This is to certify that the

thesis entitled

AQUEOUS PHASE ADSORPTION OF BENZALDEHYDE,
BENZOIC ACID AND BENZYL ALCOHOL AND THEIR MIXTURES

presented by

Chirag Ashok Shah

has been accepted towards fulfillment
of the requirements for

M.S. degree in Chemical Engineering

Major professor

Date 1/9/01

AQUEOUS PHASE ADSORPTION OF BENZALDEHYDE, BENZOIC ACID AND BENZYL ALCOHOL AND THEIR MIXTURES.

By

Chirag Ashok Shah

A THESIS

Submitted to
Michigan State University
in partial fulfillment of the requirements
for the degree of

MASTER OF SCIENCE

Department of Chemical Engineering

2001

ABSTRACT

AQUEOUS PHASE ADSORPTION OF BENZALDEHYDE, BENZOIC ACID AND BENZYL ALCOHOL AND THEIR MIXTURES.

By

Chirag Ashok Shah

Aqueous-phase adsorption equilibria of benzaldehyde, benzyl alcohol and benzoic acid are measured in the concentration range 0.2-2.0 mol/m^3 at room temperature on synthetic SP-850 resin. Several two and three parameter isotherm equations are tested. Among the models tried, the two-parameter Langmuir equation is found to be the most satisfactory. Experiments are presented to study the fixed-bed breakthrough behavior for single component liquid adsorption. The Thomas model based on the Langmuir equation is found to predict the breakthrough behavior satisfactorily for process design, and is superior to the Hougen and Marshall model using linear model. Multicomponent liquid-phase adsorption was studied for systems comprising benzaldehyde, benzyl alcohol and benzoic acid. Ideal Adsorbed Solution theory is used to model the breakthrough patterns for multicomponent systems using a linear driving force model where intraparticle diffusion is the rate-limiting step.

The process to recover benzaldehyde and benzyl alcohol from cherry pits by adsorption was studied. Various experimental variables were optimized. Knowledge of equilibrium adsorption data and breakthrough behavior data of benzaldehyde, benzyl alcohol and benzoic acid was used to predict the adsorption behavior of hydrolyzate obtained from cherry pits.

I dedicate this finished product to my Dad, who taught me to value education.

ACKNOWLEDGMENTS

I would like to thank my advisor Dr. Carl Lira for his patience and support as I have struggled to produce this finished product from my education. I would also like to thank Joel Dulebohn and Xiao Ning for their support and guidance in conducting the cherry pit experiments.

Regards to all the friends who have come and gone over the years. You will see me again.

Credit goes to Jamie Morgan, Khanghy, Amber and Shannon for assisting in the adsorption runs and issues related to the GC.

TABLE OF CONTENTS

LIST OF TABLES

LIST OF FIGURES

Chapter 1:
INTRODUCTION

The use of solids for removing substances from either gaseous or liquid solutions has been widely used since biblical times. This process, known as adsorption, involves simply the preferential partitioning of substances from the gaseous or liquid phase onto the surface of a solid substrate. From the early days of using bone char for decolorization of sugar solutions and other foods, to the later implementation of activated carbon for removing nerve gases from the battlefield, to today's thousands of applications, the adsorption phenomenon has become a useful tool for purification and separation.

Adsorption phenomena are operative in most natural physical, biological, and chemical systems, and adsorption operations employing solids such as activated carbon and synthetic resins are used widely in industrial separations and for purification of waters and waste-waters.

The process of adsorption involves separation of a substance from a fluid phase accompanied by its accumulation or concentration at the surface of a solid phase. The adsorbing phase is the adsorbent, and the material concentrated or adsorbed at the surface of that phase is the adsorbate(Suzuki et al). Adsorption is thus different from absorption, a process in which material transferred from one phase to another (e.g. liquid) interpenetrates the second phase to form a "solution". The term sorption is a general expression encompassing both processes. Physical adsorption is caused mainly by van der Waals forces and electrostatic forces between adsorbate molecules and the atoms

which compose the adsorbent surface. Thus adsorbents are characterized first by surface properties such as surface area and polarity(Slejko et al).

A large specific surface area is preferable for providing large adsorption capacity, but the creation of a large internal surface area in a limited volume inevitably gives rise to large numbers of small sized pores with increased diffusivity resistance. The size of the micropores also determines the accessibility of adsorbate molecules to the internal adsorption surface, so the pore size distribution of micropores is another important property for characterizing adsorptivity of adsorbents. Especially materials such as zeolite and carbon molecular sieves can be specifically engineered with precise pore size distributions and hence tuned for a particular separation.

Surface polarity corresponds to affinity with polar substances such as water or alcohols. Polar adsorbents are thus called "hydrophillic" and aluminosilicates such as zeolites, porous alumina, silica gel or silica-alumina are examples of adsorbents of this type(Ruthven et al). On the other hand, nonpolar adsorbents are generally "hydrophobic". Carbonaceous adsorbents, polymer adsorbents and silicalite are typical nonpolar adsorbents. These adsorbents have more affinity with oil or hydrocarbons than water.

This thesis looks at some principles and considerations for separation processes using adsorption. Chapter 2 of the thesis involves a comprehensive study of the adsorption behavior of benzaldehyde, benzoic acid and benzyl alcohol from water onto a synthetic resin. Their equilibrium adsorption behavior and their breakthrough behavior are studied as single components and also as a mixture.

The third chapter is about the experiments and subsequent changes done to the process of manufacturing benzaldehyde from cherry pits. The process holds significance

because the natural cherry flavoring is much more valuable than the artificial flavoring. Various experimental variables such as water to pit ratio, physical condition of pits, temperature of hydrolysis were studied and modified. Several modifications were made to the filtration and the regeneration process. The desorption patterns were also studied and efforts were made to improve the desorption yields.

REFERENCES

Ruthven, D.M.; Principles of Adsorption and Adsorption Processes, Wiley Interscience, New York, 1984

Slejko, F.L.; Adsorption Technology, Marcel Dekker, New York, 1985.

Suzuki, M.; Adsorption Engineering, Elsevier,Amsterdam, 1990.

Chapter 2:
ADSORPTION BEHAVIOR OF BENZALDEHYDE, BENZYL ALCOHOL AND BENZOIC ACID

2.1 Introduction to Adsorption Isotherms

Brunauer et al.(1940)classified adsorption equilbria into five types as shown in Figure 2.1. Type I ("favorable") and Type III (" unfavorable") are concave downward and upward, respectively, while the remaining three types are of an inflecting type. The type I isotherm represents monolayer adsorption and also applies to microporous adsorbents with small pore sizes. Adsorbents with type II or III isotherms are characterized by a wide range of pore sizes such that adsorption may extend from monolayer to multilayer and ultimately to capillary condensation. An isotherm of type IV suggests that adsorption causes the formation of two surface layers while type V isotherm behavior is found in the adsorption of water vapor on activated carbon. Linear isotherms are usually identified by their slope, which equals the Henry constant, H. Basically, all the types of isotherms behave as linear isotherms at sufficiently low concentration. Linear isotherms are linear for a limited concentration range.

Isotherm equations can be derived using the thermodynamic approach or the kinetic approach or using the potential theory or capillary condensation theory. Expressions from the Gibbs Isotherm Equation and the Vacancy Solution Theory are based on the thermodynamic approach while Langmuir expression, Freundlich expression and Langmuir-Freundlich equations are all based on kinetic theory approach. Although

the Langmuir equation can be derived thermodynamically or from a statistical approach (Ruthven 1984), this expression is commonly derived through a kinetic approach. The BET equation for multilayer adsorption is also based on the kinetic theory approach.

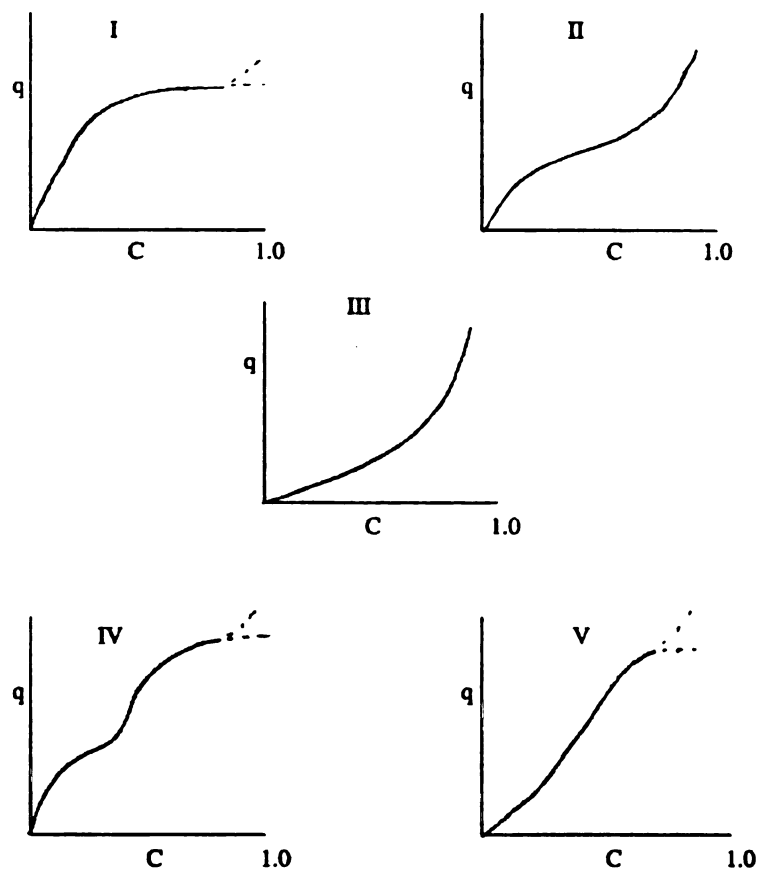

Figure 2.1 Brunauer's classification of adsorption isotherms, showing amount adsorbed versus normalised concentration in the outlet.

2.2.1 The Langmuir Model.

The earliest model of gas adsorption was suggested by Langmuir. The model is limited to monolayer adsorption. It is assumed that gas molecules striking the bare surface have a given probability of sticking, i.e. adsorbing. Molecules already adsorbed similarly have a given probability of leaving the surface, i.e. desorbing. At equilibrium a steady state exists in which as many molecules desorb as adsorb at any time. The probabilities are related to the strength of the interaction between the adsorbent surface and the adsorbate gas.

This model leads to the following isotherm:

$$\theta = \frac{q}{q_m} = \frac{bP}{1+bP} \qquad 2.1$$

where θ = fractional coverage, i.e. the fraction of the maximum coverage possible.

q = volume of gas adsorbed at pressure P usually expressed in cm^3/g at STP,

q_m = volume of the maximum gas adsorbed usually taken to be a monolayer,

b = a constant characteristic of the system. b is related to the strength of the interaction between the adsorbing gas and the surface.

As the strength of the interaction between the adsorbent (the surface of the solid) and the adsorbate (the gas adsorbing on the surface) increases the value of b increases and the surface coverage increases faster as the pressure is increased.

In practice it has been found that the Langmuir model is rarely a useful model to calculate the surface area from gas adsorption data. The Langmuir model is useful when there is a strong specific interaction between the surface and the adsorbate so that a single adsorbed layer forms and no multi-layer adsorption occurs. Strongly held adsorption from solution may fit the Langmuir model.

2.2.2 The BET Model.

Brunauer, Emmett and Teller developed several models of gas adsorption on solids, which have become the effective standard for surface area measurements. The models were generalisations of Langmuir theory monolayer adsorption to multilayer adsorption.

The assumptions underlying the simplest BET isotherm are: Gas adsorbs on the flat, uniform surface of the solid with a uniform heat of adsorption due to van der Waals forces between the gas and the solid. There is no lateral interaction between the adsorbed molecules. After the surface has become partially covered by adsorbed gas molecules additional gas can adsorb either on the remaining free surface or on top of the already adsorbed layer. The adsorption of the second and subsequent layers occurs with a heat of adsorption equal to the heat of liquefaction of the gas. There is no limit to the number of layers which can adsorb.

Other isotherms developed by Brunauer, Emmett and Teller were based on more complex models which included the assumptions that the thickness of the adsorbed layers cannot exceed some finite number of layers n and the second adsorbed layer has a heat of adsorption intermediate between the first layer and the heat of liquefaction.

The standard 2-parameter BET isotherm based on the simplest BET model may be written in various ways. The isotherm form, which gives the amount of gas adsorbed as a function of the relative pressure of the adsorbing gas is:

$$\frac{q}{q_m} = \frac{\alpha(P/P_s)}{(1-P/P_s)(1+(\alpha-1)(P/P_s))} \qquad 2.2$$

or

$$\frac{q}{q_m} = \frac{\alpha x}{(1-x)(1+(\alpha-1)x)} \qquad 2.3$$

where, q = Volume of gas adsorbed at pressure P

q_m = Volume of gas which could cover the entire adsorbing surface with a monomolecular layer

P_s = Saturation pressure of the gas, i.e. the pressure of the gas in equilibrium with bulk liquid at the temperature of the measurement.

$x = P/P_s$ = relative pressure.

α = a constant for the gas/solid combination.

The constant α is related to the difference between the heat of adsorption of the first layer ($q_1^{\wedge}$) and the heat of liquefaction ($q_L^{\wedge}$) in the form

$$\alpha = \exp\{(q_1^{\wedge} - q_L^{\wedge})/RT\} \qquad 2.4$$

or $(q_1^{\wedge} - q_L^{\wedge}) = RT \ln \alpha$

$q_1^{\wedge} - q_L^{\wedge}$ is also known as the net heat of adsorption.

R = gas constant (8.31447 J K^{-1} mol^{-1})

T = temperature (K)

2.2.3 Freundlich Model.

The Freundlich isotherm, frequently described as the classical equation, is widely used, particularly in the low to intermediate pressure range. It is expressed as

$$q = K(P)^{1/n} \qquad 2.5$$

where q = volume of gas adsorbed at pressure P usually expressed in cm^3/g at STP,

K = a constant characteristic of the system.

n= another constant restricted to values greater than unity.

The Freundlich equation, in many ways is the simplest equation for data representation. The biggest limitation of the Freundlich model is, it fails to observe Henry's law behavior in the limiting situations of $P \rightarrow 0$.

2.2.4 Langmuir-Freundlich Expression.

The Langmuir-Freundlich expression combines the Langmuir and Freundlich Equations and is given as

$$\theta = \frac{q}{q_m} = \frac{bP^{1/n}}{1 + bP^{1/n}} \qquad 2.6$$

This equation follows the same asymptotic behavior as the Langmuir equation as $P \rightarrow \infty$. And the expression translates to Langmuir equation at n=1.

2.3 Isotherm Expressions for Liquid Adsorption

In contrast to gas phase adsorption, the density of pure adsobate in liquid phase is essentially invariant. For liquid systems, the term single-component adsorption isotherm refers to the adsorption of a single adsorbate from liquid solutions in which the activity of the solvent is constant. Giles et al.(1960, 1962) examined several liquid adsorption isotherms and classified them into four categories- S, L, H and C types with subdivisions for each time. Their classification is based on the initial curvature of the isotherm curve at the origin. The S type is convex and the L type is concave which correspond to types III and I respectively, in the BET classification for gas adsorption isotherms. The C type exhibits linear behavior at least part of the adsorption range, while the H-type isotherms show a strong preferential adsorption of the adsorbate and are steep at low concentration.

Most of the gas phase isotherm expression can be extended to liquid systems by replacing the pressure term with concentration and with corresponding changes in the units of the various parameters. In liquid phase adsorption, it is not easy to assume a monolayer coverage as the adsorbed molecules are not necessarily tightly packed with identical orientation. This and other complications such as the presence of solvent molecules and the formation of micelles from adsorbed molecules make the liquid phase adsorption much more complex than the gas phase adsorption.

The following isotherm expressions can however be used for liquid phase adsorption.

Linear Isotherm $$q = Kc \qquad (2.7)$$

Langmuir Isotherm $$\frac{q}{q_m} = \frac{bc}{1+bc} \quad \text{or} \quad q = \frac{ac}{1+bc} \qquad (2.8)$$

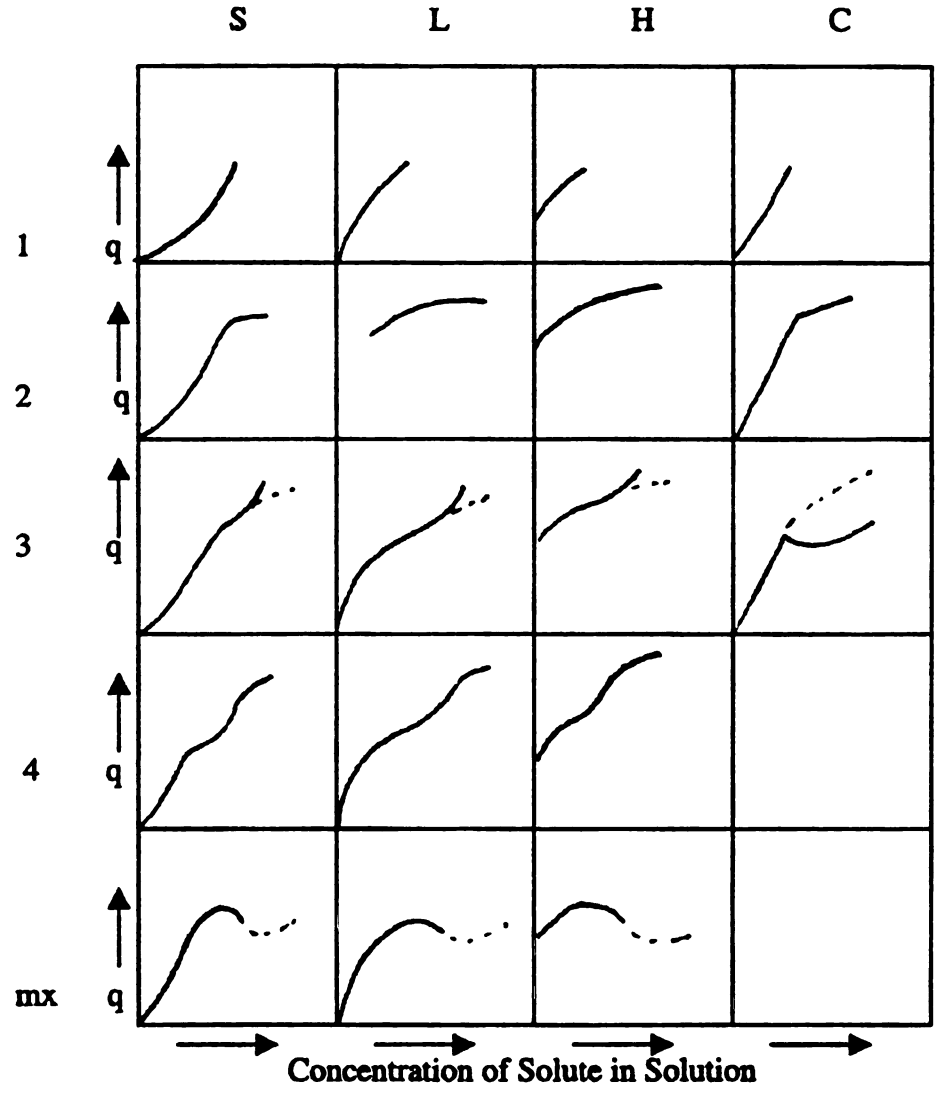

Figure 2.2 Classification of isotherms for adsorption from solution.

Freundlich Isotherm $$q = K(c)^{1/n}$$ 2.9

Langmuir-Freundlich Isotherm $$\frac{q}{q_m} = \frac{bc^{1/n}}{1 + bc^{1/n}}$$ 2.10

2.3.1 Benzaldehyde, Benzyl-alcohol and Benzoic Acid Liquid Phase Adsorption

Equilibrium adsorption behavior of benzaldehyde, benzyl alcohol and benzoic acid at room temperature was studied in a liquid phase adsorption from water. The initial liquid concentrations were varied as well as the quantities of SP-850 resin. The procedure followed in finding the equilibrium adsorption behavior and the raw data is given in Appendix C-2. All the experiments were done at room temperature.

The data were fitted using a C++ code to find the best fit for linear model, Langmuir model, Freundlich model and the Langmuir-Freundlich model. The concentration of the adsorbate in the solution at equilibrium was provided in mol/m^3 while the amount of adsorbate adsorbed was given in gm adsorbate/gm resin. Since the code was written in C++, which is not a very powerful language for mathematical calculations, the code fails for extremely low concentrations in order of E-8. The concentrations of benzaldehyde, benzyl alcohol and benzoic acid in the feed for single component and multicomponent fixed bed adsorption experiments were around 0.95 mol/m^3, 0.45 mol/m^3 and 0.15 mol/m^3 respectively. The linear adsorption model was made to fit data points around these concentrations. The least square method for linear model was applied for data points up till 1 mol/m^3, 1 mol/m^3 and 0.25 mol/m^3 for benzaldehyde, benzyl alcohol and benzoic acid respectively. The fits are summarized in Figures 2.3 to 2.14.

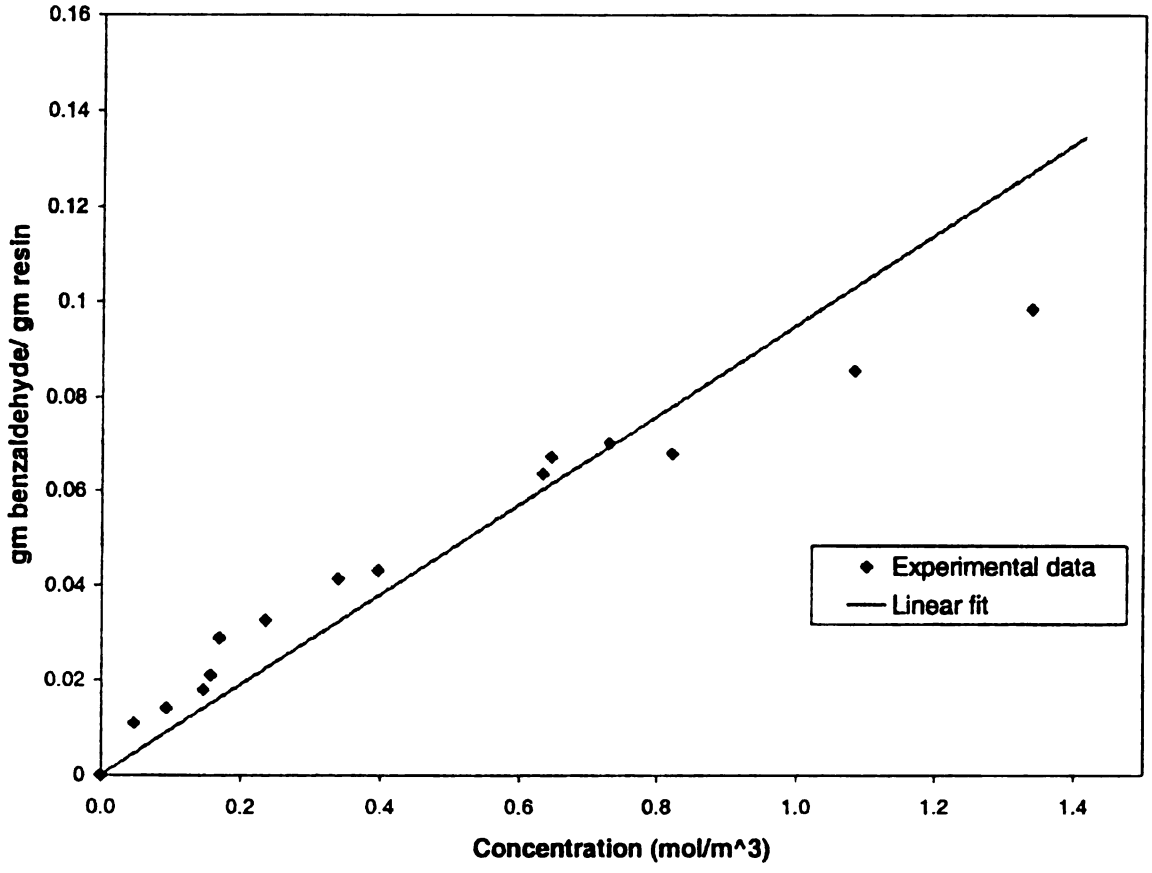

Figure 2.3 Benzaldehyde Equilibrium Adsorption Isotherm and Linear Fit

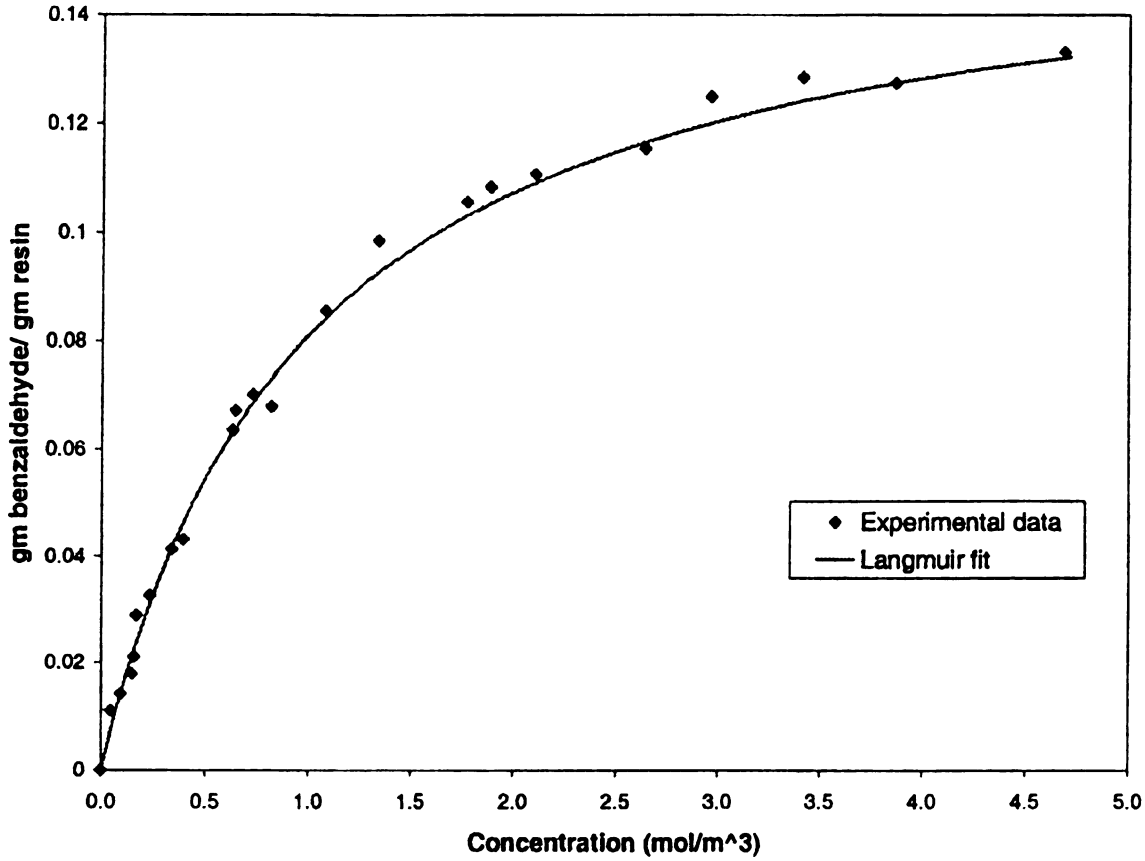

Figure 2.4 Benzaldehyde Equilibrium Adsorption Isotherm and Langmuir Fit

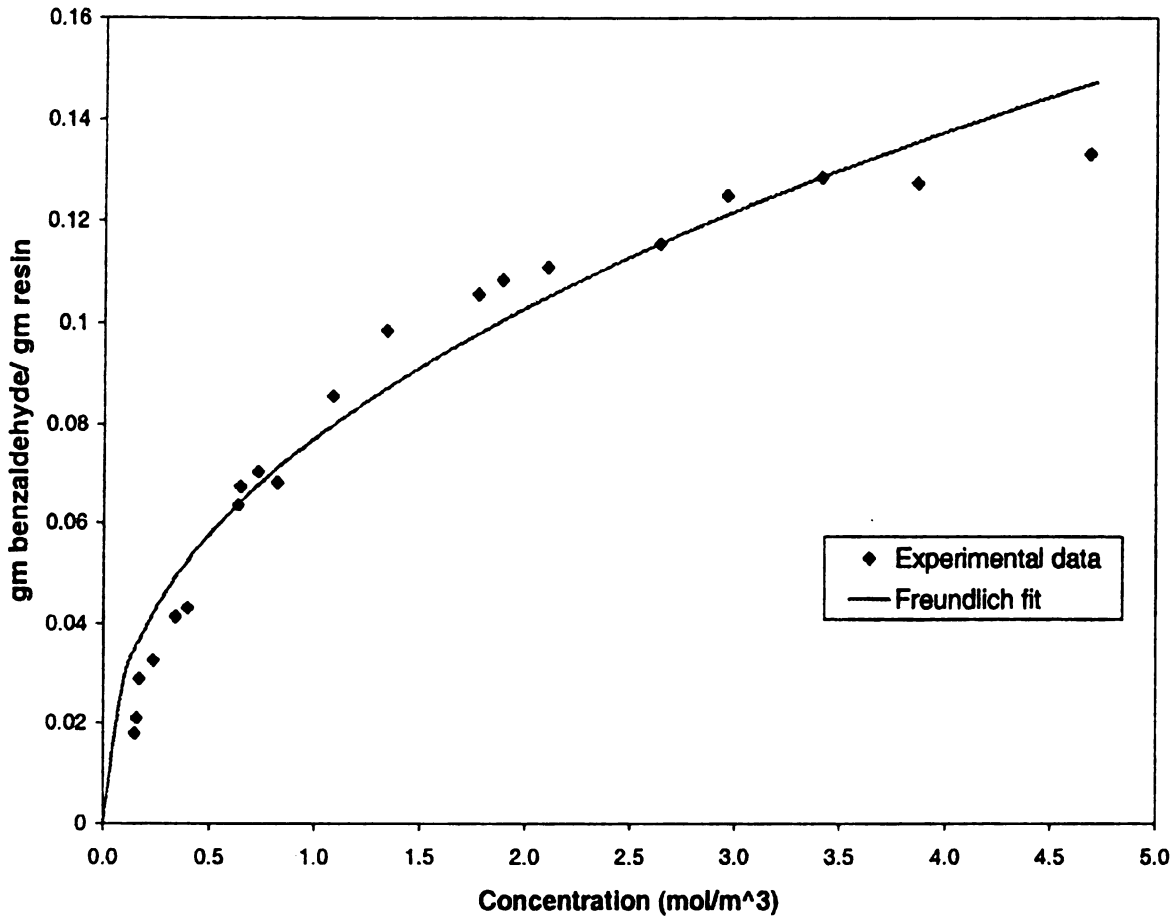

Figure 2.5 Benzaldehyde Equilibrium Adsorption Isotherm and Freundlich Fit

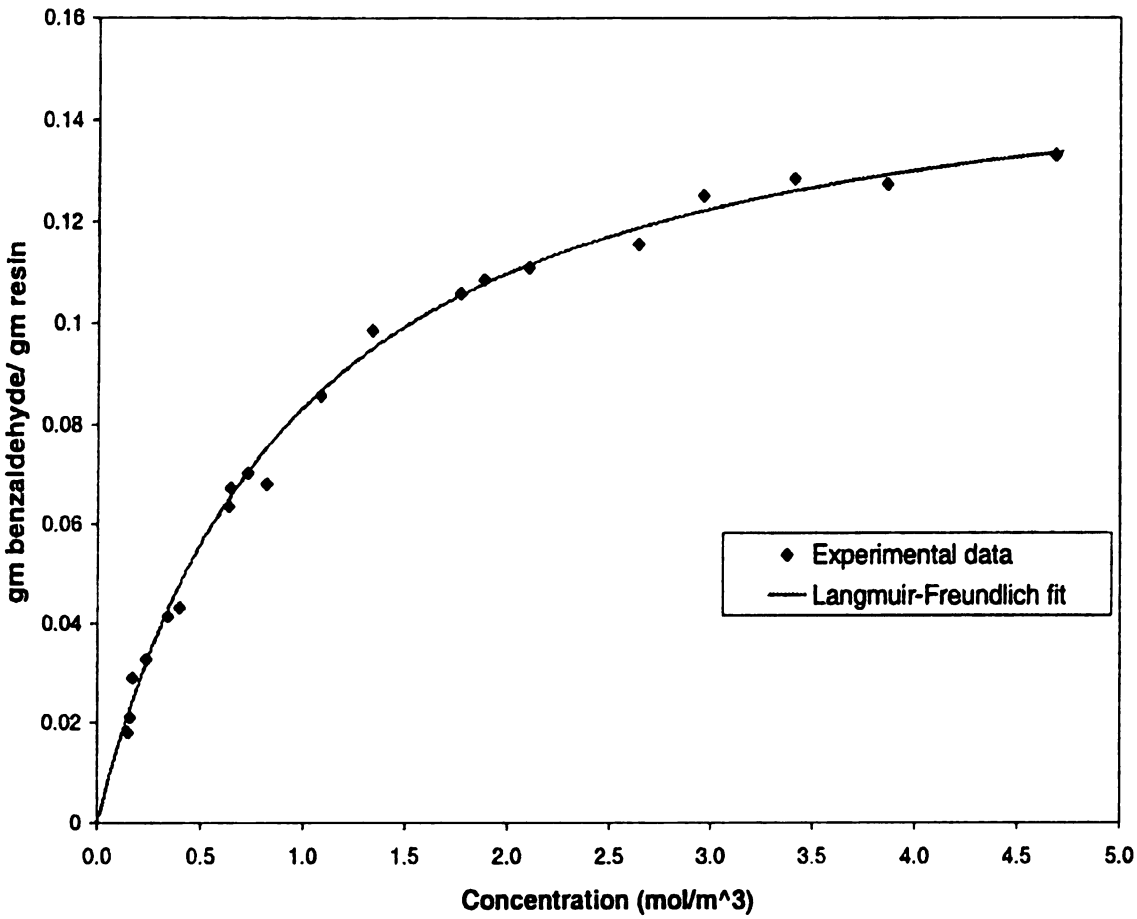

Figure 2.6 Benzaldehyde Equilibrium Adsorption Isotherm and Langmuir-Freundlich Fit

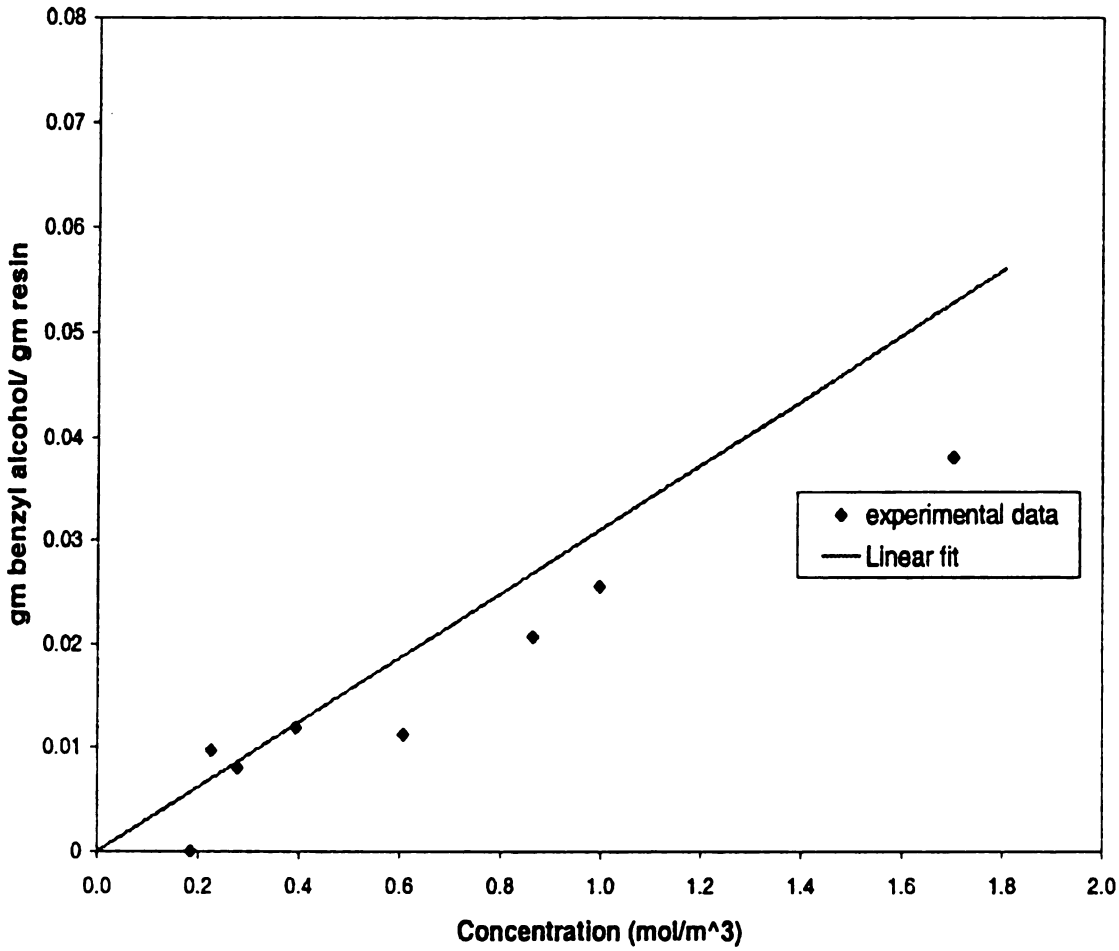

Figure 2.7 Benzyl Alcohol Equilibrium Adsorption Isotherm and Linear Fit

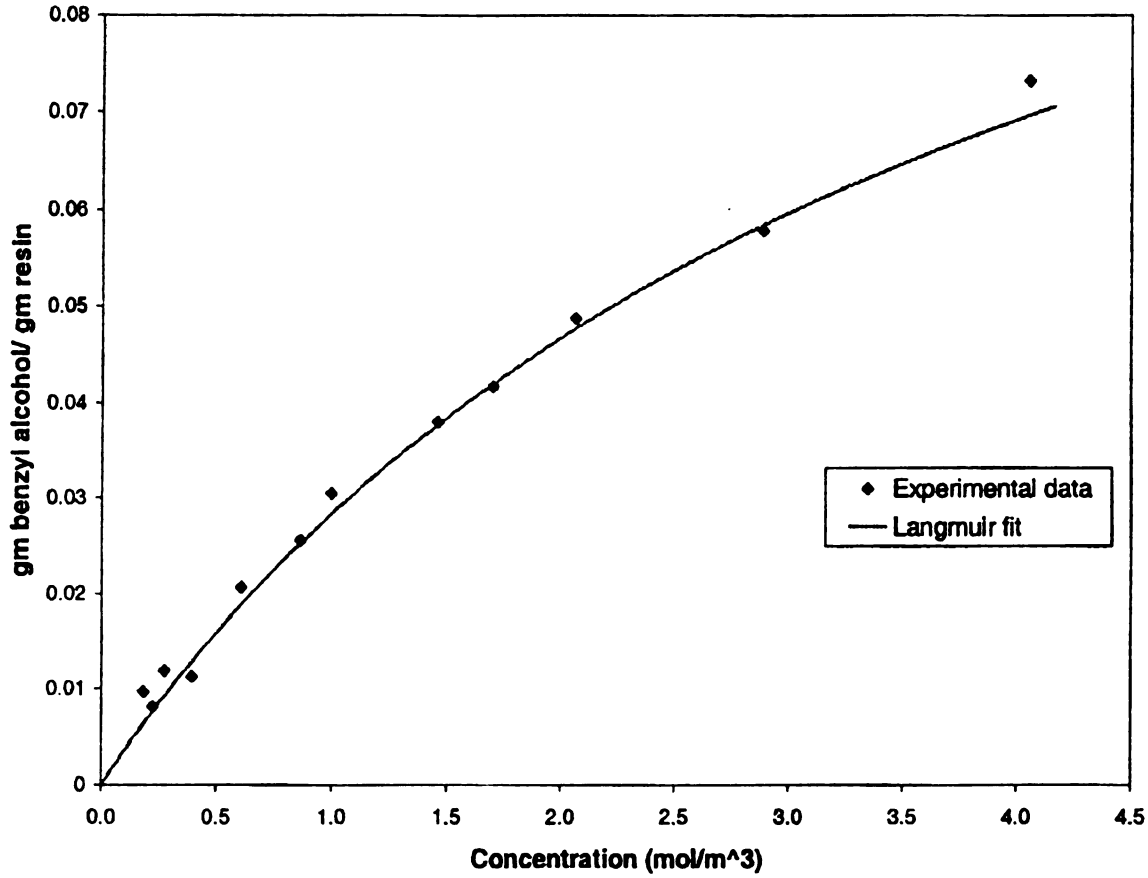

Figure 2.8 Benzyl Alcohol Equilibrium Adsorption Isotherm and Langmuir Fit

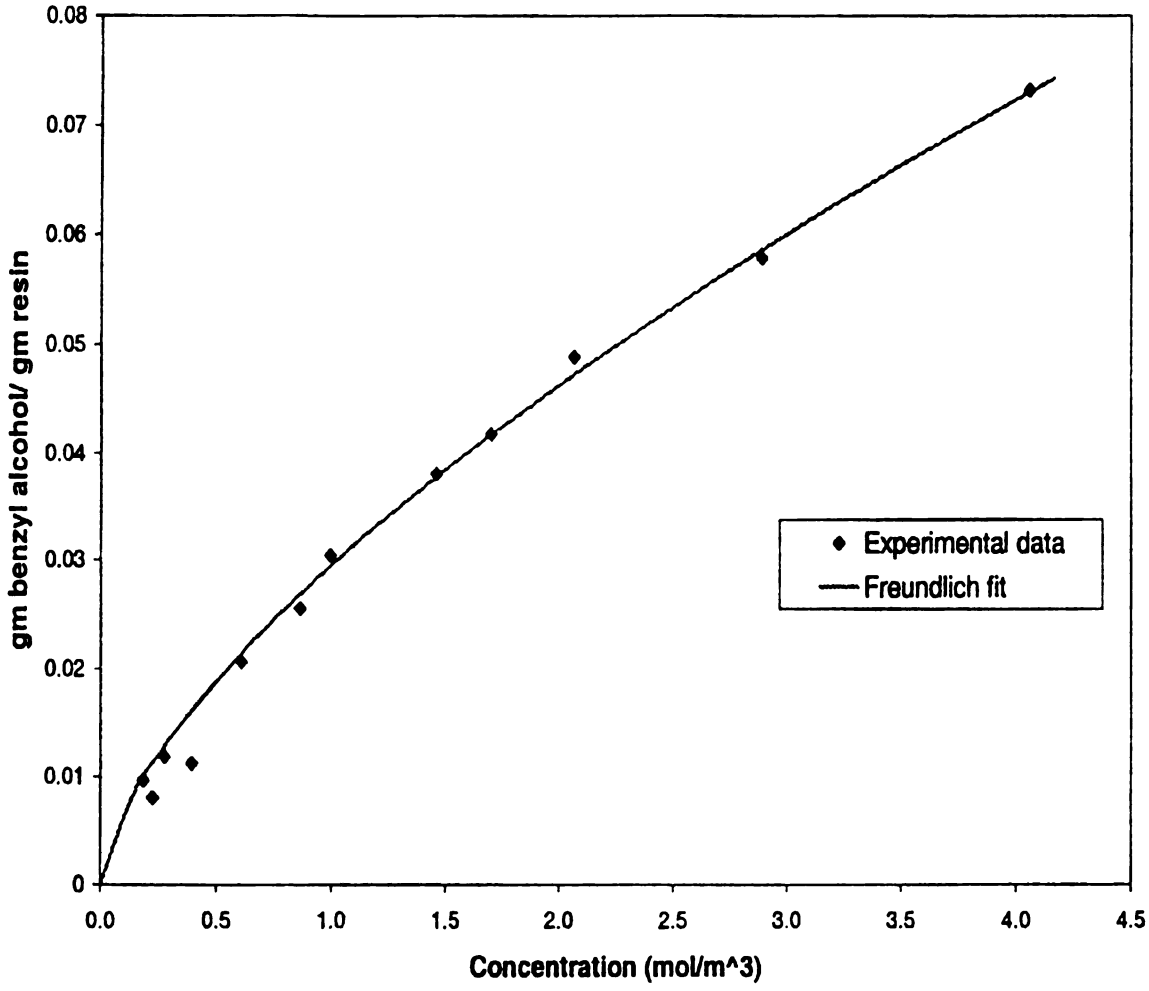

Figure 2.9 Benzyl Alcohol Equilibrium Adsorption Isotherm and Freundlich Fit

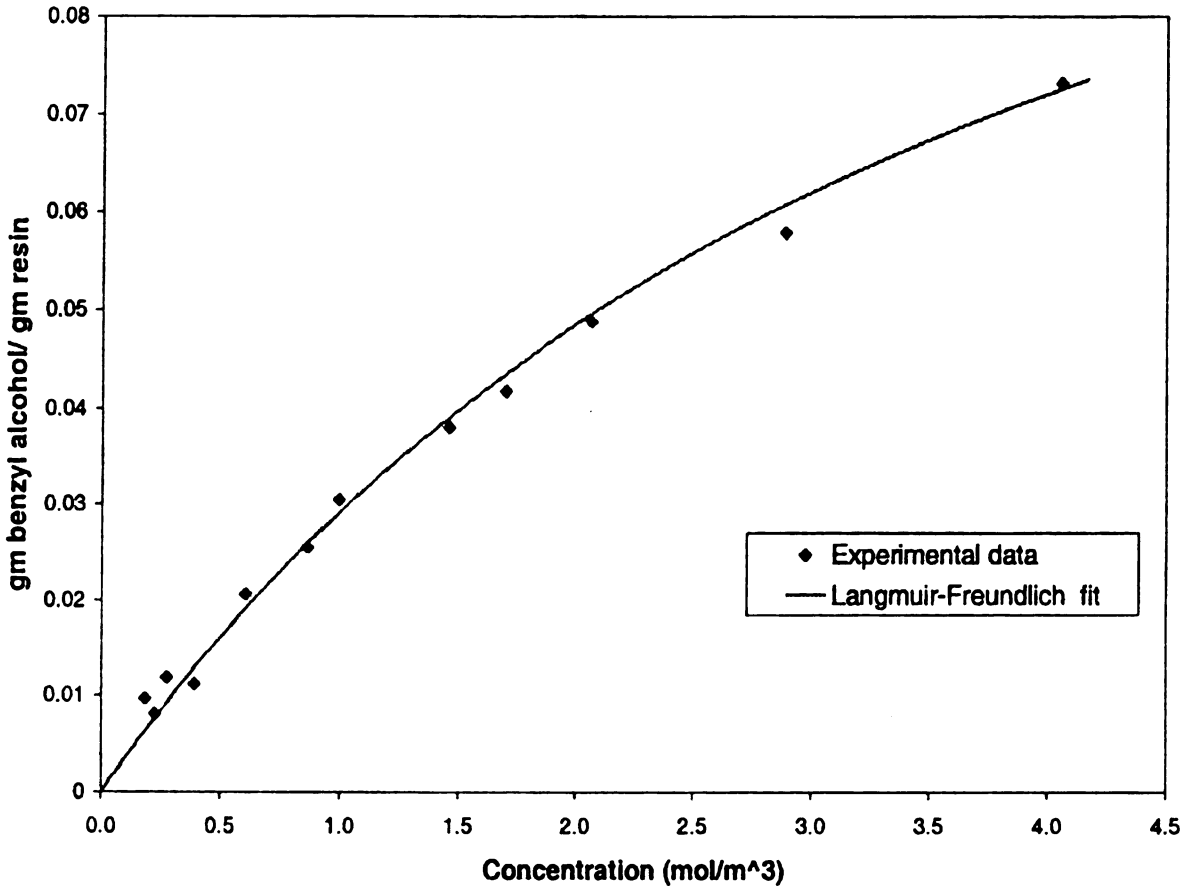

Figure 2.10 Benzyl Alcohol Equilibrium Adsorption Isotherm and Langmuir-Freundlich Fit

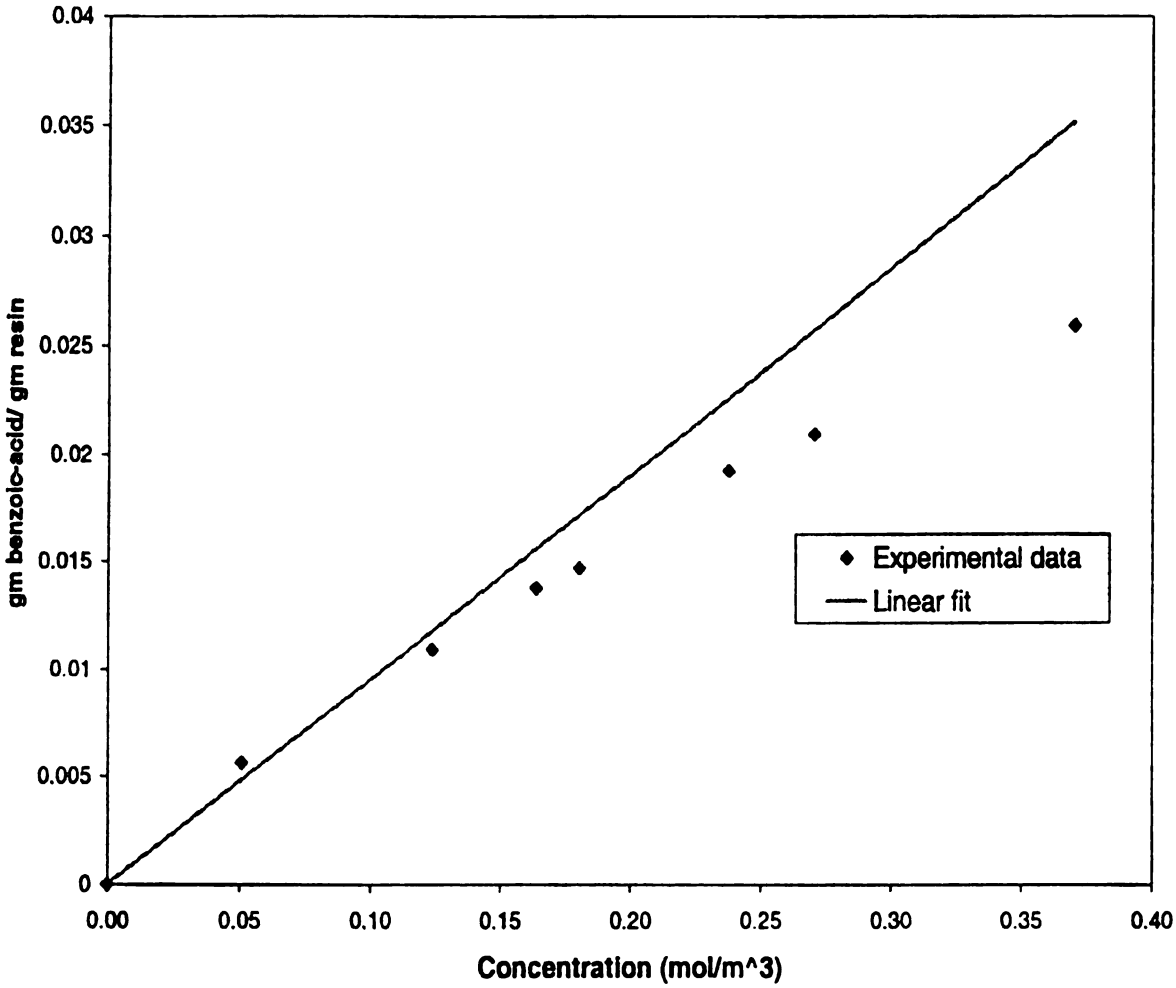

Figure 2.11 Benzoic Acid Equilibrium Adsorption Isotherm and Linear Fit

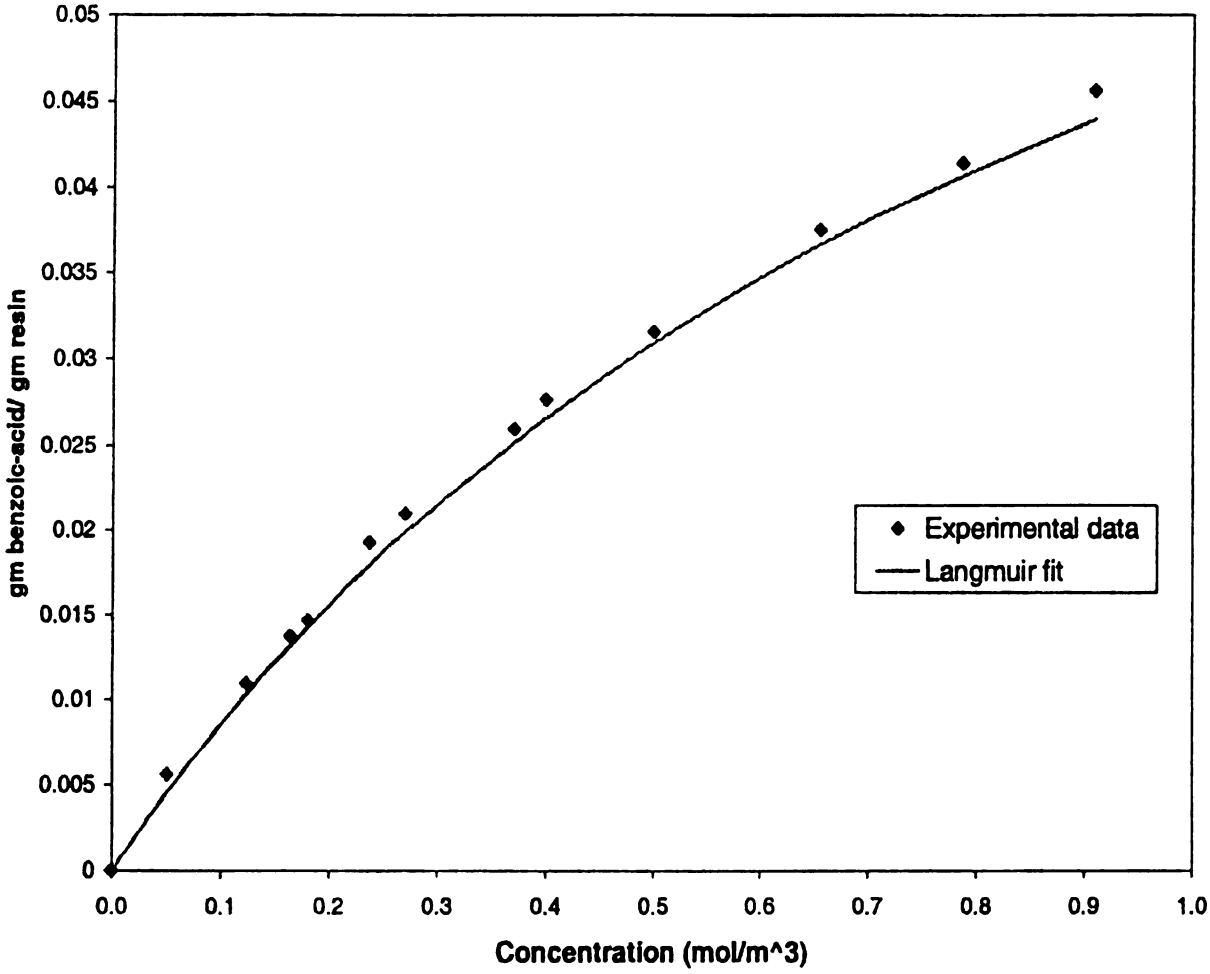

Figure 2.12 Benzoic Acid Equilibrium Adsorption Isotherm and Langmuir Fit

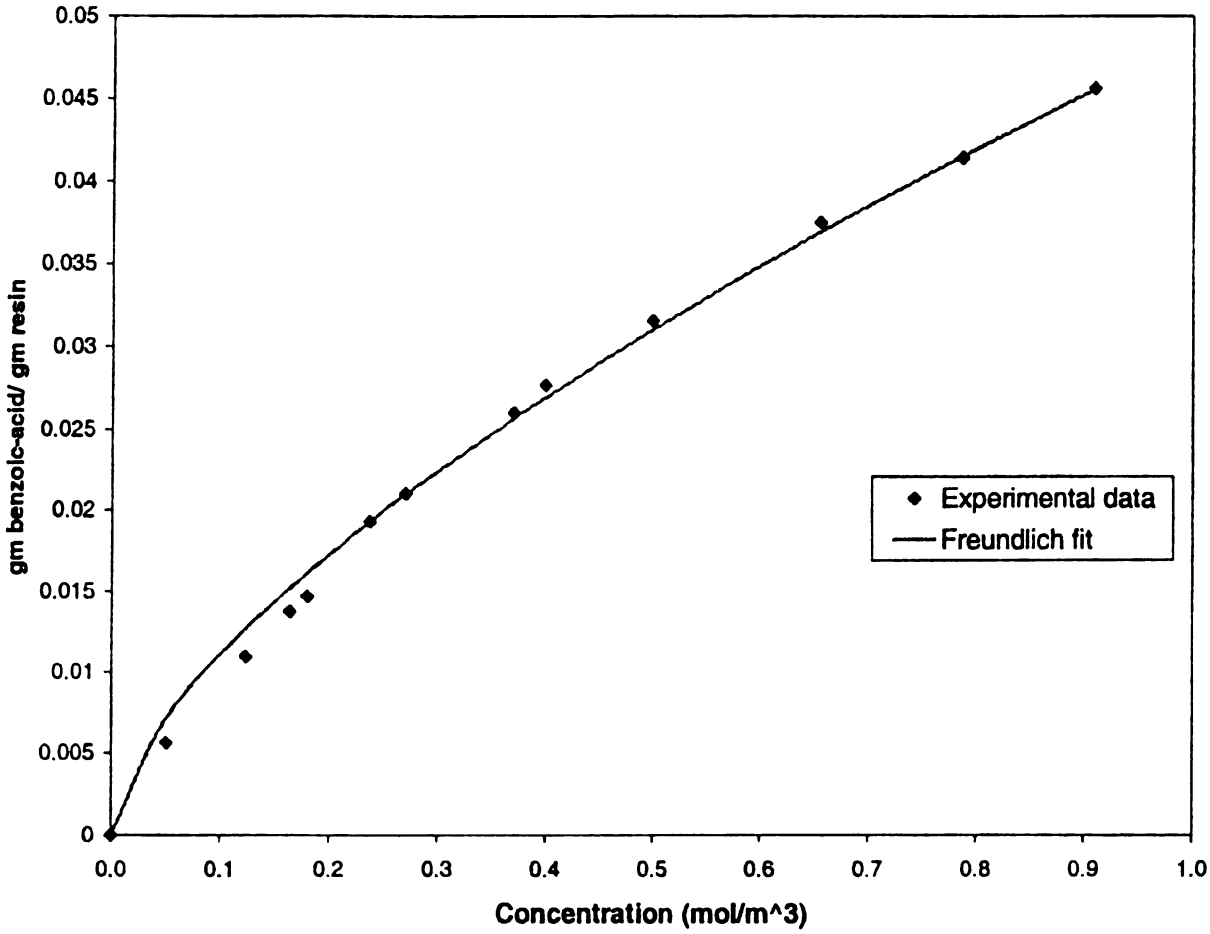

Figure 2.13 Benzoic Acid Equilibrium Adsorption Isotherm and Freundlich Fit

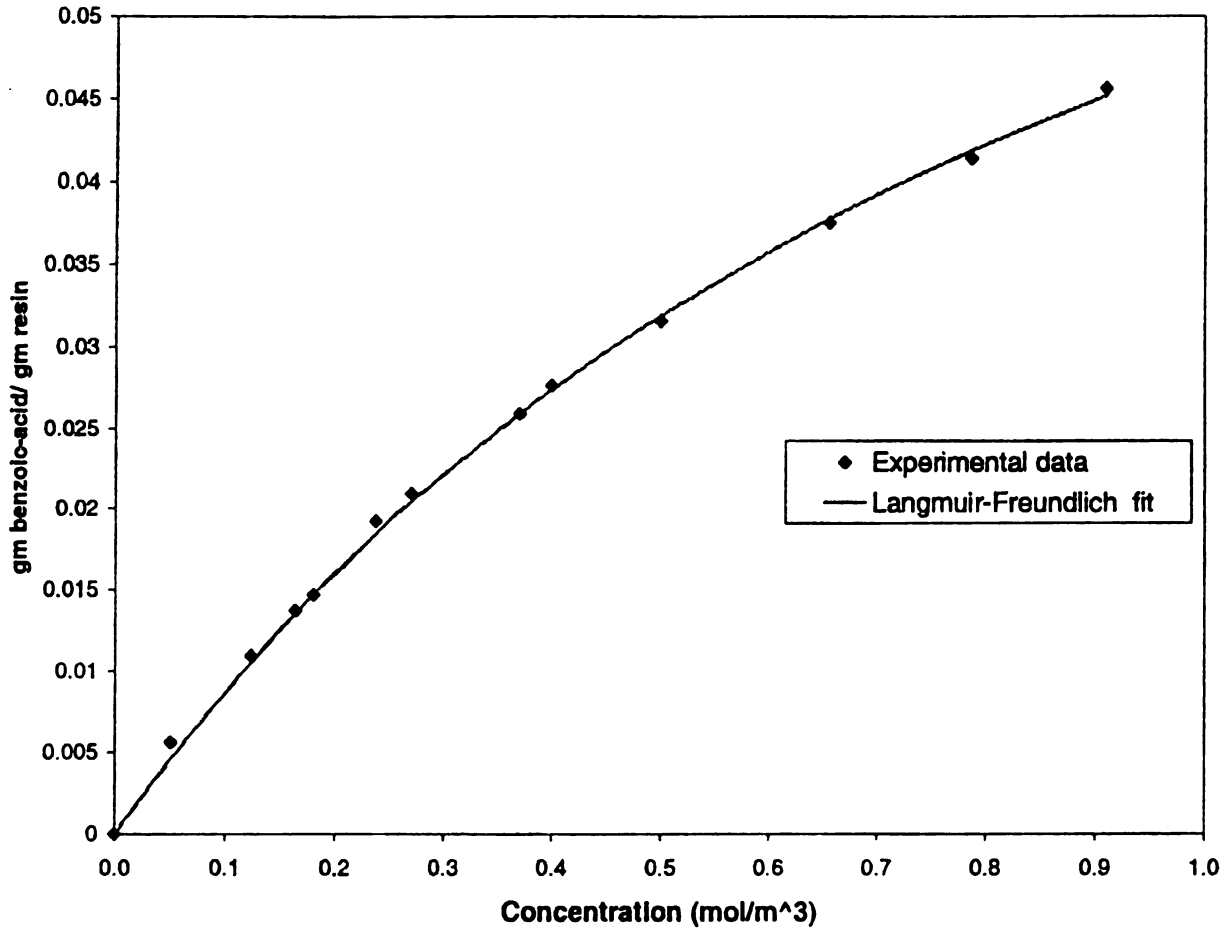

Figure 2.14 Benzoic Acid Equilibrium Adsorption Isotherm and Langmuir-Freundlich Fit

The concentrations were provided in mol/m^3 and the adsorbed amount in mass unit adsorbate per mass unit adsorbent. The constants corresponding to the best fits are tabulated below. The mean error for all the fits are calculated. The mean error(ε) is given by the following equation :

$$\varepsilon = \frac{1}{n}\sum\left(\frac{X_E - X_C}{X_C}\right)^2$$

where, ε= Dimensionless mean error for every data point.

n= Number of data points

X_E=Experimental Value of Amount adsorbed for a particular y

X_C=Calculated Value of Amount adsorbed for the same y

Table 2-1: Results of Best Linear Fit.

Compound	K(m^3/mol)	ε(unitless)
Benzaldehyde	0.095	0.140
Benzyl-alcohol	0.031	0.084
Benzoic-acid	0.095	0.070

Table 2-2: Results of Best Langmuir Fit.

Compound	a(m^3/mol)	b(m^3/mol)	ε(unitless)
Benzaldehyde	0.165	1.036	0.014
Benzyl-alcohol	0.036	0.270	0.032
Benzoic-acid	0.094	1.040	0.005

Table 2-3: Results of Best Freundlich Fit.

Compound	K((m^3/mol)^n)	n(unitless)	ε(unitless)
Benzaldehyde	0.077	2.393	0.048
Benzyl-alcohol	0.029	2.234	0.041
Benzoic-acid	0.048	1.558	0.006

Table 2-4: Results of best Langmuir-Freundlich Fit.

Compound	a($(m^3/mol)^n$)	b($(m^3/mol)^n$)	n(unitless)	ε(unitless)
Benzaldehyde	0.175	1.102	0.986	0.013
Benzyl-alcohol	0.037	0.270	1.008	0.031
Benzoic-acid	0.101	1.112	0.983	0.004

Comparing the mean error between the experimental values and the calculated values, the Langmuir fit was found to be the best fit for equation up to two constants for all the three compounds. Langmuir-Freundlich isotherm provided almost the same model as Langmuir Isotherm. The value of n for Langmuir-Freundlich model for all the three components was almost unity. And with n as 1, the Langmuir-Freundlich model reduces to a Langmuir model. It can be realized from equation 2.8 that

$$q_m = a/b \qquad 2.11$$

Comparing the Langmuir constants obtained by fitting, the values of q_m were found to be 0.159, 0.133 and 0.090 g adsorbate/g adsorbent for benzaldehyde, benzoic acid and benzyl alcohol respectively. Since q_m is a measure of the amount of adsorbate needed for saturation of the adsorbent, it can be understood that the resin adsorbs a lot more of benzaldehyde than benzyl alcohol and benzoic acid for a saturated coverage, when adsorbing from aqueous solutions.

2.3.2 Dynamic Behavior of Fixed Bed Adsorption of Single Component.

Generally, practical applications of adsorption for separation and purification are carried out in the fixed bed mode. The type of adsorption processes carried out in fixed bed operations include saturation, desorption and their combinations. The important feature of the dynamic behavior of fixed bed adsorption is the history of effluent concentration. The effluent history is generally depicted as concentration-time curve. This concentration-time curve is known as the breakthrough curve. The time at which the effluent concentration reaches a particular threshold value, which makes it impractical to continue further is known as the breakthrough time. Accurate predictions of the breakthrough curves are essential for the rational design of the adsorption system.

Breakthrough behaviors of aqueous benzaldehyde, benzyl alcohol and benzoic acid were studied on SP-850 resin. The resin was washed with 20 % ethanol solution in water and then washed with water. The feed solution containing a single adsorbate was passed through the resin bed at a superficial velocity of 2.7 cm/min. A detailed procedure is in Appendix C-3. Breakthrough patterns for benzaldehyde, benzyl alcohol and benzoic acid were followed for different amounts of resin, different heights of bed and different flow rates. However, the superficial velocity U_S of the feed flowing through the bed was kept constant. The superficial velocity is a velocity averaged over the entire cross section of the preform. In a one-dimensional flow, superficial velocity is defined as:

U_S = Volumetric Flow Rate/ Cross Section Area of Bed

The superficial velocity is related to the interstitial velocity, U_Z by $U_s = \varepsilon U_z$, where ε is the void fraction ratio of the adsorbent.

2.3.1.1 Prediction of Breakthrough Curves using Linear Adsorption Iisotherms.

Hougen and Marshall (1947) developed a model to predict the breakthrough curves for cases in which the mass transfer of the solid adsorbent was controlled by a fluid phase mass transfer coefficient. Their model was based on the assumptions that the equilibrium between the fluid and solid phases could be expressed by a linear isotherm equation.

The general mass balance for solute A through a differential column section neglecting the transport by axial diffusion can be given as:

(rate of A in) – (rate of A out) = (rate of A accumulation)

$$\varepsilon S(C_A U_Z)_{Z,t} - \varepsilon S(C_A U_Z)_{Z+\Delta Z,t} = S\Delta Z\left[\left(\varepsilon\frac{\partial C_A}{\partial t}\right)_Z + \left((1-\varepsilon)\frac{\partial C_{As}}{\partial t}\right)_Z\right] \qquad 2.12$$

Where,

Z= Bed height, m.

ε= Void fraction ratio for the SP-850 resin.

U_z= Interstitial velocity, m/min.

S= Cross sectional area of the column, m^2

t= Time, minutes.

C_A= Concentration of adsorbate in the fluid phase, mol/m^3

C_{As}= Average concentration of adsorbate in the solid phase, mol/m^3

Applying the limiting process for ΔZ after dividing equation 2.12 by $\varepsilon S\Delta Z$ gives

$$-U_Z\left(\frac{\partial C_A}{\partial z}\right)_t = \left(\frac{\partial C_A}{\partial t}\right)_Z + \left(\frac{(1-\varepsilon)}{(\varepsilon)}\frac{\partial C_{As}}{\partial t}\right)_Z \qquad 2.13$$

Introducing $\rho_s = \rho_b/(1-\varepsilon)$ and $q_A = C_{As}/\rho_s$ into equation 2.13 and assuming that the fluid content of the bed is small compared to the total volume of fluid throughput, the mass balance for the bed can be expressed by a partial differential equation:

$$\frac{-\varepsilon U_Z}{\rho_b}\left(\frac{\partial C_A}{\partial Z}\right)_t = \left(\frac{\partial q_A}{\partial t}\right)_Z \qquad 2.14$$

where,

ρ_b= Bulk adsorbent density, kg/m^3.

ρ_s= Skeletal adsorbent density, kg/m^3.

q_A=Equilibrium uptake, g adsorbed/g resin.

The change in the adsorbate content of the adsorbent and the fluid can be given by the rate expression.

$$\left(\frac{\partial q_A}{\partial t}\right)_Z = \frac{K_f a}{\rho_b}\left(C_A - C_A^*\right) \qquad 2.15$$

While the equilibrium fluid-phase concentration for a linear isotherm can be related to the adsorbate concentration in the solid by the following equations.

$$q_A = K_D C_A^* \qquad 2.16$$

$$q_A^\infty = K_D C_{A0} \qquad 2.17$$

Where,

$K_f a$= Rate constant, (min^{-1})(m^3 adsorbate/m^3 bed).

K_D= Distribution coefficient, m^3/mol.

C_{A0}= Concentration of adsorbate in the inlet feed stream, mol/m^3

q_A^{∞} =Saturation capacity of the bed corresponding to concentration C_{A0} of the adsorbate in the influent

C_A^* =Concentration of A in the fluid phase that is in equilibrium with uptake q_A in solid.

The entire model can be expressed in terms of dimensionless variables:

$$\tau = \frac{K_f a}{K_D \rho_b}\left(t - \frac{Z}{U_z}\right) \qquad 2.18$$

$$\overline{X} = \frac{C_A}{C_{A0}} \qquad 2.19$$

$$\zeta = \frac{ZK_f a}{\varepsilon U_z} \qquad 2.20$$

Where,

ζ= Dimensionless bed length parameter.

τ= Dimensionless time parameter.

$\overline{X}$ = Dimensionless concentration parameter.

A solution can be obtained using the Laplace transforms. The solution is

$$\overline{X} = 1 - \int_0^{\tau} e^{-(\zeta+\tau)} J_0(i\sqrt{4\tau\zeta})d\zeta = \overline{J}(\tau,\zeta) \qquad 2.21$$

Where,

J_0 = Zero Order Bessel solution of the first kind.

An approximation of the $\bar{J}(\tau,\zeta)$ function for large values of τ and ζ was given by Thomas in 1944. The approximation in terms of the error function is given as under.

$$\bar{J}(\zeta,\tau)=\frac{1}{2}\left[1-erf(\sqrt{\zeta}-\sqrt{\tau})+\frac{e^{-(\sqrt{\zeta}-\sqrt{\tau})^2}}{\sqrt{\pi}(\sqrt{\tau}+\sqrt[4]{\tau\zeta})}\right] \qquad 2.22$$

The above equation is accurate to within 1% when $\zeta\tau \geq 36$ (Vermeulen et al.). When $\zeta\tau \geq 3600$, the last term may be neglected.

The procedure followed in performing experiments for studying the breakthrough behavior is given in Appendix C-3. ρ_s, ρ_b and void ratio ε were calculated by performing experiments shown in Appendix C-1. Table 2.5 summarizes the experimental conditions.

Table 2-5. Summary of Experimental Conditions for Single Component Adsorption.

No	Compound	Z(m)	C_{A0} (mol/m^3)	Diameter of bed(m)	Amount of resin(ml)	Figure no
1	Benzaldehyde	0.0635	0.83	0.0222	13.0	2.15
2		0.0853	1.13	0.0222	18.0	
3		0.1219	1.05	0.0603	172.0	
4		0.1117	1.09	0.0603	152.0	
5	Benzyl alcohol	0.0508	0.63	0.0222	11.0	2.16
6		0.0660	0.48	0.0222	13.5	
7		0.0812	0.48	0.0603	112.0	
8		0.0838	0.48	0.0603	125.0	
9	Benzoic acid	0.0508	0.26	0.0222	11.0	2.17
10		0.0808	0.26	0.0222	16.5	
11		0.1219	0.19	0.0603	170.0	
12		0.0750	0.19	0.0603	100.0	

The superficial velocity, U_z was kept constant at 2.7 cm/min for all the runs. The experimental data obtained by running the synthetic feeds containing benzaldehyde, benzyl alcohol or benzoic acid were analyzed using the Hougen and Marshall model. The

experimental data was entered in a Microsoft® Excel sheet along with the equations and was fitted by iterating the parameter $K_f a$. The results are shown in Figures 2.15, 2.16 and 2.17.

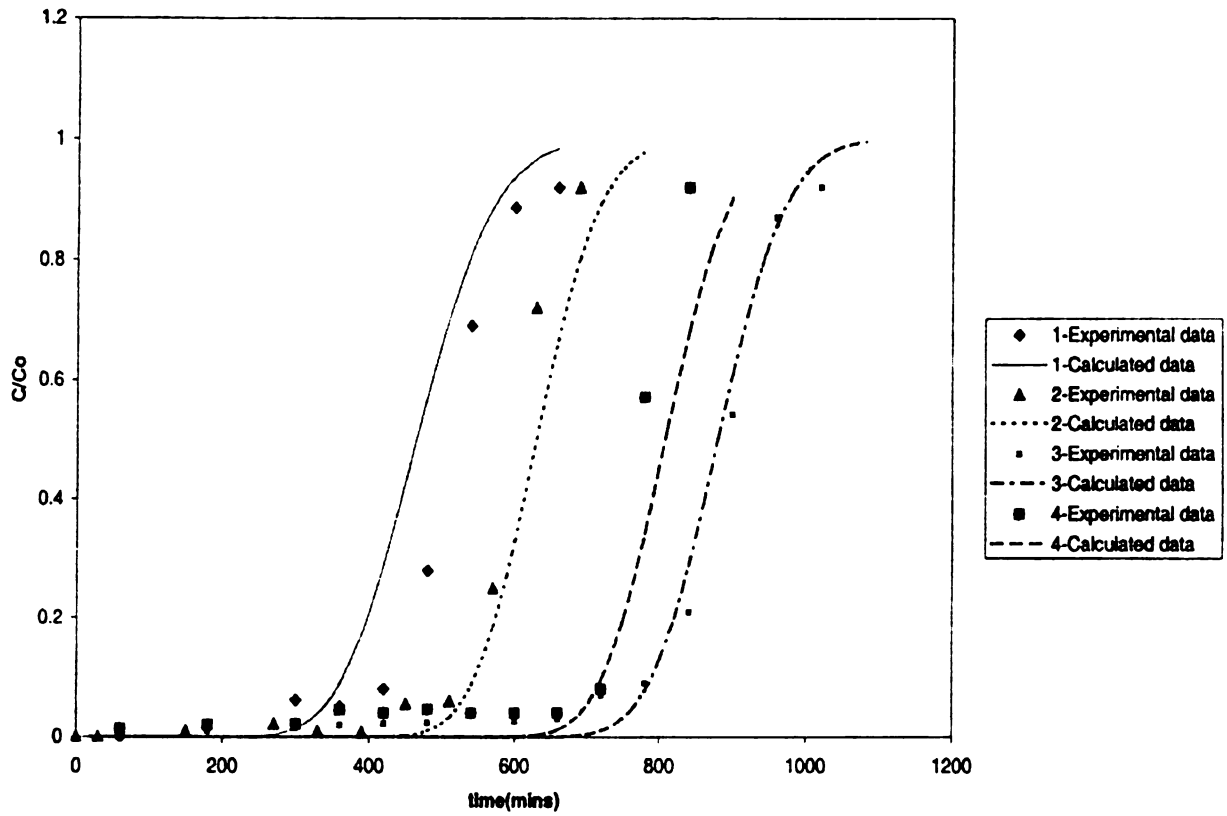

Figure 2.15 Benzaldehyde Breakthrough Behavior using Linear Adsorption Isotherm.

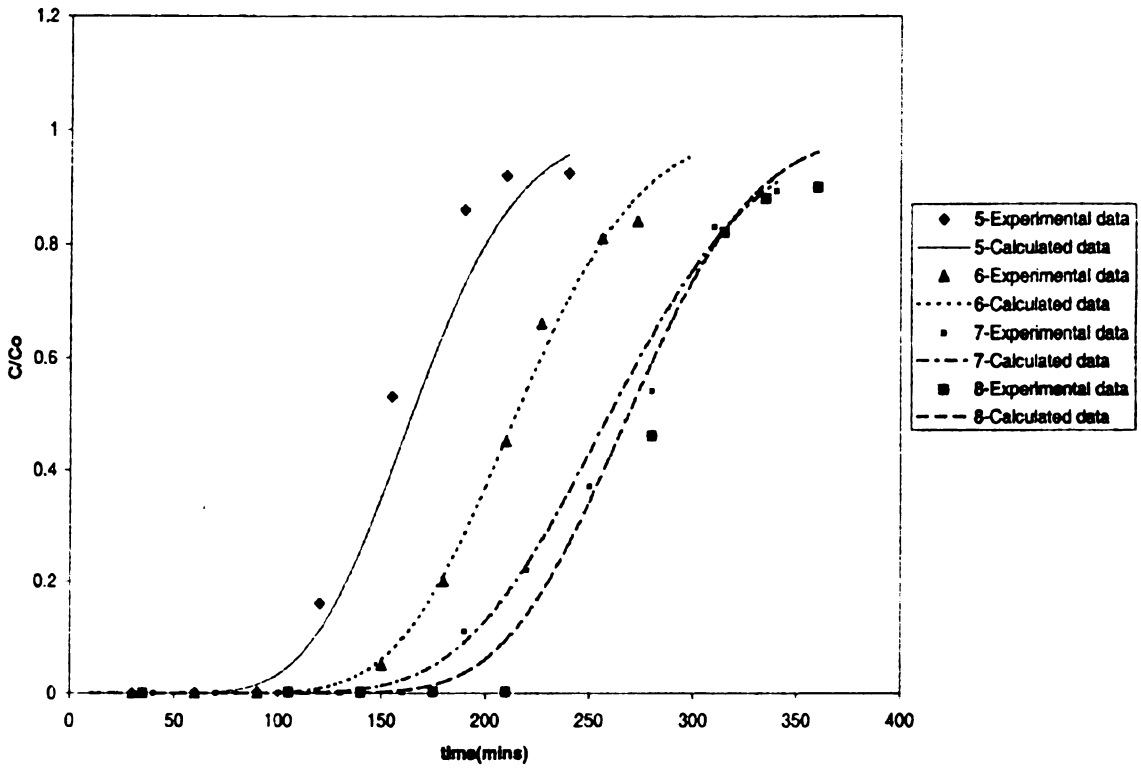

Figure 2.16 Benzyl Alcohol Breakthrough Behavior using Linear Adsorption Isotherm.

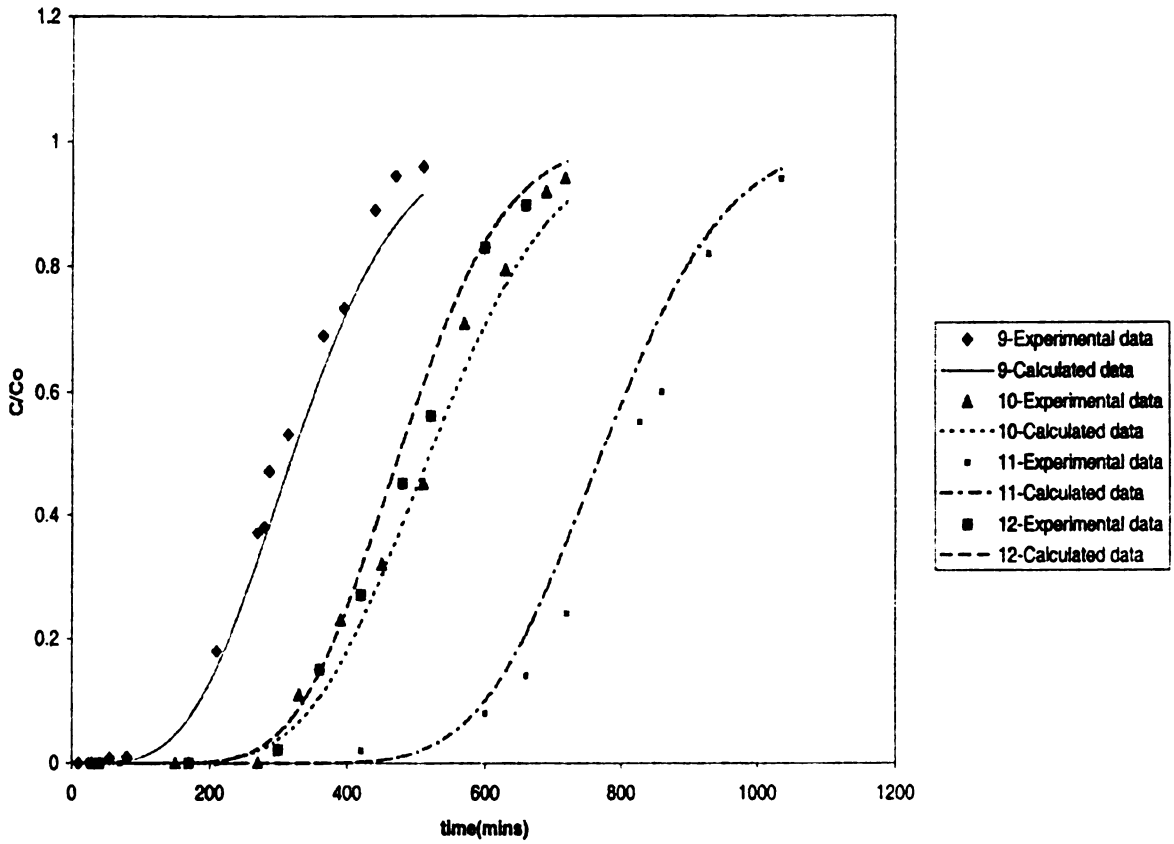

Figure 2.17 Benzoic Acid Breakthrough Behavior using Linear Adsorption Isotherm.

It can be realized from equation 2.22 that the value of $\bar{J}(\zeta,\tau)$ becomes 0.5 when $\zeta = \tau$. So, the necessary condition to reach a 50 % breakthrough is that both these values are equal. Comparing equation 2.18 and equation 2.20 for these dimensionless variables, the time required for a 50 % breakthrough ($t_{0.5}$) can be given as under.

$$t_{0.5} = \frac{Z}{U_z}\left(1 + \frac{K_D \rho_b}{\varepsilon}\right) \qquad 2.23$$

Since $t_{0.5}$ is not a function of $K_f a$, the time required to reach 50 % breakthrough actually doesn't change by changing $K_f a$.

It was observed that $K_f a$ decides the slope of the breakthrough sigmoid curve while the value of K_D decides the time at which the breakthrough occurs. Increasing the value of K_D increases the time interval at which the breakthrough occurs. While, lowering its value shortens the time period when the breakthrough occurs. The other parameter $K_f a$ doesn't have any hold on the time frame but just determines the slope. As the value decreases, the slope of the sigmoid curve gets closer to 0 while increasing the value makes it closer to vertical line. And, hence decides the time required for running from a 20 percent breakthrough to a 80 percent breakthrough. However, the sigmoid curve just keeps pivoting around a 50 % breakthrough time.

Since the time required for a 50 % breakthrough was obtained by experiments, the value of K_D was calculated using equation 2.23 and the value found for each fit is given in Table 2.6. The values should have been identical to those listed in Table 2.1.

Table 2-6: Comparision of K_D from Fitting Equilibrium Adsorption Data and Fitting Breakthrough Behavior Data using Hougen and Marshall Model

Compound	K_D (m^3/mol) from equilibrium data(Table 2.1)	K_D (m^3/mol) from breakthrough data
Benzaldehyde	0.095	0.18
Benzyl-alcohol	0.031	0.08
Benzoic-acid	0.095	0.16

It was found that the values aren't identical. However, the breakthrough data required K_D almost twice the value predicted from equilibrium data for all the three compounds. This might have originated from the inefficiency of the linear model to accurately predict the breakthrough behavior. The results of the breakthrough data fitted by iterating K_fa and using the value of K_D obtained from the breakthrough data are given below.

Table 2-7 Results of Data-fitting for Benzaldehyde using Hougen and Marshall Model

No	Height of bed(m)	Diameter of bed(m)	K_fa (dimensionless)	K_D(m^3/mol)
1	0.0635	0.0222	25.77	0.18
2	0.0853	0.0222	50.07	0.18
3	0.1219	0.0603	62.78	0.18
4	0.1117	0.0603	63.80	0.18

Table 2-8 Results of Data-fitting for Benzyl-Alcohol using Hougen and Marshall Model

No	Height of bed(m)	Diameter of bed(m)	K_fa (dimensionless)	K_D(m^3/mol)
5	0.0508	0.0222	17.62	0.08
6	0.0660	0.0222	17.46	0.08
7	0.0812	0.0603	13.88	0.08
8	0.0838	0.0603	20.00	0.08

Table 2-9 Results of Data-fitting for Benzoic acid using Hougen and Marshall Model

No	Height of bed(m)	Diameter of bed(m)	K_fa (dimensionless)	K_D(m^3/mol)
9	0.0508	0.0222	7.54	0.16
10	0.0808	0.0222	8.92	0.16
11	0.1219	0.0603	12.76	0.16
12	0.0750	0.0603	11.60	0.16

It was observed that while fitting the data with the Hougen and Marshall model, there was a lot of discrepancy between the experimental data and the model fit. It was observed that the value of K_fa varied a lot for benzaldehyde. The model fitted well for benzyl alcohol. This could probably be attributed to the lower value of K_D. With the value of K_fa found by iteration, the product $\zeta\tau$ was greater than 36 and reached as high as 36000. But since the value was greater than 36, the $\bar{J}(\zeta,\tau)$ function given by equation 2.22 could be used. The values of $\zeta\tau$ and the $\bar{J}(\zeta,\tau)$ function for experiment 1 mentioned in Table 2.6 are given in Table 2.10.

Table 2-10 Values of $\zeta\tau$ and $\bar{J}(\zeta,\tau)$ Function for Experiment 1 for Single Component Adsorption

Time(min)	$\zeta\tau$	$\bar{J}(\zeta,\tau)$
6	37.44	0.00
30	331.30	0.00
60	504.16	0.00
90	763.45	0.00
120	1022.74	0.00
150	1282.08	0.00
270	2319.17	0.00
390	3356.32	0.17
450	3874.90	0.43
510	4393.47	0.70
630	5344.19	0.95

It can be realized from the table that the product $\zeta\tau$ becomes greater than 36 in the first 6 minutes.The term follows the same pattern for all the other experiments. However, all the fits predicted a higher concentration in the outlet stream towards the end of the run.

2.3.1.2 Prediction of Breakthrough Curves using Langmuir Adsorption Isotherms.

The solution given by Thomas (1944) stands out to be most widely cited and used among all the analytical solutions available for fixed bed adsorption. The solution was originally developed to describe ion exchange in fixed beds in which the exchange process is described by reversible second-order kinetics. He developed the solution assuming surface kinetics as the rate-limiting step. However, Hiester and Vermeulen (1952) showed that the solution could be used for cases in which rate controlling steps other than surface kinetics applied. For this model, the Langmuir isotherm describes equilibrium between the fluid and solid phase. The kinetic derivation for adsorption described by this model can be derived by making a mass balance of the adsorbate.

$$\frac{\partial q_A}{\partial t} = k_a\left[C_A\left(\frac{a}{b} - q_A\right) - \frac{1}{b}q_A\right] \qquad 2.24$$

where, q_A=Equilibrium uptake of adsorbate on the adsorbent, g adsorbed/g resin.

t= time, minutes.

C_A= Concentration of adsorbate in the fluid phase, mol/m^3

k_a= Adsorption rate constant, m^3/mol

a,b=Langmuir constants, m^3/mol

Saturation capacity of the bed (q_A^{∞}) corresponding to concentration C_{A0} of the adsorbate in the influent can be given by

$$q_A^{\infty} = \frac{aC_{A0}}{1 + bC_{A0}} \qquad 2.25$$

where,

C_{A0}= Concentration of adsorbate in the influent fluid phase mol/ m^3

Dividing equation 2.24 by equation 2.25 ,

$$\frac{\partial(q_A / q_A^{\alpha})}{\partial t} = k_a\left(\frac{1+bC_{A0}}{aC_{A0}}\right)\left[C_A\left(\frac{a}{b}-q_A\right)-\frac{1}{b}q_A\right] \qquad 2.26$$

Introducing dimensionless variables $\bar{Q}$, $\overline{X}$, r^* and Δ_a into equation 2.26

$$\frac{\partial \bar{Q}}{\partial t} = \Delta_a\left[\bar{X}(1-\bar{Q})-r^*\bar{Q}\left(1-\bar{X}\right)\right] \qquad 2.27$$

where,

$$\bar{Q} = q_A / q_A^{\alpha} \qquad 2.28$$

$$\Delta_a = k_a.\frac{1+bC_{A0}}{b} \qquad 2.29$$

$$\overline{X} = \frac{C_A}{C_{A0}} \qquad 2.30$$

$$r^* = \frac{1}{1+bC_{A0}} \qquad 2.31$$

Introducing dimensionless time parameter and dimensionless bed length parameter into equation 2.27,

$$\frac{\partial \bar{Q}}{\partial \tau} = \left[\bar{X}(1-\bar{Q}) - r^{*}\bar{Q}\left(1-\bar{X}\right) \right] \qquad 2.32$$

$$\zeta = \frac{Z(1-\varepsilon)q_A'''\Delta_a}{U_z C_{A0}\varepsilon} \qquad 2.33$$

$$\tau = \Delta_a\left(t - \frac{Z}{U_Z}\right) \qquad 2.34$$

Where,

Z= Bed Height in m.

ε= Void Fraction ratio for the SP-850 resin.

U_Z= Interstitial Velocity in m/min.

Hiester and Vermeulen expressed Thomas' results in terms of $\bar{J}$ Function. The $\bar{J}$ function is defined as shown in equation 2. 20. The dimensionless concentration parameter is expressed in terms of $\bar{J}$ function as below

$$\bar{X} = \frac{\bar{J}(\tau, r^{*}\zeta)}{\bar{J}(\tau, r^{*}\zeta) + \left[1 - \bar{J}(\tau, r^{*}\zeta)\exp[(r^{*}-1)(\tau-\zeta)]\right]} \qquad 2.35$$

It can be observed that for $r^{*} = 1$, the Thomas model and Hougen and Marshall soltuions are the same. r^{*} can be 1 only when b is equal to zero. And with b=0, the Langmuir model is same as the Linear model. The same experimental data tabulated in Table 2.5 was analyzed using the Thomas model. The experimental data was entered in a Microsoft® Excel sheet along with the equations and was fitted by iterating the parameter k_a. Results are shown in Figures 2.18-2.20.

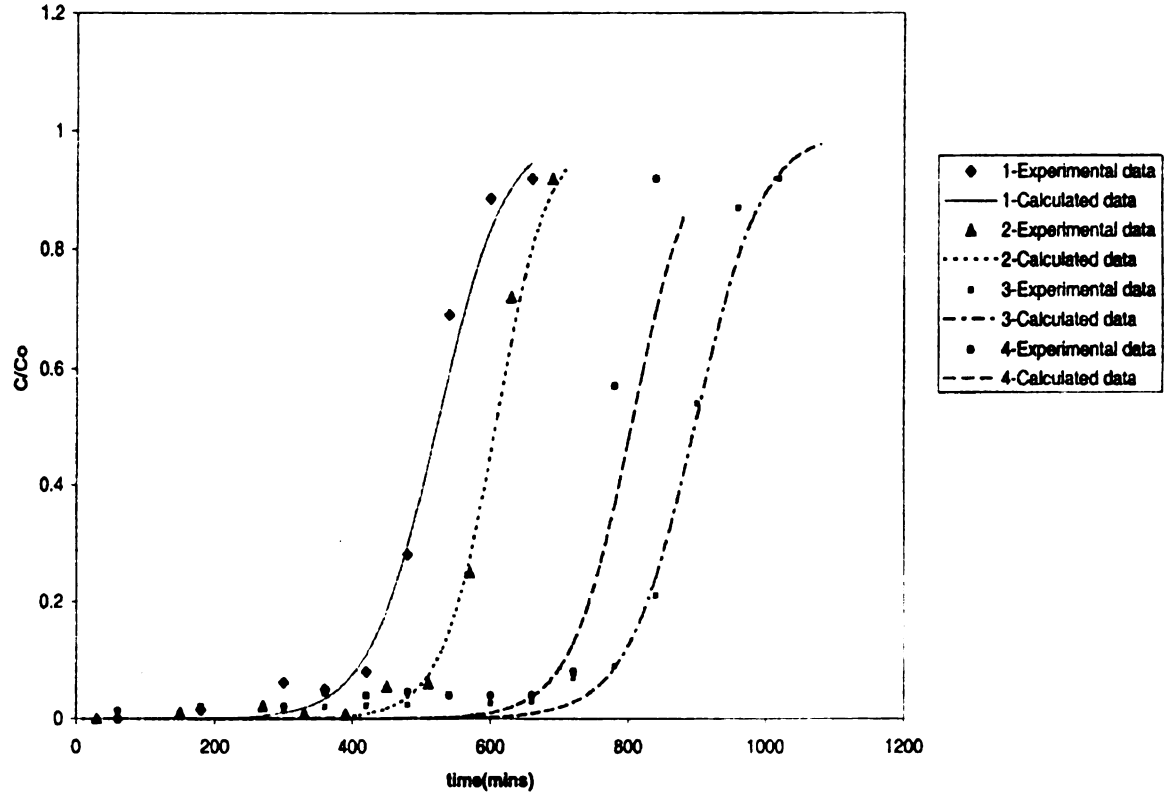

Figure 2.18 Benzaldehyde Breakthrough Behavior using Langmuir Adsorption Isotherm.

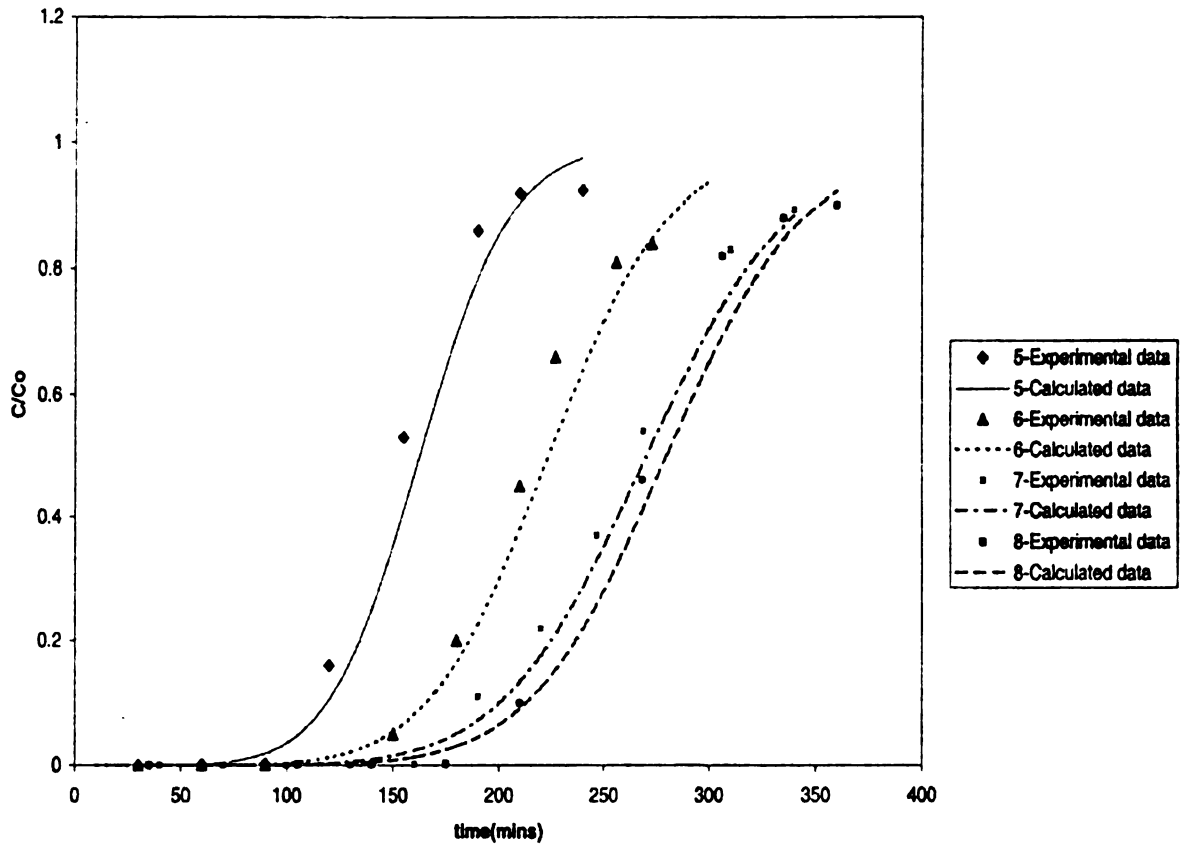

Figure 2.19 Benzyl Alcohol Breakthrough Behavior using Langmuir Adsorption Isotherm.

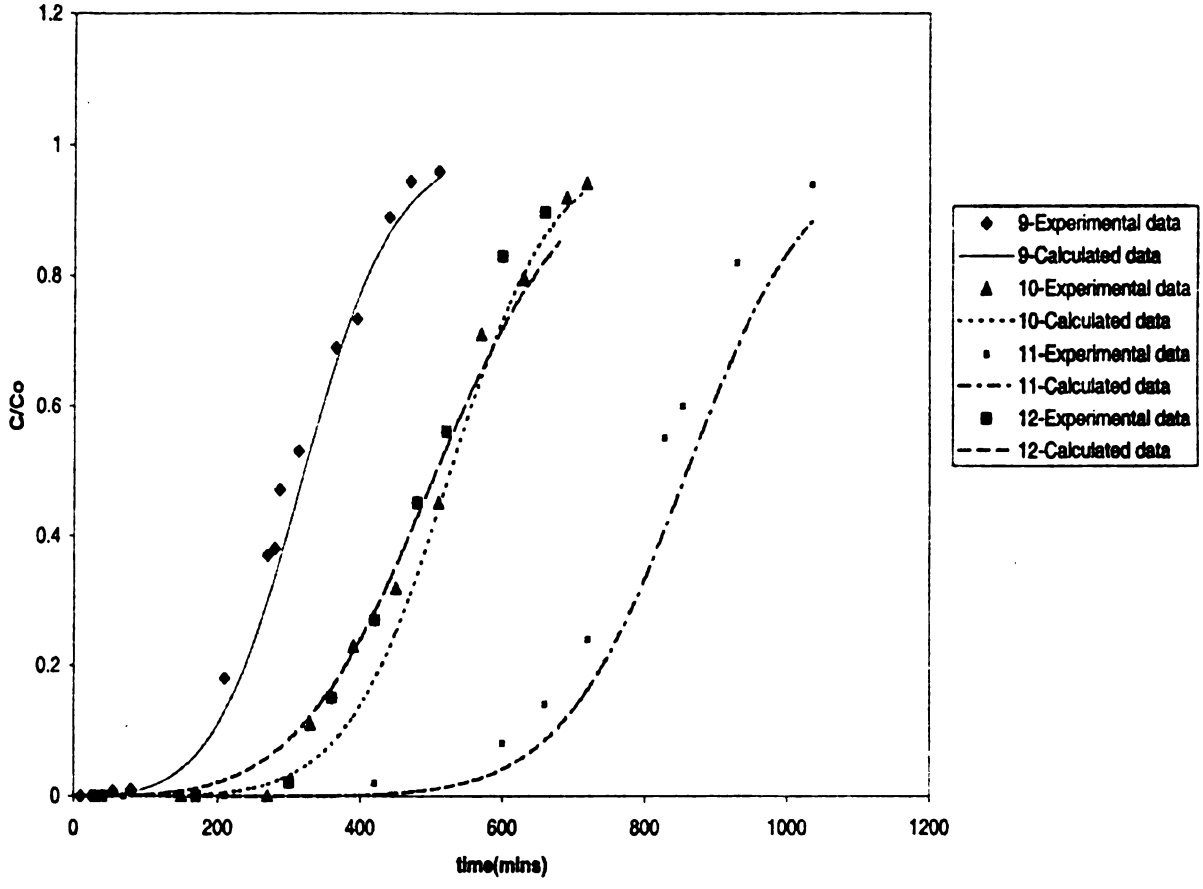

Figure 2.20 Benzoic Acid Breakthrough Behavior using Langmuir Adsorption Isotherm.

Results of fitting the experimental data with the behavior predicted by Thomas model are given in Tables 2.11, 2.12 and 2.13

Table 2-11 Results of Data-fitting for Benzaldehyde using Thomas Model

No.	Height of bed(m)	Diameter of bed(m)	$k_a(m^3/mol)$,
1	0.0635	0.0222	0.014
2	0.0853	0.0222	0.014
3	0.1219	0.0603	0.012
4	0.1117	0.0603	0.013

Table 2-12 Results of Data-fitting for Benzyl-Alcohol using Thomas Model

No.	Height of bed(m)	Diameter of bed(m)	$k_a(m^3/mol)$
5	0.0508	0.0222	0.027
6	0.0660	0.0222	0.024
7	0.0838	0.0603	0.020
8	0.0812	0.0603	0.022

Table 2-13 Results of Data-fitting for Benzoic acid using Thomas Model

No.	Height of bed(m)	Diameter of bed(m)	$k_a(m^3/mol)$
9	0.0508	0.0222	0.022
10	0.0808	0.0222	0.022
11	0.1219	0.0603	0.025
12	0.0750	0.0603	0.017

The value of the adsorption rate constant (k_a) found by iteration was almost constant in all the four experiments for benzaldehyde and benzyl alcohol. There was a little discrepancy in the iterated results of benzoic acid. This could have resulted from the inaccurate means of quantification used for benzoic acid. The adsorption rate constant is a function of temperature and it is inversely proportional to the molecular weight of the

compound. Hence the adsorption rate constant for benzaldehyde, benzyl alcohol and benzoic acid were expected in a descending order. However, the value of k_a found for benzaldehyde was a little lower than benzyl alcohol. Comparing Figures 2.18, 2.19 and 2.20 to 2.15, 2.16 and 2.17 respectively, it can be realised that the Thomas model could account for the sigmoidal curve better than the Hougen and Marshall model. Effort was made to find a constant value of k_a for each compound, which would be successful in predicting the breakthrough behavior for all the breakthrough experiments done with that compound. By observing the model predictions with different values of k_a within the range given in Table 2.12, 21.3 and 2.14, it was found that the best overall value of k_a for benzaldehyde, benzyl alcohol and benzoic acid were 0.013 m^3/mol, 0.022 m^3/mol and 0.022 m^3/mol respectively. Figures 2.21, 2.22 and 2.23 illustrate the behavior predicted by Thomas model with the best overall value of k_a for the three compounds.

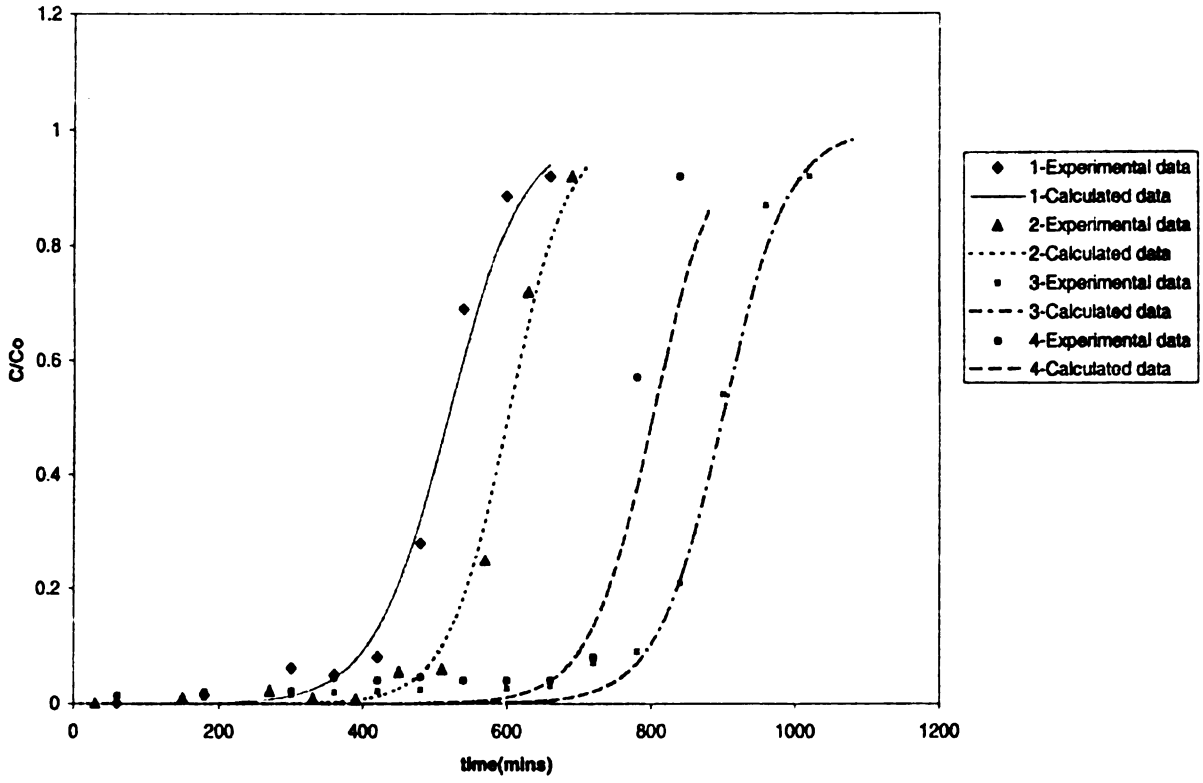

Figure 2.21 Benzaldehyde Breakthrough Behavior using Langmuir Adsorption Isotherm and Constant ka.

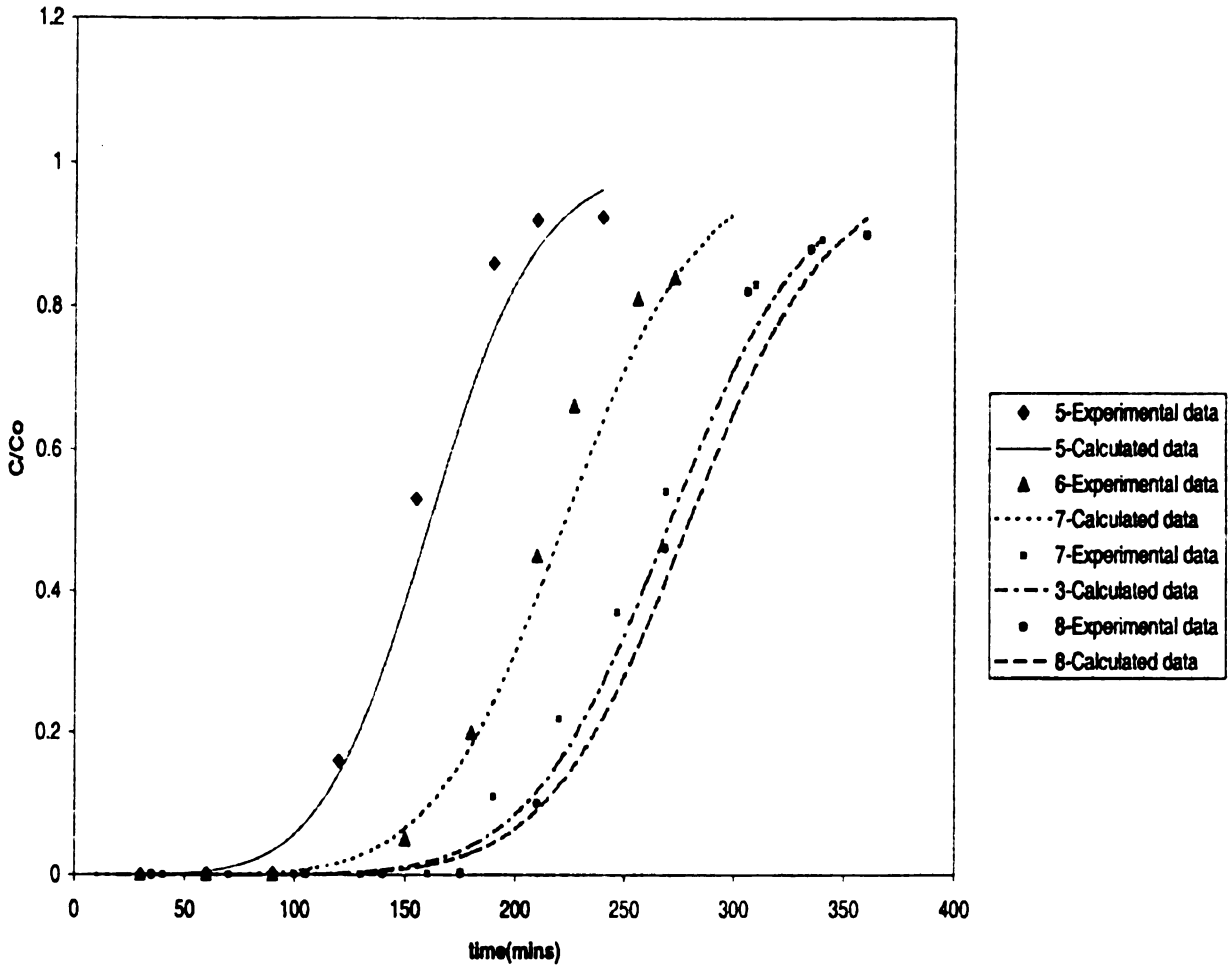

Figure 2.22 Benzyl Alcohol Breakthrough Behavior using Langmuir Adsorption Isotherm and Constant ka.

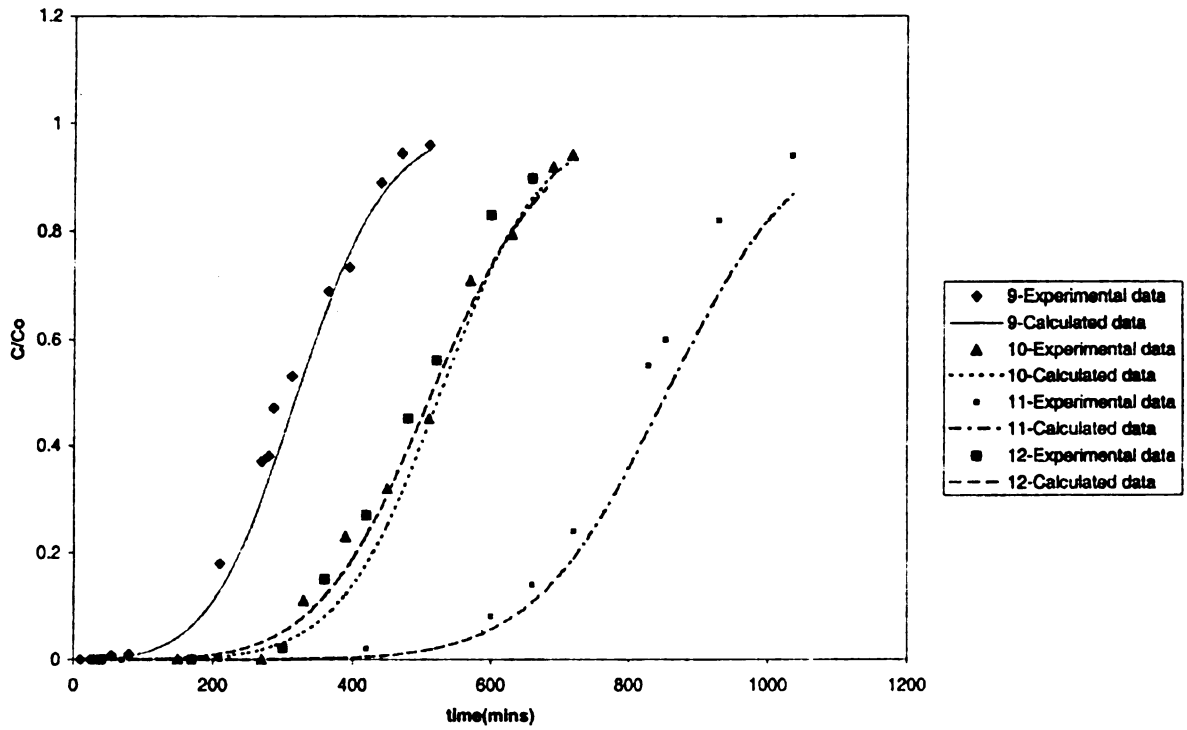

Figure 2.23 Benzoic Acid Breakthrough Behavior using Langmuir Adsorption Isotherm using Constant ka.

2.4 Multicomponent Adsorption

Adsorption exists because of a naturally occurring attractive force between the molecules on the surface of the adsorbent and those in the adsorbate phase. Multicomponent adsorption is when each adsorbate molecule competes for and occupies several sites, whilst interacting with each other. For optimal process design, accurate adsorption equilibria data for both single and multicomponent systems are required. Although adsorption isotherm data for pure components are relatively easy to measure, multicomponent equilibrium data is generally obtained by numerous, elaborate experiments for the adsorbate, adsorbent and temperature range of concern. Eliminating the reliance on multicomponent experimental data seems to be an excellent method for economic feasibility for most process industries. This has fuelled a maturing interest in possibility of efficient analytical models, able to predict multicomponent adsorption equilibria. Of the various theories which have been proposed to describe the physical adsorption properties of gases and vapours on solids, the Ideal Adsorbed Solution Theory, developed by Myers and Prausnitz in 1965, appears to be the most successful.

Myers and Prausnitz(1965) proposed the ideal adsorbed solution (IAS) theory for the adsorption of gas mixtures. The theory was subsequently extended to multicomponent liquid phase adsorption by Radke and Prausnitz(1972). The IAS theory for gas mixtures is based on the assumption that the various fundamental thermodynamic equations of liquid are applicable to the adsorbed phase and that the solution in the adsorbed phase is ideal, such that Raoult's law is valid. Hence, applying the criterion of equilibrium between the gas and adsorbed phase gives the following relation

$$Py_i = p_i^0(\pi_i, T)x_{i,} \qquad i=1,2,\ldots\ldots,N \qquad 2.36$$

where

P=Total pressure of the gas phase.

$x_{i,}$ =Mole fraction of the ith adsorbate in the adsorbed phase

$y_{i,}$ =Mole fraction of the ith adsorbate in the gas phase.

p_i^0 =Hypothetical pressure of the ith adsorbate in its pure component adsorption that yields a spreading pressure π

π_i =Spreading pressure equal to that of the multicomponent adsorption case($\pi_i = \pi_j = \pi$)

The spreading pressure can be given by Gibbs adsorption isotherm as under

$$\pi_i = \frac{RT}{A}\left(\int_0^{p_i^0} \frac{q_i^0}{p_i^0} dp_i^0\right) \qquad 2.37$$

where 0= Pure component adsorption state

q_i^0 =Equilibrium adsorbed phase concentration in the pure component adsorption of the ith adsorbate.

The total adsorbed phase concentration can be calculated by

$$q_t = \left[\sum_{j=1}^{N} \frac{x_j}{q_j^0}\right]^{-1} \qquad 2.38$$

The amount of adsorption of the ith adsorbate is given as

$$q_i = q_t x_i \qquad 2.39$$

Equations 2.36 , 2.37, 2.38 and 2.39 constitute the system of equations describing the multicomponent adsorption equilibrium between the gas phase and the adsorbed phase. The theory extended by Radke and Prausnitz for multicomponent liquid phase adsorption revolves around the same system of equations. The system constitutes equation 2.38, 2.39 and equations 2.36 and 2.37 with the pressure term replaced by concentration giving

$$c_i = c_i^0(\pi_i, T)x_i \qquad 2.40$$

$$\pi_i = \frac{RT}{A}\left(\int_0^{c_i^0} \frac{q_i^0}{c_i^0} dc_i^0\right) \qquad 2.41$$

Intrapellet Mass Transfer.

The linear driving force model for intrapellet mass transfer is based on the postulate that the uptake rate of adsorbate by a pellet is linearly proportional to a driving force, defined as the difference between the surface concentration and the average adsorbed-phase concentration.

$$\frac{d\bar{q}}{dt} = \frac{15D_e}{a_P^2}\left(q_s - \bar{q}\right) \qquad 2.42$$

where,

$\bar{q}$ =Average adsorbed phase concentration at the exterior surface of the pellet, mol adsorbate/kg resin.

q_s =Adsorbed phase concentration of the pellet, mol adsorbate/kg resin.

D_e =Effective intrapellet diffusivity, m^2/sec.

a_P =Particle radius, m.(4.25E-4, from product literature, Mitsubishi Chemicals)

Interphase Mass Transfer

The transport of the adsorbate species from the bulk of the fluid phase to the external surface of adsorbent pellets is given by the following equation.

$$\frac{d\bar{q}}{dt} = \frac{3k_f}{a_p \rho_p}\left(c_b - c_s\right) \qquad 2.43$$

where,

c_b=Adsorbate concentration in the bulk of fluid, mol/m^3.

c_s = Adsorbate concentration at the fluid-pellet interface, mol/m^3.

ρ_p=Pellet density, kg/ m^3.

k_f =Interphase mass transfer coefficient, m/sec.

Experiments were done to study multicomponent adsorption. A solution of benzaldehyde, benzyl alcohol and benzoic acid was passed through a fixed bed of SP-850 resin. The procedure observed in doing these experiments and the raw data is given in the appendix. A FORTRAN code by Moon (1987) was used to predict the multicomponent breakthrough behavior, which could accept the equilibrium behavior represented in terms of the piecewise Freundlich equation. However, the one-piece Freundlich equation as given by Equation 2.9 was used for all the analysis, while the values for Freundlich constants were taken from Table 2.3. These values predicted a very high adsorbate capacity. Hence, the equilibrium adsorption data for the concentration range of interest was fitted to get the Freudlich constants. The experimental and the predicted results are shown in Figures 2.24 and 2.25 respectively, while the Freudlich constants and the concentration range of interest are tabulated in Table 2.14.

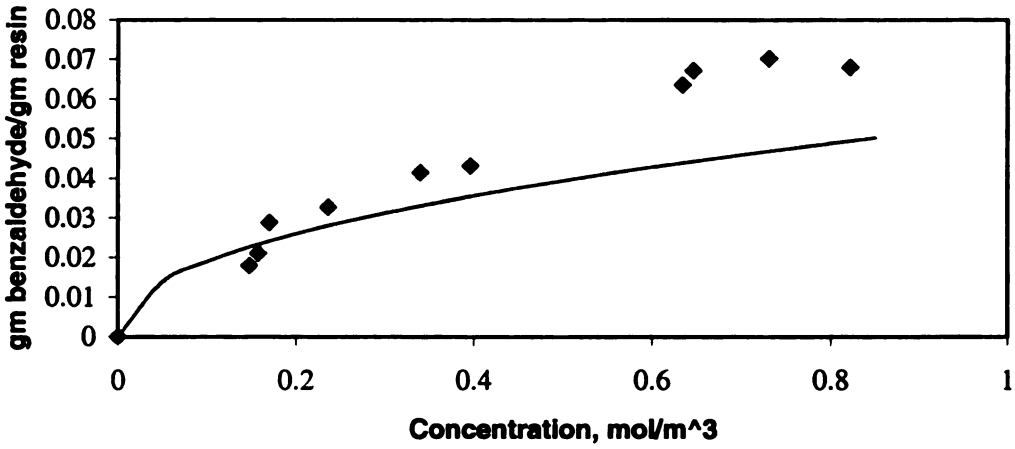

Figure 2.24 Prediction of Equilibrium Adsorption Data of Benzaldehyde by Freundlich Model for 0-0.9 mol/m^3 Concentration Range

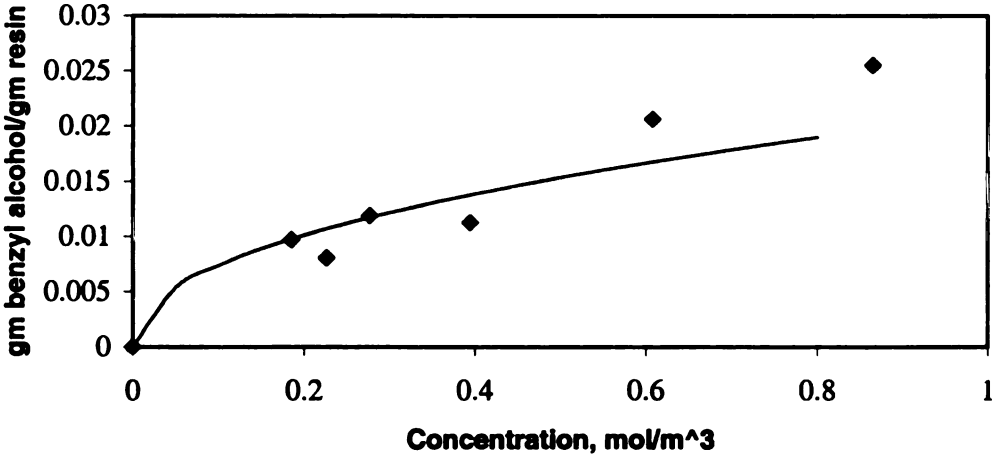

Figure 2.25 Prediction of Equilibrium Adsorption Data of Benzyl Alcohol by Freundlich Model for 0-0.5 mol/m^3 Concentration Range

Table 2.14 Summary of Freudlich Parameters used for Multicomponent Adsorption

Compound	Concentration Range, mol/m^3	K((m^3/mol)^n)	n(unitless)
Benzaldehyde	0-0.90	0.054	2.43
Benzyl Alcohol	0-0.50	0.021	2.20

In this program, the linear driving force approximation is used and the dispersion effect is neglected. The multicomponent adsorption equilibrium is assumed to obey the IAS theory. Adsorption equilibrium is assumed at the fluid-pellet interface as a result of the fact that surface diffusion is the rate controlling mechanism in intrapellet mass transfer. The governing equations for this program are obtained by extending equation 2.14 for N adsorbates and by equating equation 2.42 and 2.43

$$\frac{U_S}{\rho_b}\left(\frac{\partial C_{bi}}{\partial Z}\right)_t = \left(\frac{\partial \overline{q_i}}{\partial t}\right)_Z \qquad 2.44$$

$$\frac{d\bar{q}}{dt} = \frac{3k_f}{a_P\rho_p}\left(c_b - c_s\right) = \frac{15D_e}{a_P^2}\left(q_s - \bar{q}\right) \qquad 2.45$$

Finite difference analysis is used to calculate the adsorbate concentration in the bulk of fluid and the average adsorbed phase concentration at the exterior surface of the pellet, corresponding to a particular grid point. These values are used to find the surface concentration of the adsorbate and the adsorbed phase concentration at the surface.

Table 2.15 and 2.16 summarises the experimental conditions. The concentrations of the adsorbate in the feed are given in Table 2.15 while the other experimental variables are listed in Table 2.16

Table 2.15 Adsorbate Concentrations in Feed

No	Benzaldehyde conc in feed, mol/m^3	Benzyl alcohol conc in feed, mol/m^3	Benzoic acid conc in feed, mol/m^3
1	0.90	0.48	0.20
2	0.88	0.46	0.20
3	0.88	0.46	0.20
4	0.90	0.50	0.20
5	0.90	0.50	0.20
6	0.90	0.50	0.20
7	0.90	0.46	0.20
8	0.90	0.46	0.20
9	0.90	0.46	0.20

The concentration of benzoic acid wasn't actually measured in all the experiments. However the amount of benzoic acid added to the feed was constant in all the experiments. The concentration of benzoic acid was found by making a feed stream with the same concentration and measuring the pH. However, the concentrations of benzaldehyde and benzyl alcohol were almost constant for all the experiments. The variation in concentration was less than 3 % for benzaldehyde and 8% for benzyl alcohol.

All the experiments were done in a glass bed of 2.22 cm diameter. The experiments were carried out at room temperature.

Table 2.16 Summary of Experimental Conditions for Multicomponent Adsorption.

No	Bed height, m	Superficial velocity, m/sec	Amount of resin, ml	Flow-rate, ml/min
1	0.075	0.00042	15	10
2	0.075	0.00063	20	15
3	0.075	0.00084	25	20
4	0.106	0.00042	15	10
5	0.106	0.00063	20	15
6	0.106	0.00084	25	20
7	0.121	0.00042	15	10
8	0.121	0.00063	20	15
9	0.121	0.00084	25	20

The experimentally observed behavior and the predicted behavior by the program are given in figures 2.26 to 2.34.

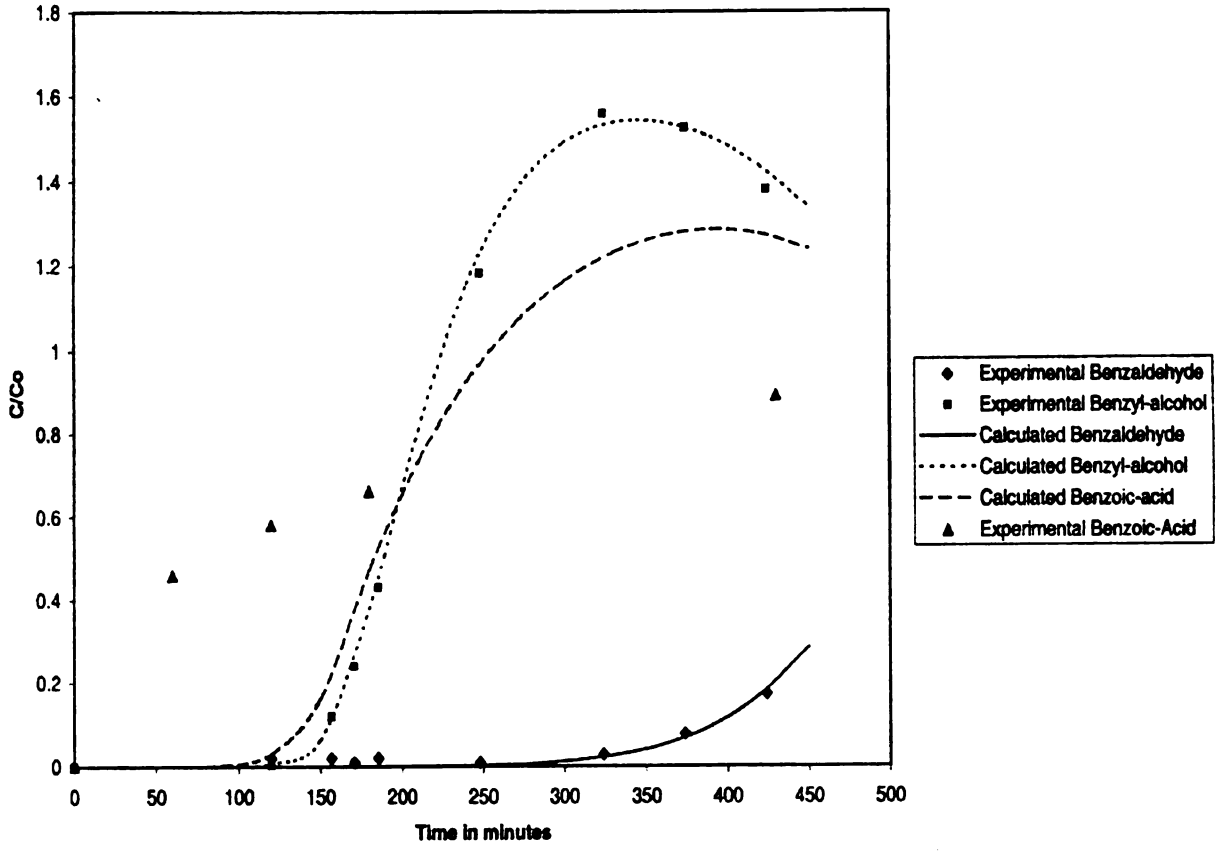

Figure 2.26 Breakthrough Behavior of Mixtures (15 ml resin at 10 ml flow rate)

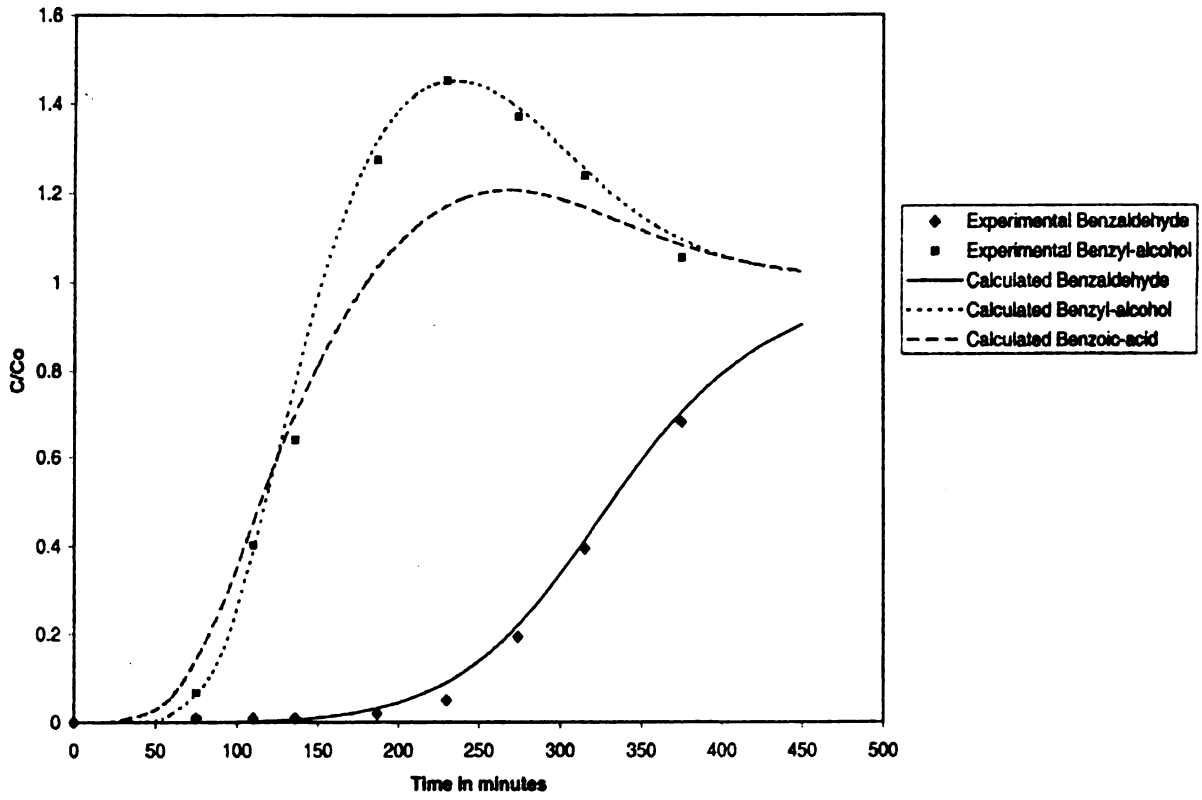

Figure 2.27 Breakthrough Behavior of Mixtures (15 ml resin at 15 ml flow rate)

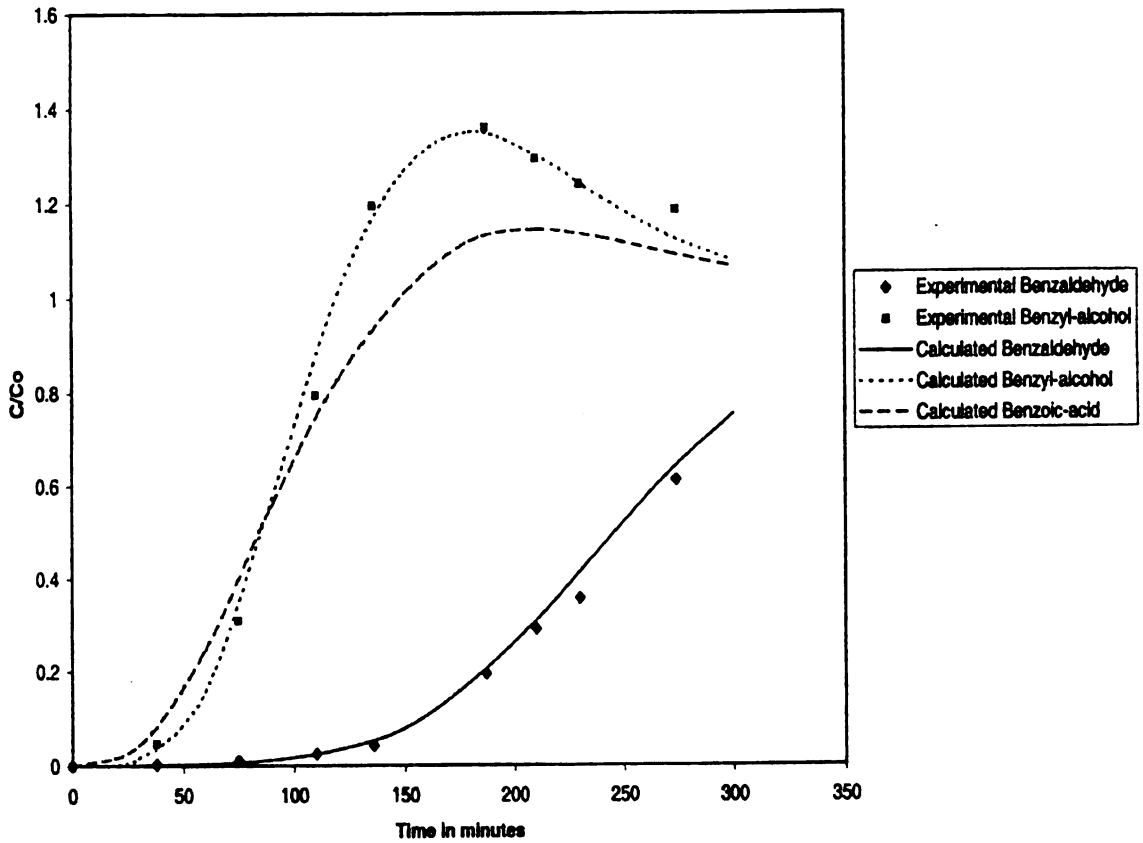

Figure 2.28 Breakthrough Behavior of Mixtures (15 ml resin at 20 ml flow rate)

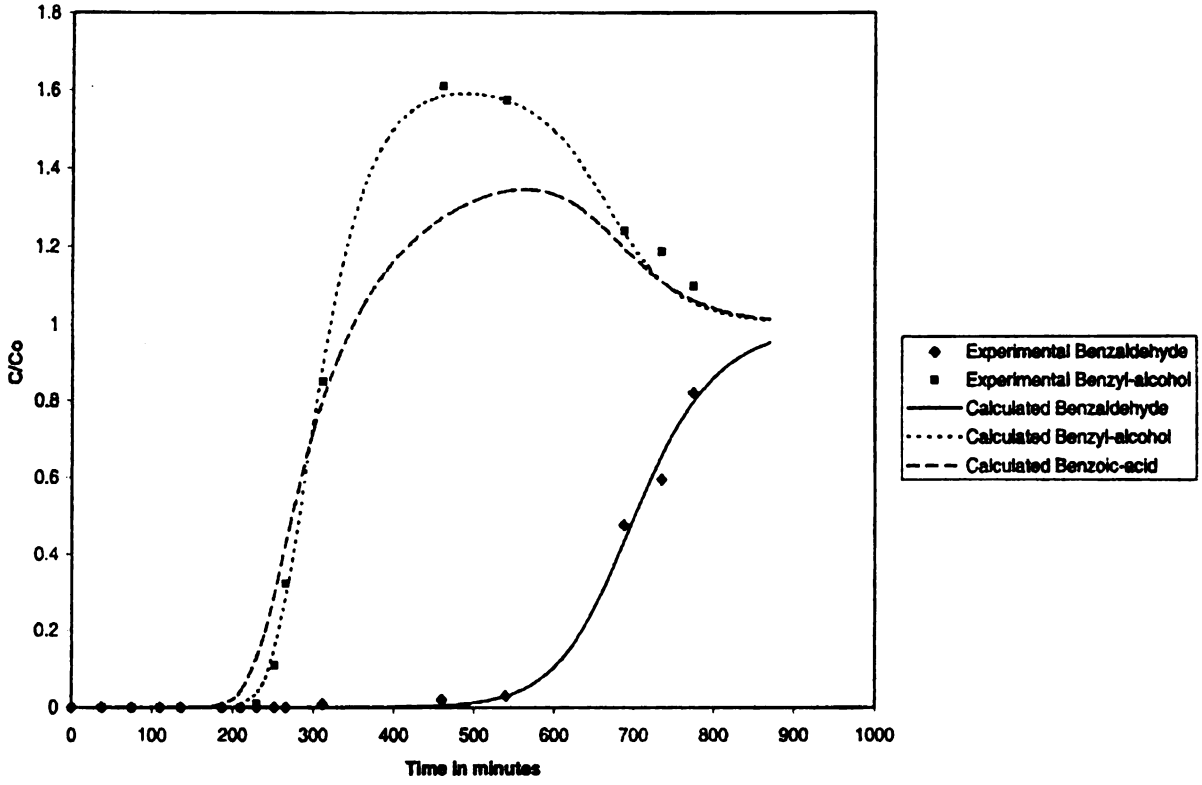

Figure 2.29 Breakthrough Behavior of Mixtures (20 ml resin at 10 ml flow rate)

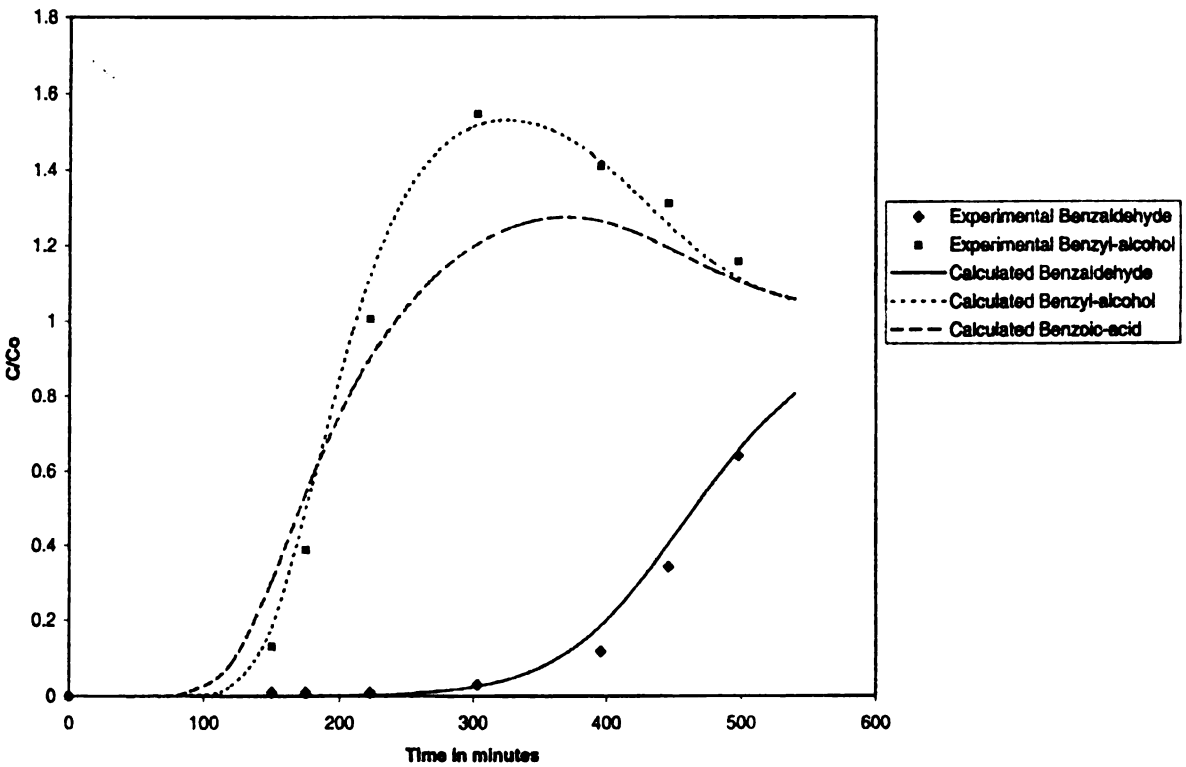

Figure 2.30 Breakthrough Behavior of Mixtures (20 ml resin at 15 ml flow rate)

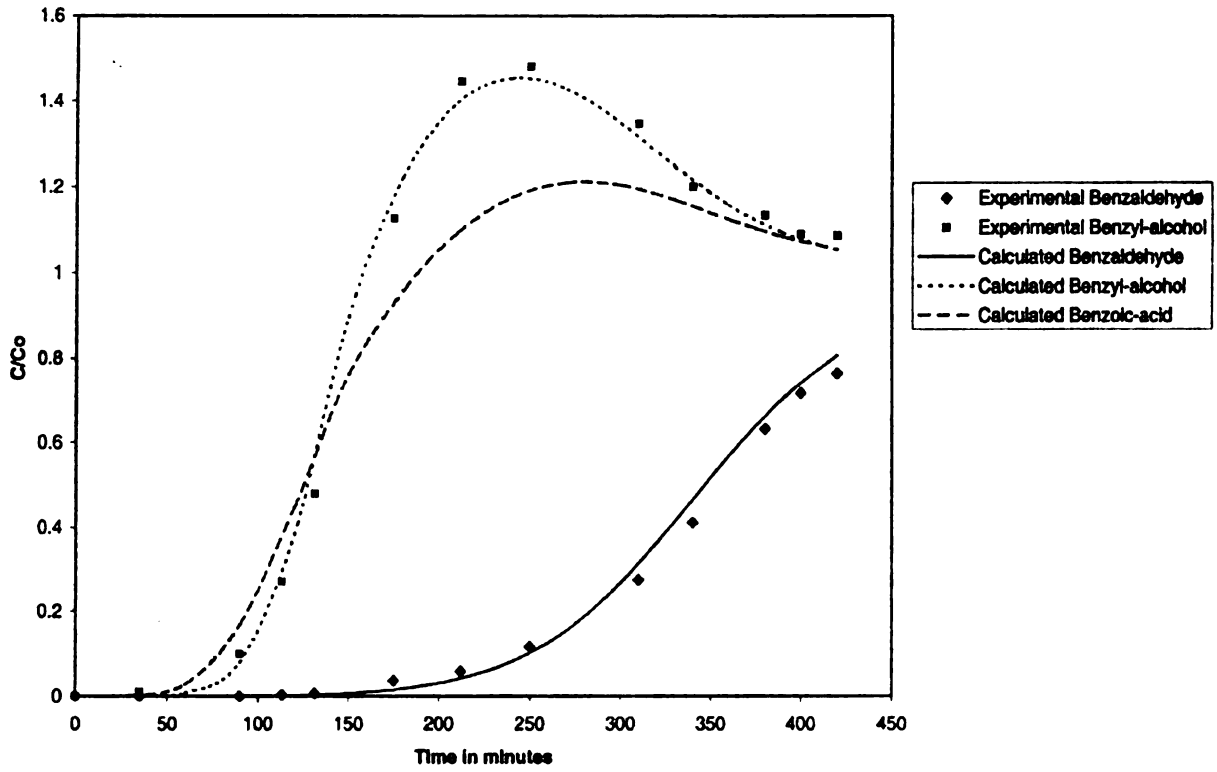

Figure 2.31 Breakthrough Behavior of Mixtures (20 ml resin at 20 ml flow rate)

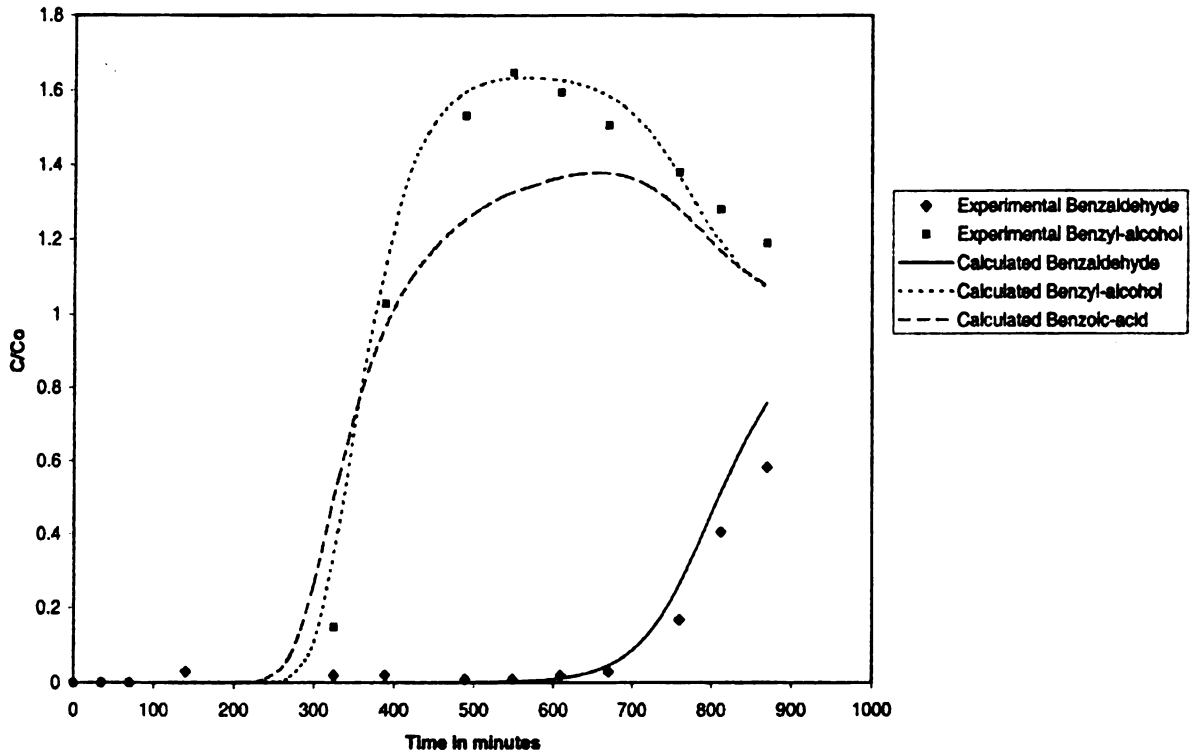

Figure 2.32 Breakthrough Behavior of Mixtures (25 ml resin at 10 ml flow rate)

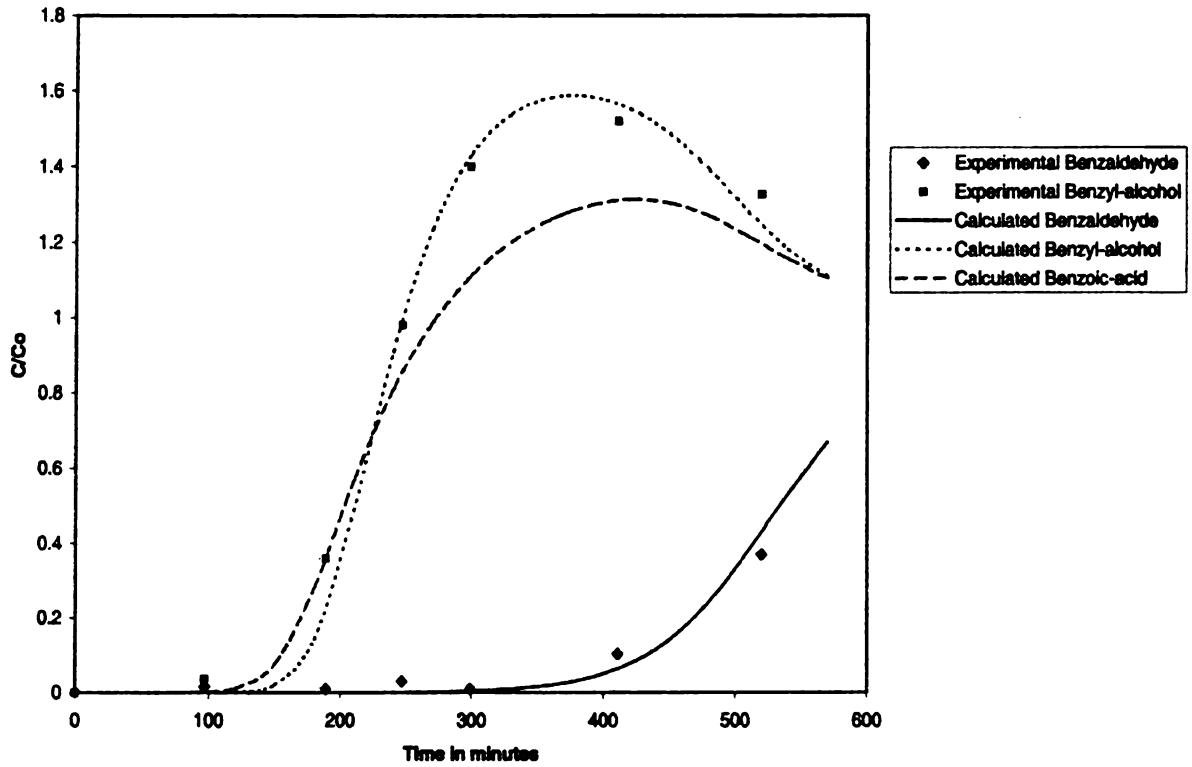

Figure 2.33 Breakthrough Behavior of Mixtures (25 ml resin at 15 ml flow rate)

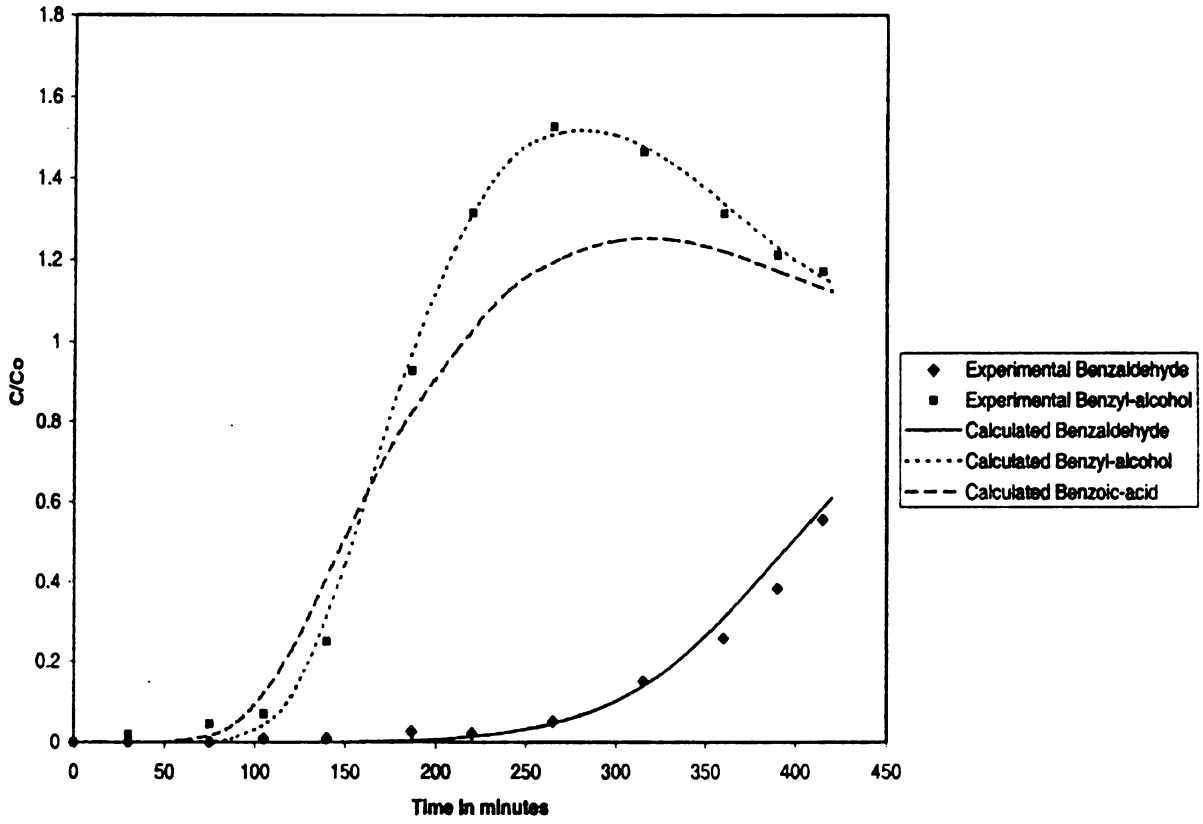

Figure 2.34 Breakthrough Behavior of Mixtures (25 ml resin at 20 ml flow rate)

The intrapellet mass transfer coefficients and the effective surface diffusivity of the three compounds were the only unknowns. Since the molecular size of benzaldehyde, benzyl alcohol and benzoic acid is quite close, the coefficients are assumed to be same for all the three compounds. The mass transfer coefficient and the surface diffusivity were not varied for different superficial velocity. Hence, the experimental data was fitted to the IAS theory predicted results by iterating the value of these two coefficients. The intrapellet mass transfer coefficient was found to be 0.2E-4 m/sec and the surface diffusivity was found to be 0.26E-11 m^2/sec. Wang and Tien(1982) studied multicomponent breakthrough behavior for a system of p-nitrophenol, p-chlorophenol and propionic acid. They found that the mass transfer coefficient and surface diffusivity were 0.17E-4 m/sec and 0.2E-11 m^2/sec for all the three compounds. Since their obtained values were of the same order of magnitude as the values obtained for our experiments, the values seemed to be realistic. However, with the same values it wasn't possible to predict the single component breakthrough behavior. The program predicted a very late breakthrough for all the experiments.

The code was successful in predicting the breakthrough behavior for benzaldehyde and benzyl alcohol. Since the gas chromatograph couldn't accurately sense the concentration of benzoic acid, it was not possible to check the correctness of the predicted behavior of benzoic acid. However, for Experiment-1, HPLC was used to check the correctness of the benzoic acid breakthrough pattern predicted by the computer program. A Waters 600 solvent delivery system equipped with a model 410 refractive index detector was used for liquid phase analysis of the experimental samples. Data from the analysis was interpreted with a Waters WIRC software program version 1.0 on a IBM

XT. The data was transferred through a Waters System Interface Module (SIM). The column used in the analysis was manufactured by Alltech Associates. The Alltima Narrow-Bore Column contained a C-18 silicon bonded phase which was 5 microns in size. The column was 250 mm long by 4.6 mm diameter and its catalog number was 88371. The column was protected with cartridge columns of the same composition. The solvent was 15 weight percent methanol, 25 weight percent ethyl acetate in water. The HPLC results didn't coincide with the results predicted by the program. The HPLC analysis showed that benzoic acid started coming out from the start of the run and the concentration of benzoic acid in the outlet didn't surpass the concentration of benzoic acid in the feed even after 7 hours. This can be attributed to the failure of the Freundlich model to predict the equilibrium adsorption behavior of benzoic acid. Since the HPLC was not used for all the other experiments, it is impractical to draw a conclusion from a single experiment.

It was observed that benzoic acid starts coming out first immediately followed by benzyl alcohol. The outlet concentration of both benzoic acid and benzyl alcohol exceeds the concentration of the feed, indicating that some other compound is displacing them. And after lapse of some more time, the concentration in the outlet for benzoic acid and benzyl alcohol get close to their concentration in the feed. Benzaldehyde is the last compound to break through. And as the concentration of benzaldehyde in the outlet equals its concentration in the inlet, there is nothing being adsorbed on the resin.

REFERENCES

Brunauer, S., Emmett, H. and Teller, E.,Amer. Chem. Soc., 60, 309-319 (1938).

Brunauer, S.P.,The Adsorption of Gases and Vapors, vol. 1, Physical Adsorption, p.97, 133, Princeton University Press, Princeton, NJ(1945).

Giles, C.H., MacEwan, T.H., Nakhwa, S.N., and Smith, D., J Chem Soc. 3973 (1960).

Giles, C.H., and Nakhwa, S.N., J. Appl. Chem. 12, 266(1960).

Hiester, N.K., and Vermeulen, T., Chem. Eng. Prog., 48, 505 (1952).

Hougen, O. A., and. Marshall, W. R., Chem. Eng. Prog., 43, 197 (1947).

Langmuir, J. Am. Chem Soc., 38, 2219,(1916); 40, 1368, (1918).

Moon, H., and Tien, C., AIChE Symposium Series 84(264), 94 (1988a).

Moon, H., and Tien, C., AIChE Symposium Series 84(264), 23 (1988b).

Radke, C.J., and Prausnitz, J.M. 1972. Thermodynamics of multi-solute adsorption from dilute liquid solutions. AIChE Journal, 184): 761-768(1972).

Polanyi, M., Z. Phys., 2, 111 (1920).

Prausnitz, J.M., and Myers, A.L., Molecular Thermodynamics of Physical Adsorption, Chem. Eng. Prog., 54, (1964). Rosen, J. B., Ind. Eng. Chem., 46, 1590 (1954

Ruthven, D.M., Principles of Adsorption and Adsorption Processes, Wiley Interscience, New York (1984).

Thomas, H. C., J. Amer. Chem. Soc., 66, 1664 (1944).

Vermeulen, T., Klein, G., and Hiester, N.K., J.H. Perry, Ed., Chemical Engineers' Handbook, McGraw Hill, New York, 1973.

Chapter 3:
PRODUCTION OF BENZALDEHYDE AND BENZYL ALCOHOL FROM CHERRY PITS.

The flavor industry uses both natural and chemically synthesized flavors. In the case of cherry flavor, the use of synthetic benzaldehyde has grown over the years as the flavor component in candies, desserts and carbonated beverages such as Cherry Coke and Dr Pepper. While from a technical point of view there may be a marginal difference, the public perception and desire is changing in favor of all natural ingredients in food and drinks. The high demand for natural cherry flavor has driven the price of bitter almond oil and naturally derived benzaldehyde. Because of the limited supply and high price of the natural product, synthetic benzaldehyde is often used as a substitute. However, the application of the less expensive artificial flavor has to be indicated, and it is suspected that this is not always done. Although artificial flavor components and natural flavor components are identical in taste quality, they can be distinguished by their ^{14}C content (Krueger, 1987). The natural form of the cherry flavor is the benzaldehyde in bitter almond oil, available in the pits of cherries, apricots, peaches, cherry laurel and plums.

Recovery of Natural Benzaldehyde is on-going research that was initially started in 1990. A Phase I USDA grant was provided for developing a process to recover benzaldehyde and benzyl alcohol from cherry pits. A Phase II grant was provided in 1999 to optimize experimental variables and improve the yield of benzaldehyde and benzyl alcohol. This work was performed in conjunction with Natura, Inc. The recovery of benzaldehyde from cherry pits involve several experimental steps. It was essential to optimize the hydrolysis conditions to get the maximum yield of benzaldehyde . Changes

to the filtration step were impending , since the earlier filtration process wasn't efficient and took a lot of time. It was essential to understand the kinetics of the adsorption process to better the yield results. Changes were also made to the process used for the regeneration of the adsorbent.

3.1 **Hydrolysis and Reaction Kinetics**

The earlier experiments were carried out using the hydrolysis conditions suggested in Aaron Soule's thesis. The pits were dried and were ground up before adding to water preheated to 50°C. A 5:1 water-to-pit mass ratio was used. The water and pits were mixed together for 1 hour and then filtered. However, due to discrepancy in the pit yields in previous work, various tests were performed analyzing optimal hydrolysis conditions as well as the chemical processes occurring during hydrolysis. Macroscopic variables such as water to pit ratio, temperature of the water and the condition of the cherry pits were studied to find the optimum condition for hydrolysis.

Research at Michigan State University showed that benzaldehyde can be recovered from cherry kernel by hydrolysis (Grethlein et al, 1990) or mechanical crushing. Mechanical crushing releases oil containing a lot of triglyceride and some benzaldehyde. The pits are expected to contain quanitities of amygdalin and mandelonitrile (Li et al., 1992; Zheng and Poulton, 1995), which break down in water producing cyanide and benzaldehyde. The chemical structures of benzaldehyde, mandelonitrile, and amygdalin are shown in Figure 3.1. Soule's work shows that mandelonitrile and amygdalin breaks down in water to produce benzaldehyde, but doesn't affect the concentration of benzyl alochol.

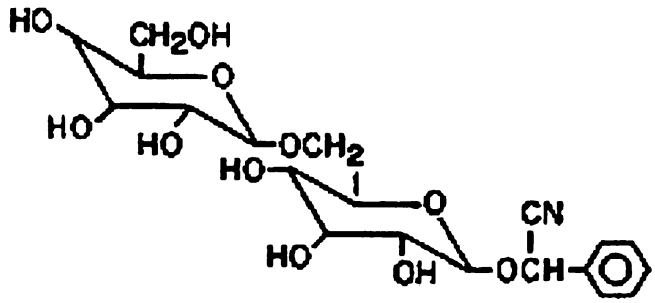

Amygdalin

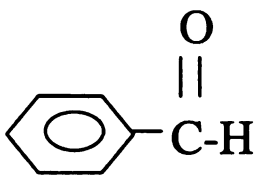

Benzaldehyde

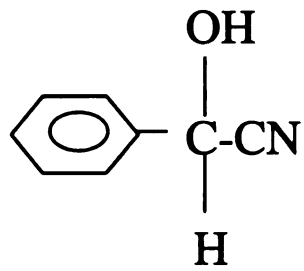

Mandelonitrile

Figure 3-1. Chemical Structures of Benzaldehyde, Mandelonitrile and Amygdalin.

Experiments were done to study the optimum hydrolysis temperature. 250 ml of water was heated to a particular temperature in a three necks, angled standard wall 500 ml glass flask and 50 gms of air-dry ground cherry pits were added and allowed to hydrolyze for an hour. The concentrations of benzaldehyde and benzyl-alcohol in the hydrolyzate were analyzed by running the sample on the gas shromatograph. The peak at 3.09 corresponds to benzaldehyde while the one at 4.62 corresponds to benzyl-alcohol. The retention time depends on the type of column used in the gas chromatograph. Currently, we are using the EC-Wax column. Specifications of the column are given in

Appendix B. With the earlier column, benzaldehyde and benzyl alcohol used to appear at 2.67 and 4.02 respectively. The response factor also changed with the change of column. The current response factors are 73.97E-6 µl/area count and 53.91E-6 µl/area count for benzaldehyde and benzyl-alcohol respectively. The response factors were calculated by running sample of known concentrations and observing their peak area. The details of the experiments are given in Appendix B. The results of hydrolysis carried out at different temperatures are tabulated below.

Table 3-1: Hydrolyzate composition for different temperatures

Retention Time (min.)	Peak Area	Parts Per Million
Hydrolysis at 45 C		
3.09 (benzaldehyde)	1.32	97.64
4.62 (benzyl alcohol)	0.39	21.02
Hydrolysis at 50 C		
3.09 (benzaldehyde)	1.43	105.77
4.62 (benzyl alcohol)	0.41	22.10
Hydrolysis at 55 C		
3.09 (benzaldehyde)	1.60	118.35
4.62 (benzyl alcohol)	0.42	23.04
Hydrolysis at 60 C		
3.09 (benzaldehyde)	1.59	117.61
4.62 (benzyl alcohol)	0.43	23.181
Hydrolysis at 65 C		
3.09 (benzaldehyde)	1.54	113.71
4.62 (benzyl alcohol)	0.43	23.181

Since all the pits were taken from the same bucket, the change in composition can be attributed to the temperature of hydrolysis. It was observed that the concentration of benzaldehyde in the hydrolyzate was higher for hydrolysis carried out at 55 C than one carried out at 45 C or 50 C temperature. Concentration of benzaldehyde and benzyl alcohol was same for 55 C and 60 C. However, the concentration of benzaldehyde was marginally less for hydrolysis carried out at 65 C. The higher temperature might be inciting some side reaction, but, since the difference is so small, it is impractical to draw

such conclusions. It was observed that the benzaldehyde concentration of hydrolyzate from different pit buckets varied a little. But for all the subsequent experiments, the hydrolysis was done at 55 C.

Experiments were also conducted to optimize the water to pit ratio for hydrolysis. A particular amount of water was heated to 55 C and then 25 gms of cherry pits were added for hydrolysis. The following are the results of hydrolysis done with different water to pit ratio. Yield is given as the total amount of benzaldehyde or benzyl alcohol recovered from the cherry pits.

Table 3-2: Hydrolyzate composition for different water- dry pit ratio

Retention Time (min.)	Peak Area	Parts Per Million	Amount of hydrolyzate (ml)	Yield, ml
Water:Pit 3:1				
3.09 (benzaldehyde)	1.89	139.80	58ml(75ml water used)	8.10E-3
4.62 (benzyl alcohol)	0.49	26.41	58ml(75ml water used)	1.53 E-3
Water:Pit 5:1				
3.09 (benzaldehyde)	1.60	118.35	103ml(125ml water used)	12.19 E-3
4.62 (benzyl alcohol)	0.42	22.64	103ml(125ml water used)	2.33E-3
Water:Pit 7:1				
3.09 (benzaldehyde)	1.42	105.03	152ml(175ml water used)	15.96E-3
4.62 (benzyl alcohol)	0.33	17.79	152ml(175ml water used)	2.70E-3
Water:Pit 8:1				
3.09 (benzaldehyde)	1.36	100.59	176ml(200ml water used)	17.70E-3
4.62 (benzyl alcohol)	0.28	15.09	176ml(200ml water used)	26.55E-3
Water:Pit 10:1				
3.09 (benzaldehyde)	0.954	70.56	225ml(250ml water used)	15.87E-3
4.62 (benzyl alcohol)	0.20	10.78	225ml(250ml water used)	2.42E-3

The total hydrolyzate obtained after hydrolysis is always found to be close to the total amount of water added minus the amount of cherry pits added to it. This loss of hydrolyzate is due to the water lost with the wet cherry pits after the hydrolysis. This trend is also observed in bigger runs. Only 20 L of hydrolyzate was generally collected in a bigger run with 25 L of water and 5 kgs of cherry pits. Although the ppm concentration

of benzaldehyde and benzyl alcohol is higher for 7:1 ratio than 8:1 ratio, the yield obtained from 8:1 ratio is higher than a 7:1 ratio. Earlier, a ratio of 5:1 was used, because it reduced the amount of hydrolyzate to be processed.

Experiments were performed with wet cherry pits instead of air dry cherry pits. The same procedure was followed to analyze the effect on the hydrolyzate composition. The observations are as under

Table 3-3: Hydrolyzate composition for different water- wet pit ratio

Retention Time (min.)	Peak Area	Parts Per Million	Amount of hydrolyzate, ml	Yield, ml
Water:Pit 3:1				
3.09 (benzaldehyde)	1.68	124.92	74ml(75ml water used)	9.24E-3
4.62 (benzyl alcohol)	0.34	18.32	74ml(75ml water used)	1.35E-3
Water:Pit 5:1				
3.09 (benzaldehyde)	1.43	105.77	123ml(125ml water used)	13.00E-3
4.62 (benzyl alcohol)	0.29	15.64	123ml(125ml water used)	1.93E-3
Water:Pit 7:1				
3.09 (benzaldehyde)	1.32	97.64	172ml(175ml water used)	16.79E-3
4.62 (benzyl alcohol)	0.27	14.55	172ml(175ml water used)	2.50E-3
Water:Pit 8:1				
3.09 (benzaldehyde)	1.27	93.94	197ml(200ml water used)	18.50E-3
4.62 (benzyl alcohol)	0.26	14.01	197ml(200ml water used)	2.75E-3
Water:Pit 10:1				
3.09 (benzaldehyde)	0.89	65.83	247ml(250ml water used)	16.26E-3
4.62 (benzyl alcohol)	0.19	10.24	247ml(250ml water used)	2.33E-3

It was realized that the concentrations of benzaldehyde and benzyl alcohol were lower when wet cherry pits were used instead of dry cherry pits, but the amount of hydrolyzate was higher. There was a bigger difference observed in benzaldehyde and benzyl alcohol concentration at lower water to pit ratio, with a difference of around 12 percent and 30 percent for benzaldehyde and benzyl alcohol respectively at 3:1 ratio to a difference of 6 percent and 5 percent for benzaldehyde and benzyl alcohol respectively at

10:1 ratio. But the total quantity of hydrolysate obtained using wet cherry pits was much higher than amount obtained using dry cherry pits. Since the cherry pits were already wet, the total overhead in wetting the cherry pits was minimal.

When the total amount of benzaldehyde and benzyl alcohol extracted for each ratio were plotted for wet and dry cherry pits, the results obtained are as shown in Figure 3.2.

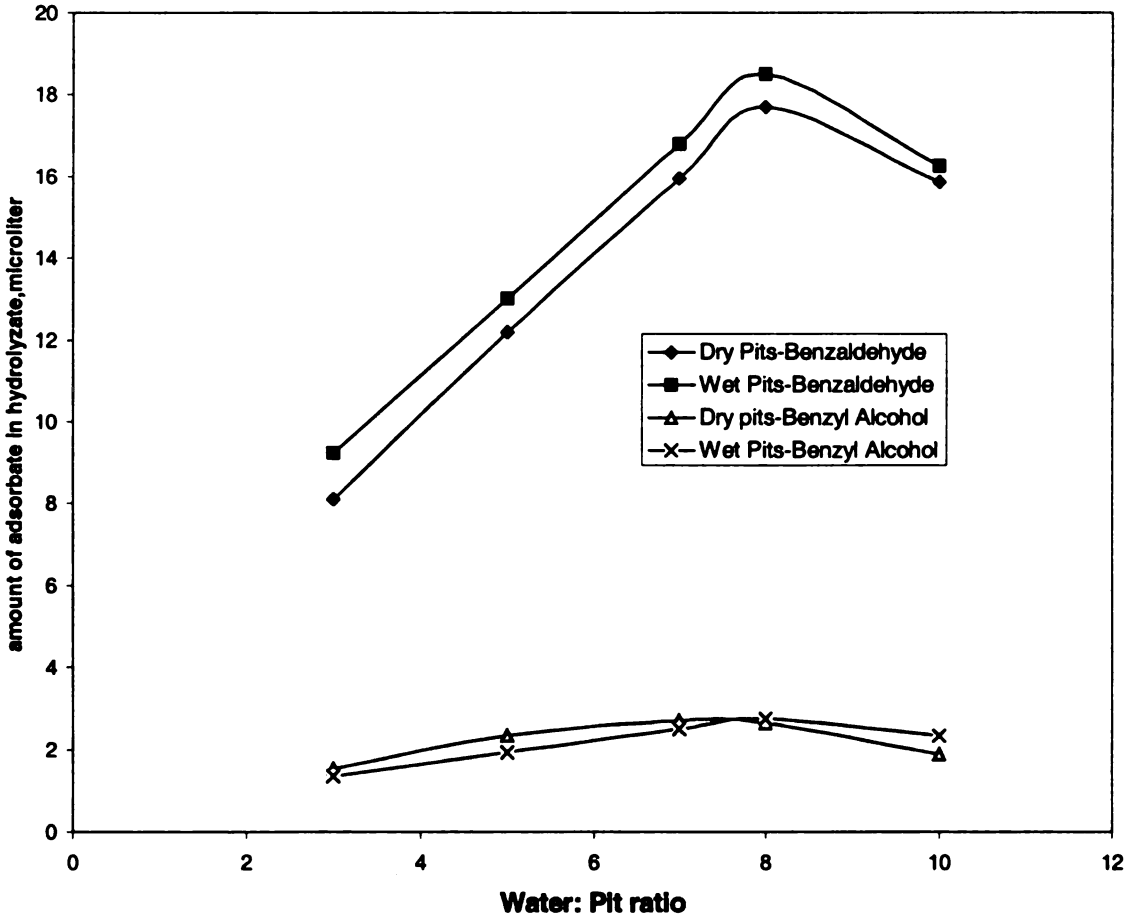

Figure 3.2 Comparison of wet cherry pits with dry cherry pits

It was observed that the total amount of benzaldehyde extracted from the pits with 8:1 water to pit ratio was more with wet pits than dry pits. However, there was a no change in the amount of benzyl alcohol recovered from the cherry pits. Using wet cherry pits also eliminated the necessity of drying the cherry pits, as the pits are shipped wet and stored in a freezer before use. Thus hydrolysis carried out with 8:1 water to wet cherry pit ratio at 55 C seemed to have the best yield. It was observed that the amount of benzaldehyde and benzyl alcohol extracted in the hydrolysis changed with different pits. There was a 20 % drop in the amount of benzaldehyde recovered by hydrolysis from cherry pits which were dried and stored in the laboratory for more than two months, than the newly dried cherry pits. However, for all kind of cherry pits, a 7:1 ratio using wet cherry pits was found to be the optimum choice.

3.2 Filtration

The preliminary filtration of the hydrolyzate, necessary to get rid of the cherry pit shells and kernels, is done by passing it through a sieve of 180 microns. This process is very quick, and it is efficient in removing the large particles. The hydrolyzate is poured into a Nalgene™ cylindrical tank with No 80. sieve manufactured by Dual Company, placed on the top. The pits are emptied out of the sieve pan as necessary. The hydrolyzate still constitutes lot of compounds besides benzaldehyde, benzyl alcohol and benzoic acid. If the hydrolyzate is passed through the adsorption bed without further filtration, there is a deposit of cake on the surface of the resin. As the thickness of the cake increases, it becomes impermeable to the fluid and finally builds up backpressure. In order to avoid this, the hydrolyzate is filtered and then passed through the adsorption bed.

Earlier, filtration was performed in a metal cylinder with a diameter of about 3 inches and a length of about 15 inches. The following items composed the filter (bottom to top): 4 grams of glass wool, 32 grams of diatomaceous earth (normally used in swimming pool filters), 130 grams of sand, and 50 grams of cherry pits for the purpose of spreading liquid flow over the entire diameter of the filter. A pump pushed the hydrolyzate through the filter from a feed tank. While this filter effectively removed all noticeable particulates from the hydrolyzate, the filter cake caused it to plug very quickly. In spite of adding diatomaceous earth to the hydrolyzate feed to make the filter cake sufficiently porous to avoid plugging, the filtration bed had to be recharged twice with glass-wool, sand and earth for filtering 20 liters of hydrolyzate and there was a loss of around 1 liter of hydrolyzate in this process. And it was difficult to cope up with the flow rate of the fluid passing through the bed. Hence, a new filtration unit with pressure filter was set up. The hydrolyzate is passed through a pressure filter with 5-micron polypropylene filter bag. It is then passed through the same pressure filter with 1-micron polypropylene filter bag. This filtration technique is faster and the wastage of hydrolyzate in this method is minimal. The filtered hydrolyzate is then stored in a 20-L glass jar, which in turn was placed in an ice bath. The chilled condition helps to slow down the bacterial growth in the hydrolyzate.

3.3 Adsorption

PharMed tubing carries the cooled hydrolyzate from the bottom of the jar to the Masterflex pump. The tubing then carries the hydrolyzate from the pump to the top of the adsorption bed. The adsorption bed itself consists of a glass tube measuring 6

centimeters in diameter. Silicon stoppers are placed on the top and bottom openings in order to hold the contents. The beds run completely filled with hydrolyzate. In order to avoid air entering the glass bed, the hydrolyzate is passed through an air trap before entering the glass adsorption bed. Experiments were done in the phase I of the USDA grant to find the resin best suited for the cherry pit experiments. Breakthrough behavior of benzaldehyde and benzyl alcohol were studied on XAD-4 (from Rohm and Haas) and SP-850 (from Mitsubishi Chemical), the best known resins for benzaldehyde adsorption. Experimental work revealed that SP-850 was the better resin for adsorbing benzaldehyde and benzyl alcohol from the hydrolyzate.

The waste stream flowing through the bottom of the bed is analysed every hour to determine whether benzaldehyde and benzyl alcohol are breaking through. Figure 3.3 shows the breakthrough behavior of benzaldehyde and benzyl alcohol for an experiment done with 160 ml of SP-850 resin. The superficial velocity of the feed flowing through the adsorption bed is 2.6 cm/min. The outlet concentration is normalized by the inlet feed concentration. The concentration of benzaldehyde and benzyl alcohol in the feed stream was 0.90 mol/m^3 and 0.48 mol/m^3 respectively. Except the diameter, all the parameters listed in Table C-4.1 were used without any kind of change. The bed diameter was 0.0603 m and the height of the bed was 0.105 m. The breakthrough behavior is predicted by the Fortran code given by Moon in 1987 for multicomponent liquid phase adsorption. Since it wasn't possible to quantify the concentration of benzoic acid in the feed, the benzoic acid's concentration was assumed to be 0.20 mol/m^3.

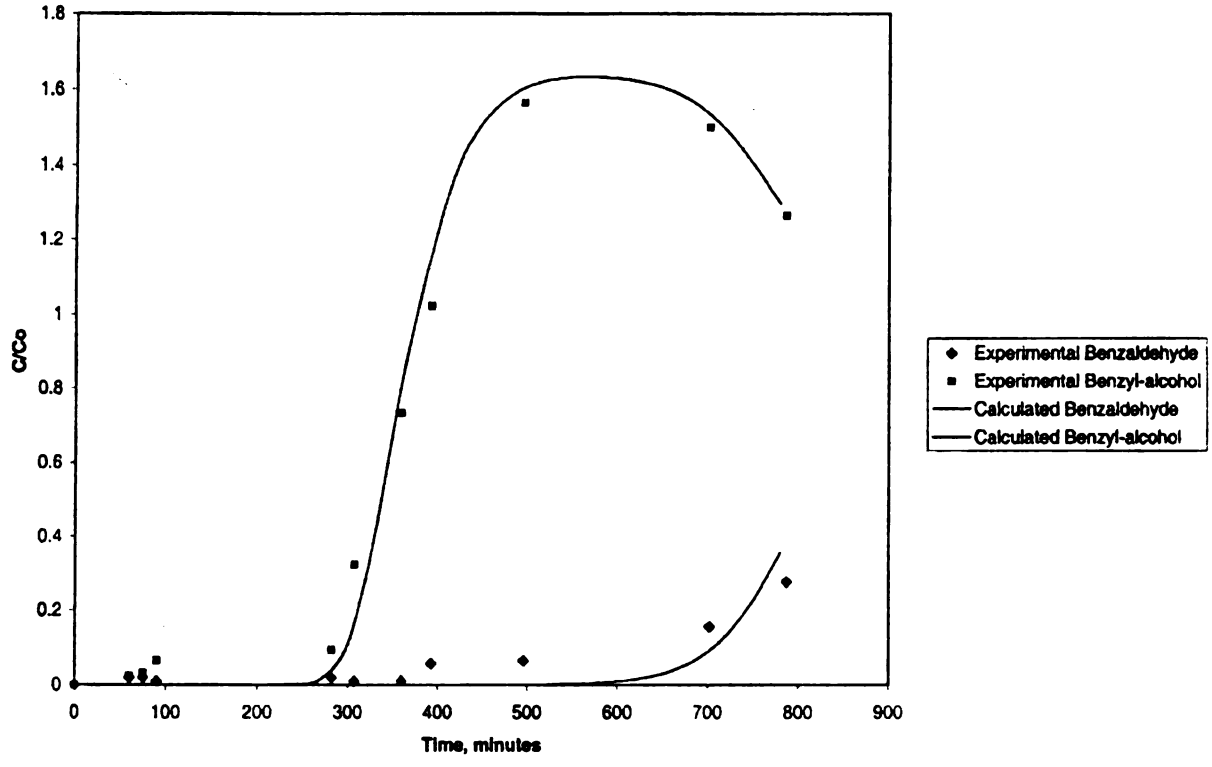

Figure 3.3 Breakthrough Behavior(1600 ml SP-850 resin) at 2.6 cm/min

3.4 **Regeneration**

After adsorption, the adsorption bed is backwashed with water to eliminate all the solids deposited on the top surface of the bed. Then the resin is regenerated at room temperature with carbon dioxide pressurized to 1200 psig in order to obtain the desired components. Benzaldehyde is completely soluble in liquid carbon dioxide (Francis, 1954). Carbon dioxide is a relatively inexpensive gas and it fulfills the all "natural" requirement for increased product value. Furthermore, its liquid and gaseous properties can both be utilized at room temperature without any heating—only pressurization and depressurization. Carbon dioxide is pressurized to its liquid state and passed through the bed where it removes adsorbates from the pores of the resin. It is then depressurized into its gaseous state where it relinquishes its solutes. Figure 3.4 gives a schematic diagram of the experimental setup used for the desorption of benzaldehyde and benzyl alcohol from the resin.

Carbon dioxide is pressurized to 1200 psi and then passed through a 500 ml regeneration chamber. At 298 K and 1200 psi, the molar density of carbon dioxide as reported by Angus and Armstrong is 0.01425 mol/cc. Around 5.739 L of pressurised carbon dioxide is passed through the bed which is equivalent to 2000 L of atmospheric carbon dioxide. The flow rate of carbon dioxide is maintained at 1L/min of atmospheric carbon dioxide which is equivalent to 0.172 L/hr of pressurised carbon dioxide. The superficial velocity of pressurised carbon dioxide through the bed is 54.83 cm/hr.To analyse the concentration of benzaldehyde and benzyl alcohol in the carbon dioxide leaving the regeneration chamber, a sampling loop is provided. The carbon dioxide can

be passed through the sampling loop by opening valves V_1 and V_2. The working of the sampling loop is given in the next section.

Carbon dioxide is depressurised to 500 psi and then passed through the collection chambers. Benzaldehyde and benzyl alcohol is collected in this stage. The lines carry carbon dioxide deep into the collection chambers. This gives them enough retention time in the collection chambers. Two chambers are provided to collect most of the benzaldehyde and benzyl alcohol from carbon dioxide.

Care must be taken to prevent the lines from freezing during depressurization. The resulting product from the collection chamber is an aqueous solution much more concentrated with the desired components than the hydrolyzate. The product contains water because of the moisture remaining in the bed after adsorption. Also, this product is a brown color. However, the product recovered from synthetic runs is pale yellow in color. Hence, the brown color can be attributed to oils, glycosides, proteins and other compounds in the hydrolysate.

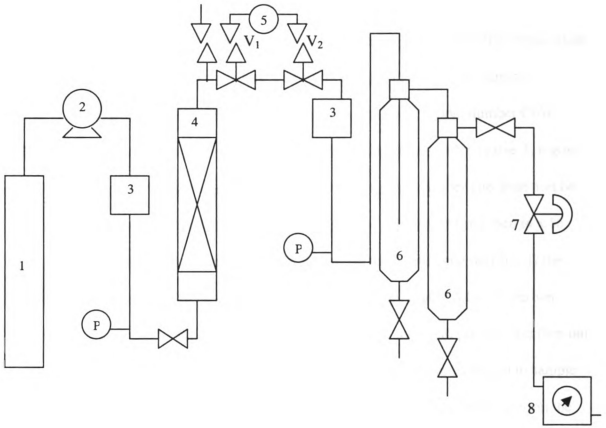

Figure 3.4 Schematic Layout of the Regeneration Setup.

1. Carbon dioxide cylinder
2. Gas booster
3. Regulator
4. Regeneration chamber
5. Sampling loop
6. Collection chamber
7. Meter valve
8. Flow meter

3.4.1 Sampling loop

The sampling section is shown in figure 3.5 and figure 3.6. From the regeneration chamber a stainless steel tubing carries the carbon dioxide to the six port sample switching valve manufactured by Valco Instruments Company, model number C6W. Figure 3.6 illustrates the load position and the sample position. A valve (valve 3, Figure 3.5) and a 16 gauge female syringe fitting is connected to port number one. Port number two is connected via 1/16 inch tubing to a valve (valve 4, Figure 3.5) and then to a 16 gauge needle. Port four is the inlet from the regeneration chamber and port five is the outlet. When the sample valve is placed in the load position, Figure 3.6a, the carbon dioxide flows into port four out of port three to the sample loop into port six and then out of port five under operating pressure. To obtain a sample, the valve is rotated to sample position, Figure 3.6b, the needle valve is opened at port two to allow material from the loop flow into a 10 ml conical volumetric flask. Another tubing extends from the evacuated test tube to a burette sealed with a silicon stopper on the top and having a tubing running from the bottom of the burette to an overflow bottle. Port three and six contains the 0.132 ml sample loop constructed from approximately 5.2 inches of 1/16 inch O.D. stainless steel tubing. The method applied in measuring the volume of the sampling loop is given in Appendix C-4 along with the raw data.

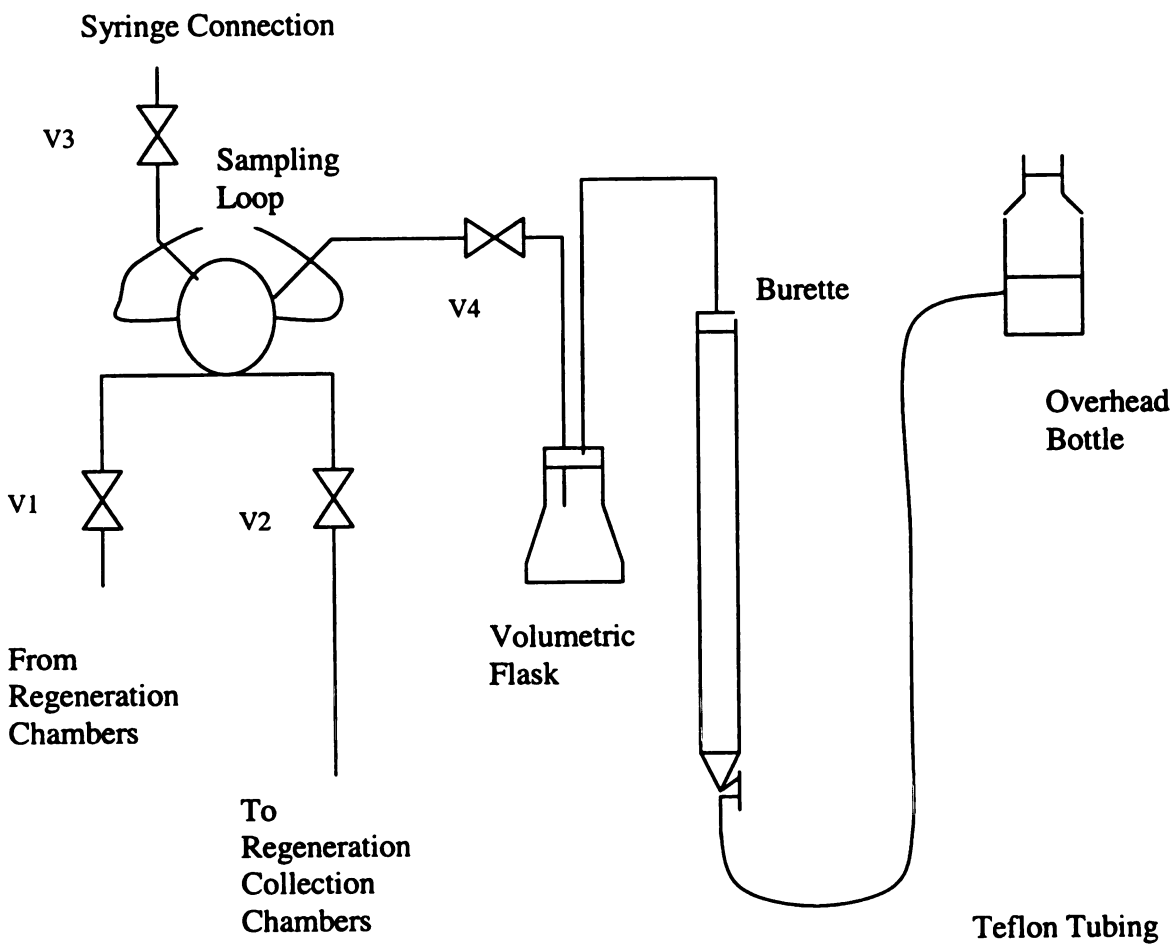

Figure 3.5 Schematics of the Sampling Loop

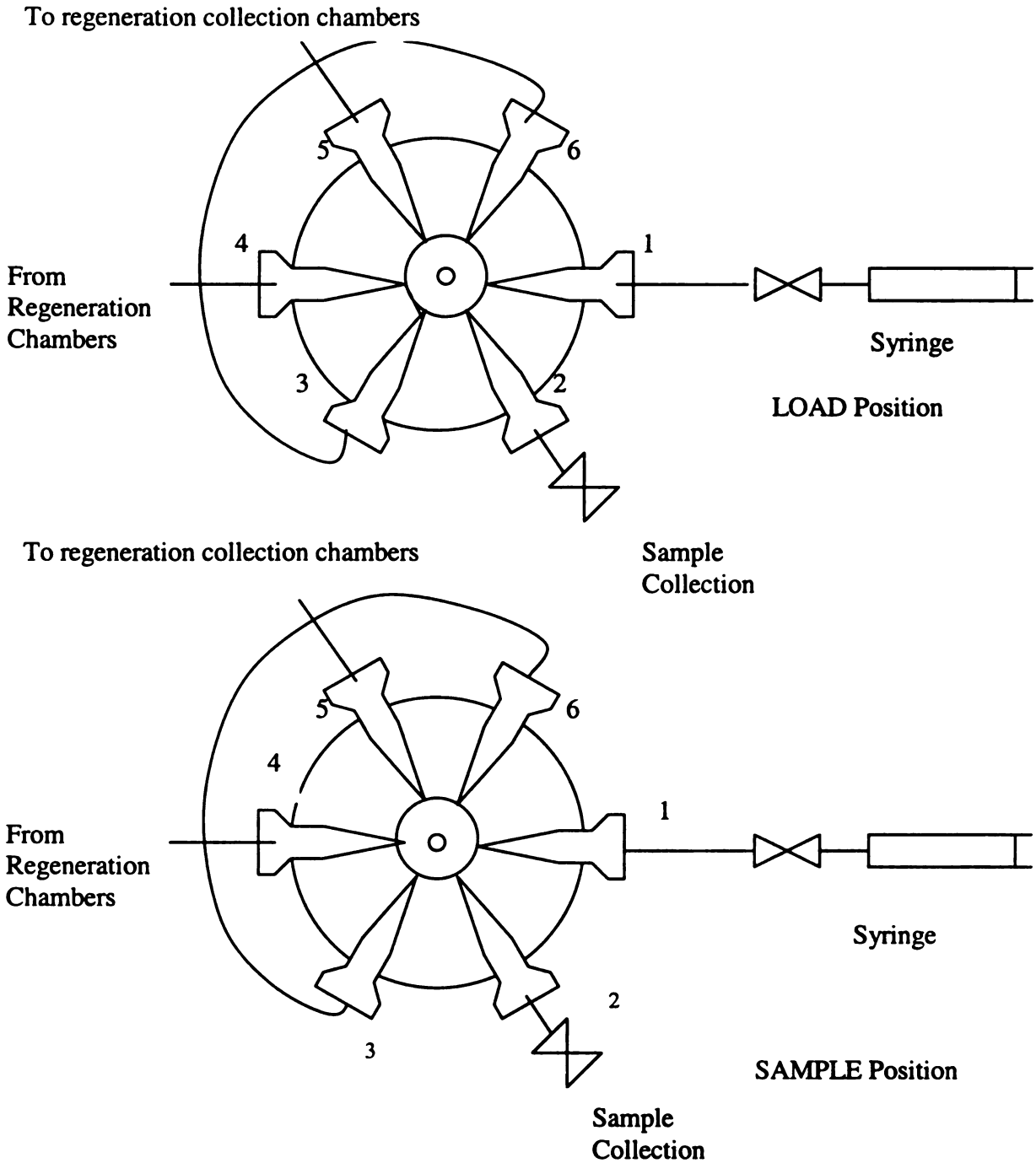

Figure 3.6 Schematic of Sampling Valve Operation in Sampling Section.

3.5 Mass balance and analysis

An attempt was made to complete the mass balance for the adsorption run illustrated in figure 3.3. By integrating the area of the benzaldehyde and benzyl alcohol breakthrough curves, it could be realized that 3.54 ml of benzaldehyde and 0.28 ml of benzyl alcohol was loaded on the resin. The displacement of benzyl alcohol molecules by benzaldehyde molecules towards the end of the run attributed to the lower amount of benzyl alcohol on the resin. The amount of benzaldehyde and benzyl alcohol lost while rinsing the resin with water after adsorption was less than 0.01 ml.

The resin was split into two halves of 80-ml resin. One half of the resin was regenerated by solvent regeneration. The method adopted for solvent regeneration was simple. 4 L of 100 % ethanol was pumped from the bottom of the bed at a superficial velocity of 2.6 cm/min and flow rate of 75 ml/min. The ethanol solution was injected into the GC after dilution. The benzaldehyde and benzyl alcohol content in the ethanol as a function of ethanol passed through the bed is given in figure 3.7. Integration of the curves showed that 1.60 ml of benzaldehyde and 0.12 ml of benzyl alcohol was recovered by solvent regeneration. Thus 89 % of the benzaldehyde and 85 % of the benzyl alcohol loaded on the resin could be recovered by solvent regeneration. However, the results from carbon dioxide regeneration weren't that encouraging. 600 L of atmospheric carbon dioxide was passed through the resin bed at the flow rate of 2 L/min. The final sample from the collection chamber carried 0.54 ml of benzaldehyde and 0.04 ml of benzyl alcohol. The pattern followed in the adsorbate desorption from the resin is illustrated in Figure 3.8. The collection chambers were washed with 100 % ethanol after the regeneration. The amount of benzaldehyde and benzyl alcohol recovered by this washing

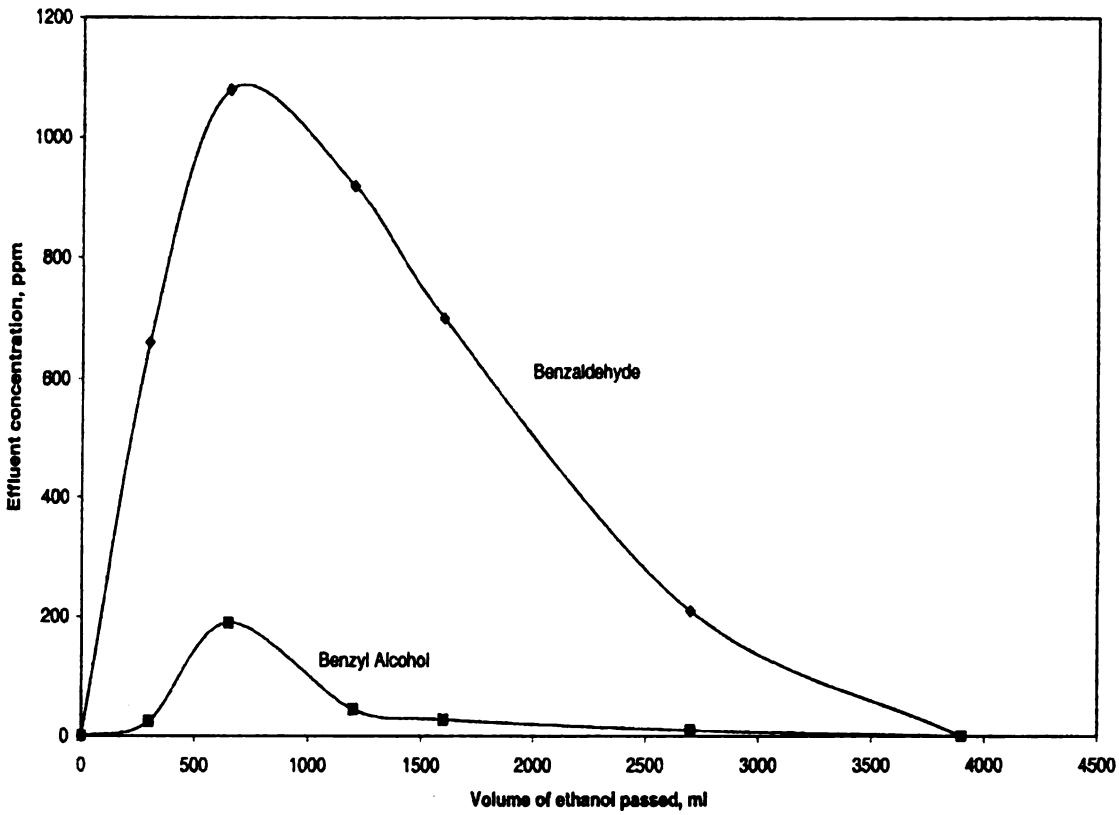

Figure 3.7 Solvent Regeneration Pattern

were 0.21 and 0.02 ml respectively. The amount of benzaldehyde and benzyl alcohol lost in the waste carbon dioxide stream was continuously monitored from a gas bulb placed before the final flow meter. GC from this bulb showed peaks of 0.3 and 0.2 area count for benzaldehyde and benzyl alcohol respectively, for a 0.5 ml gas injection. This reading accounted for 0.02 ml of benzaldehyde and 0.01 ml of benzyl alcohol. The resin was soaked in 100 % ethanol after the regeneration. GC of this ethanol showed no trace of benzaldehyde and benzyl alcohol. Hence the total benzaldehyde and benzyl alcohol traced was 0.75 and 0.07 respectively, accounting for just 46 % of the benzaldehyde and 50 % of the benzyl alcohol loaded on the resin. Table 3.4 shows the desorption results of benzaldehyde. Benzyl alcohol couldn't be followed since the concentration was too low. The overall recovery of benzyl alcohol was found by running a GC sample of the collected product.

Table 3.4 Desorption Results

Time, minutes	GC reading of sample, area count	Amount of benzaldehyde in the total sample, $ml \times 10^4$	Total amount of benzaldehyde carried by carbon dioxide, $ml/min \times 10^3$
10	0.51	3.77	8.19
20	0.43	3.18	6.90
30	0.32	2.36	5.13
40	0.31	2.29	4.97
80	0.21	1.55	3.37
140	0.09	0.66	1.44

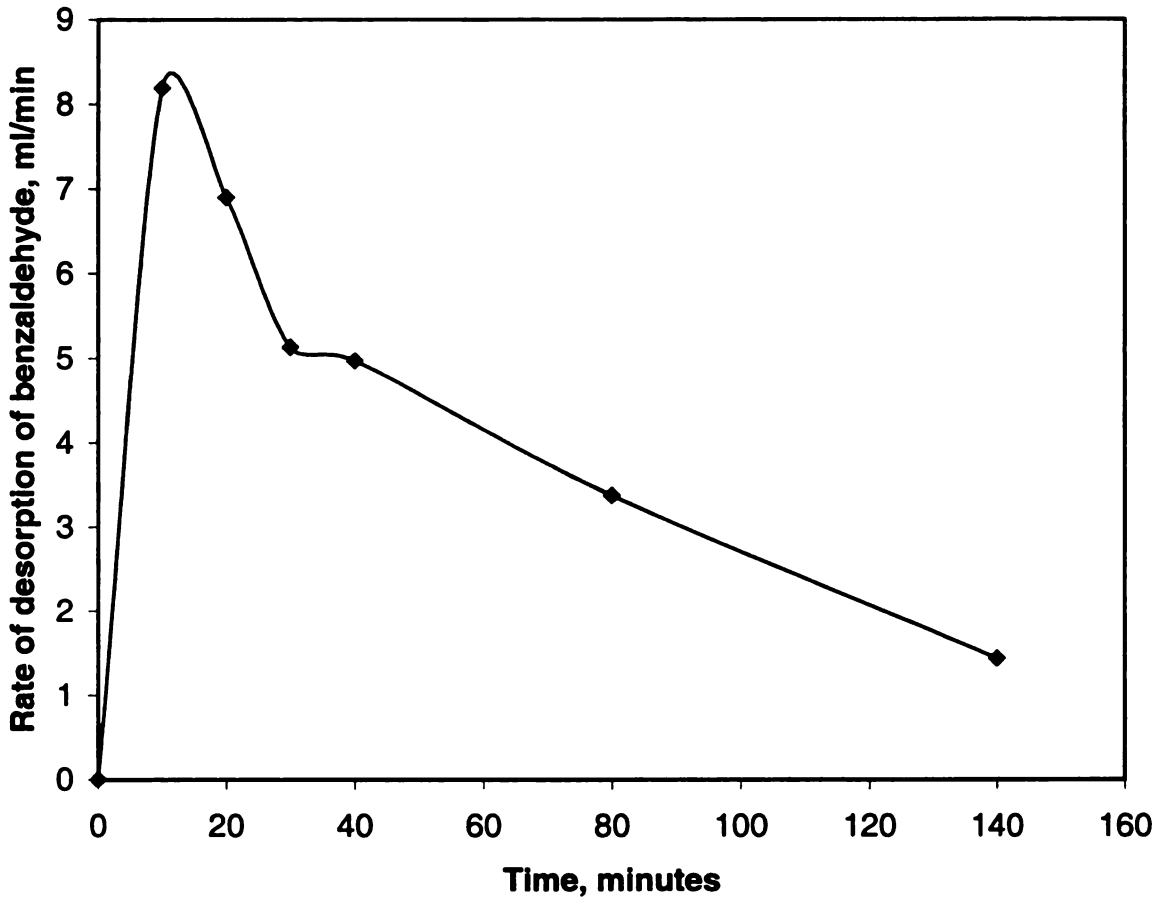

Figure 3.8 Carbon dioxide Regeneration Results

3.6 Distillation and resin reconditioning

The sample obtained from the collection chambers is distilled to get the final products. Distillation is carried out under carbon dioxide to reduce the oxidation of benzaldehyde. There is a considerable loss of benzaldehyde and benzyl alcohol in this step. However, the product obtained after distillation are found to be more than 92% pure.

The resin is stored under brine solution to prevent growth of mould. Resin is washed with ethanol and water before reuse. Around 3 lts of 20 % ethanol solution is passed through the bottom of the bed. Then, the resin bed is washed with 3 lts of water till the fluid sitting on the top of the bed becomes clear.

REFERENCES

Angus, B., and Armstrong, K.M., Thermodynamic Tables Project, International Union of Pure and Applied Chemistry, Commission on Thermodynamics and Thermochemistry,

Gribb, A., and Lira, C.T., "Benzaldehyde recovery process design", Report to the Cherry Marketing Institute, (1992)

Hagedorn, M.L.; "Differentiation of Natural and Synthetic Benzaldehydes by H Nuclear Magnetic Resonance"; *J. Agric. Food Chem.*, 1992, 40, 634.

Kawabe, T.; Morita, H.; "Production of Benzaldehyde and Benzyl Alcohol by the Mushroom Polyporus Tuberaster K2606"; *J. Agric. Food Chem.*, 1994, 42, 2556.

Krueger, H.W. and Reesman, R.H. Carbon Isotope Analyses in Food Technology. Mass Spectrometry Reviews 1 (205-236).(1983)

Krueger, D.A. and Krueger, H.W. Carbon Isotopes in Vanillin and the Detection of Falsified "Natural" Vanillin. Agricultural and Food Chemistry 31 (1265-1268).

Lamer, T.; Spinnler, H.E.; Souchon, I.; Voilley, A.; "Extraction of Benzaldehyde from Fermentation Broth by Pervaporation"; *Process Biochemistry*, 1996, 31, 533.

Li, C.P.; Swain, E.; Poulton, J.; "Prunus Serotina Amygdalin Hydrolase and Prunasin Hydrolase"; *Plant Physiology*, 1992, 100, 282.

Soule, A., Studies of Gas Adsorption on Activated Carbon and Cherry Flavor Recovery from Cherry Pits, Master's Thesis, 1999

Swain, E.; Poulton, J.; "Utilization of Amygdalin during Seedling Development of Prunus Serotina"; *Plant Physiology*, 1994, 106, 437.

Walther, D., and Maurer, G., High Pressure Vapour-Liquid Equilibria in Binary Mixtures of Carbon Dioxide and Benzaldehyde, Bromobenzene, Chlorobenzene, 1,2-Dichlorobenzene and 2-Chloro-1-Methylbenzene at Temperatures between 313 and 393 K and Pressures up to 22 Mpa, Phys Chem 96 (1992).

Zheng, L.; Poulton, J.E.; "Temporal and Spatial Expression of Amygdalin Hydrolase and Mandelonitrile Lyase in Black Cherry Seeds"; *Plant Physiology*, 1995, 109, 31.

APPENDIX A

PHYSICAL PROPERTIES

Table A-1. Physical Properties of Benzaldehyde

Formula	C_7H_6O
Molecular weight	106.12 g/gmol
Boiling point	179.0° C @ 760 mm Hg 112.5° C @ 100 mm Hg
Melting point	-26° C
Auto ignition temperature	190° C
Flash point	62° C
Vapor pressure	10mm Hg @ 62.0° C 60mm Hg @ 99.6° C 100mm Hg @ 112.5° C 400mm Hg @ 154.1° C
Solubility of benzaldehyde in water Solubility of water in benzaldehyde	0.6 % @ 20° C 1.5 % @ 20° C
Viscosity	1.4 g/cm sec @ 25° C
Relative density(water=1)	1.05
Relative vapor density(water=1)	3.65

Table A-2. Physical Properties of Benzyl Alcohol

Formula	C_7H_8O
Molecular weight	108.14g/gmol
Boiling point	205.0° C @ 760 mm Hg 142.0° C @ 100 mm Hg
Melting point	-15.3° C
Auto ignition temperature	436° C
Flash point	93° C
Vapor pressure	10mm Hg @ 92.6° C 60mm Hg @ 129.3° C 100mm Hg @ 141.7° C 400mm Hg @ 183.0° C
Solubility of benzyl alcohol in water Solubility of water in benzyl alcohol	4.4 % @ 25° C 8.0 % @ 20° C
Viscosity	8.0 g/cm sec @ 20° C
Relative density(water=1)	1.04
Relative vapor density(water=1)	3.70

Table A-3. Physical Properties of Benzoic Acid

Formula	$C_7H_6O_2$
Molecular weight	122.12 g/gmol
Boiling point	249.0° C @ 760 mm Hg 186.0° C @ 100 mm Hg
Melting point	122.4° C
Auto ignition temperature	573° C
Flash point	121.0° C
Vapor pressure	10mm Hg @ 132.1° C 60mm Hg @ 172.8° C 100mm Hg @ 186.2° C 400mm Hg @ 227.0° C
Solubility of benzoic acid in water	0.35 % @ 25° C
Viscosity	1.2 g/cm sec @ 130° C
Relative density(water=1)	1.32
Relative vapor density(water=1)	4.2

APPENDIX B

GC CALIBRATION

The analysis of the liquid and gas phases of the experimental samples was performed using a gas chromatograph. A Perkin-Elmer model 8500 equipped with a FID detector was used for the gas chromatography. The column was an Alltech Associates, Inc. Econo-cap™ capillary column, catalog number 19653, 15 m long x 1.2 mm ϕ with a EC-wax stationary phase.

Calibration standards are prepared by weighing out each component for the sample solution in the volumetric flask used as a sample container and filling the flask to the volume line with water. A clean stir bar is added to each sample and they are placed on a magnetic stirrer for at least an hour to assure that each solution will be homogeneous. The compositions of the sample solutions are given in table B.1 and table B.2. 1 μl of the sample solution was injected in the Gas Chromatograph for three to four times and a mean value of the area peak was noted. Sample solutions spanning a wide concentration range were prepared. The results are presented in table B.3 and B.4. Calibration curves were prepared as shown in figure B.1 and B.2, and a response factor for benzaldehyde and benzyl alcohol was calculated.

The column operating conditions are given in figure B.3 while a sample chromatograph is given in figure B.4.

Table B-1. Sample Solutions of Benzaldehyde/Water

Sample Description	Water ml	Benzaldehyde g	Benzaldehyde ppm
1	100	0.0068	68
2	100	0.0084	84
3	100	0.0126	126
4	100	0.0189	189
5	200	0.0462	231
6	200	0.0630	315
7	200	0.0840	420

Table B-2. Sample Solutions of Benzyl Alcohol /Water

Sample Description	Water ml	Benzyl alcohol ,g	Benzyl alcohol, ppm
1	100	0.0031	31
2	100	0.0073	73
3	100	0.0135	135
4	100	0.0166	166
5	200	0.0456	228
6	200	0.0706	353
7	200	0.0894	447

Table B-3. Benzaldehyde/Water GC Calibration Data

Sample Description	Sample Volume (µl)	Benzaldehyde (Mean Area count/µl)
1	1	0.921
2	1	1.123
3	1	1.702
4	1	2.558
5	1	3.090
6	1	4.189
7	1	5.679

Table B-4. Benzyl Alcohol/Water GC Calibration Data

Sample Description	Sample Volume (µl)	Benzyl alcohol(Mean Area count/µl)
1	1	0.573
2	1	1.360
3	1	2.510
4	1	3.121
5	1	4.271
6	1	6.564
7	1	8.301

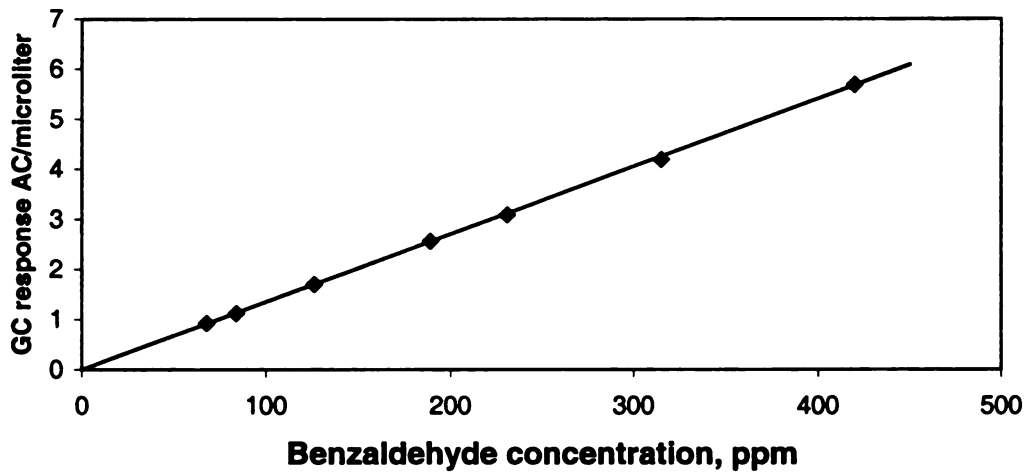

Figure B.1. Benzaldehyde Concentration Versus GC Response

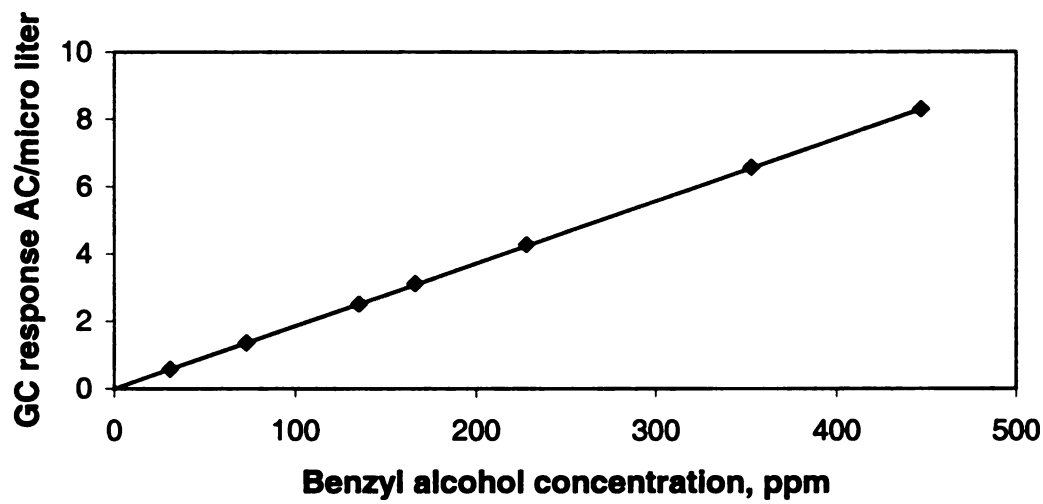

Figure B.2. Benzyl Alcohol Concentration Versus GC Response

SECTION 1 GC CONTROL

	1	2
OVEN TEMP (DEG C)	60	210
ISO TIME (MIN)	0.0	7.0
RAMP RATE (DEG C/MIN)	30.0	

HWD 1 RANGE OFF HWD 1 POLARITY A-B

FID 2 SENS LOW

DET ZERO ON

INITIAL DET 2

INJ	1	TEMP	OFF
INJ	2	TEMP	240
DET	1	TEMP	OFF
DET	2	TEMP	240

FLOW	1	5 ML/MIN
CARRIER GAS	1	HE
FLOW	2	5 ML/MIN
CARRIER GAS	2	HE
PRESSURE	3	5.0 PSIG

EQUILIB TIME 0.5 MIN

TOTAL RUN TIME 12.0 MIN

Figure B.3 Column Operating Conditions

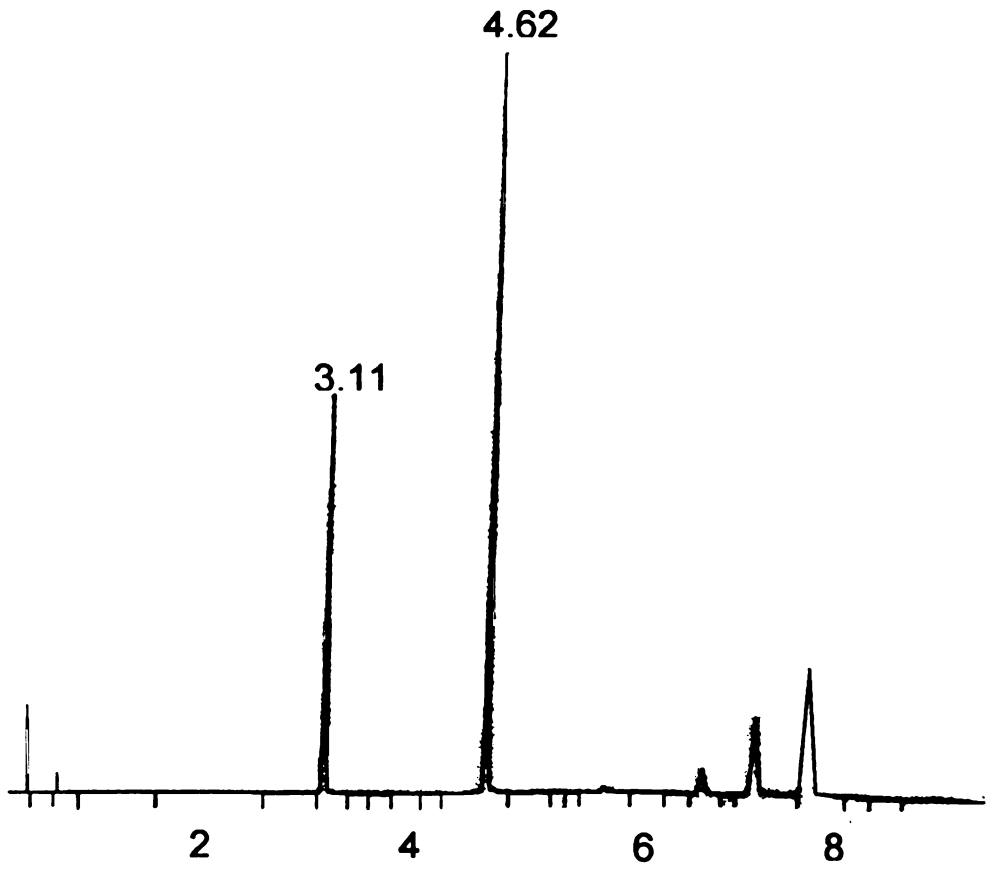

Figure B.4. A Sample Chromatograph

It was observed from Figures B.1 and B.2 that the GC response was a linear function of the concentration for benzaldehyde and benzyl alcohol. The GC response factors for a 1 μl of liquid sample were found to be 73.97E-6 μl/area count and 53.91E-6 μl/area count for benzaldehyde and benzyl alcohol respectively. Hence the area count obtained for a particular injection multiplied by their response factor would give the ppm concentration of that compound in the sample.

APPENDIX C

PROCEDURES AND RAW DATA

C-1. Void fraction calculations

The skeletal density and the bulk density were calculated to find out the void ratio of SP-850 resin. The procedure adopted and the raw data for finding them is summarized.

1. Resin was thoroughly washed with water to get rid of the salts.
2. A particular volume of washed resin (V_1 ml) was measured using a 10 ml graduated cylinder.
3. The resin was transferred using a pipette to decant the liquid and then dried in a vacuum oven for 24 hours at a temperature of 60^0C.
4. The resin was then weighed to give the final mass (m gm) of the resin.
5. The dried resin was then added to a finite volume (V_2 ml) of 40 % ethanol solution.
6. The total volume (V_3 ml) of the ethanol solution and the resin was measured after 30 minutes, thus giving the change in volume ($\Delta V = V_3 - V_2$ ml).
7. ρ_b and ρ_s were calculated using the formulas :

   $\rho_b = m/V_1$ and

   $\rho_s = m/\Delta V$.

Table C-1.1 ρ_b and ρ_s Calculations

V_1 ml	m gm	V_2 ml	V_3 ml	ΔV ml	ρ_b gm/ml	ρ_s gm/ml
10	3.40	40	43.2	3.2	0.340	1.062
12	4.10	40	43.9	3.9	0.341	1.051
18	6.25	80	85.9	5.9	0.347	1.059
20	6.80	80	86.5	6.5	0.340	1.046
24	8.20	80	87.8	7.8	0.341	1.051
25	8.60	80	88.2	8.2	0.344	1.048
30	10.20	100	109.7	9.7	0.340	1.051

The same experiments were repeated by using a different ethanol solution and the results found were exactly same. Hence, ρ_b and ρ_s used in all the calculations were 0.34 gm/ml and 1.051 gm/ml respectively. The void fraction of the resin is given by $\varepsilon = \left(1 - \frac{\rho_b}{\rho_s}\right)$, and its value is found to be 0.677.

C-2. Equilibrium adsorption behavior of benzaldehyde, benzyl-alcohol and benzoic acid solution.

Equilibrium adsorption behavior of benzaldehyde, benzyl-alcohol and benzoic acid was studied in a liquid phase adsorption at room temperature. The following

procedure was used to get a single point on the isotherm for benzaldehyde and benzyl-alcohol.

1. Water was sparged with carbon dioxide for 15 minutes.
2. 250 ml of the sparged water was put in a 400 ml PYREX™ beaker.
3. A specific volume of benzaldehyde or benzyl alcohol was measured and added to the beaker.
4. The solution was stirred on a low setting for 10 minutes to let the concentration even out.
5. A G.C of the solution was taken to measure the initial concentration.
6. A specific volume of resin was added to the flask.

   To measure the resin:

   A. Salt water was rinsed out of resin and it was put in fresh water.

   B. A pipette was used to suck some of the water/resin.

   C. All the water was drained carefully so that only resin remained in the auto pipette.

   D. A small portion of the beaker solution was put in a small Erlenmeyer flask onto the scale.

   E. The resin was carefully added, by shaking it out of the tube into the solution until desired mass.

   F. The small portion of resin/solution was added to the beaker. The resin was rinsed into the beaker using the solution.
7. The beaker was covered with parafilm and stirred for two hours.
8. The final concentration was measured after two hours.

Here, the adsorbent loading is given by the grams of adsorbate adsorbed onto the resin per gram of wet resin. The resin is washed prior to weighing to get rid of the salts. Experiments were done to calculate the ratio of dry resin weight to wet resin weight. A particular volume of resin was taken and weighed. It was then washed with water to remove the salts. A pipette was used to remove the drain the water. The resin was then weighed again. The results are tabulated in Table C.2.1.A.

Table C.2.1.A. Results of Experiments to Detect the Ratio of Dry Resin Weight / Wet Resin Weight

Weight of Dry Resin, gm	Weight of Wet Resin, gm	Ratio of Dry Resin Weight to Wet Resin Weight
5	7.50	0.666
8	12.50	0.640
10	15.65	0.638
15	23.00	0.652
20	31.25	0.64

Hence, it was found that the ratio of dry resin weight to wet resin weight is 0.64.

The same procedure was observed for collecting the equilibrium adsorption data for benzoic acid, except the method to detect the concentration. The Gas Chromatograph couldn't accurately sense the concentration of benzoic acid, so the concentration was detected using a pH test-meter. Calibration of the pH meter is given in Table C.2.1.B.

The results are given in table C.2.2, C.2.3 and C.2.4. The values of equilibrium adsorbate concentration in the adsorbent phase are tabulated in gm adsorbate/gm wet adsorbent. For model fitting, these values were converted to gm adsorbate/gm dry adsorbent by diving them by 0.64.

Table C-2.1.B Calibration of pH-meter

pH reading	Concentration of benzoic acid in mol/m^3
3.25	0.562
3.50	0.316
3.75	0.177
4.00	0.100
4.50	0.031
5.00	0.010
5.50	0.003
6.00	0.001

Table C-2.2 Equilibrium Adsorption Data for Benzaldehyde Solution

y- equilibrium adsorbate concentration in the fluid phase mol/m^3	q-equilibrium adsorbate concentration in the adsorbent phase, gm adsorbate/gm wet adsorbent
0.0470	0.0070
0.0943	0.0090
0.1475	0.0115
0.1577	0.0135
0.0169	0.0185
0.2357	0.0209
0.3397	0.0265
0.3960	0.0276
0.6338	0.0407
0.6458	0.0430
0.7304	0.0449
0.8215	0.0435
1.0842.	0.0547
1.3397	0.0630
1.7730	0.0676
1.8868	0.0694
2.1048	0.0709
2.6418	0.0739
2.9614	0.0800
3.4131	0.0822
3.8679	0.0815
4.6870	0.0852

Table C-2.3 Equilibrium Adsorption Data for Benzyl Alcohol Solution

y- equilibrium adsorbate concentration in the fluid phase mol/m^3	q-equilibrium adsorbate concentration in the adsorbent phase, gm adsorbate/gm wet adsorbent
0.1853	0.0062
0.2263	0.0051
0.2768	0.0076
0.3943	0.0072
0.6079	0.0132
0.8647	0.0163
0.9979	0.0194
1.4614	0.0243
1.7022	0.0266
2.0675	0.0312
2.8888	0.0370
4.0581	0.0468

Table C-2.4 Equilibrium Adsorption Data for Benzoic Acid Solution

y- equilibrium adsorbate concentration in the fluid phase, mol/m^3	q-equilibrium adsorbate concentration in the adsorbent phase, gm adsorbate/gm wet adsorbent
0.0508	0.0036
0.1239	0.0070
0.1639	0.0088
0.1803	0.0094
0.2377	0.0123
0.2704	0.0134
0.3704	0.0166
0.3998	0.0177
0.5002	0.0202
0.6557	0.0240
0.7868	0.0265
0.9098	0.0292

C-3. Breakthrough behavior of benzaldehyde, benzyl-alcohol and benzoic acid in a fixed bed adsorption of single component.

Experiments were performed to study the breakthrough pattern of benzaldehyde, benzyl alcohol or benzoic acid in a fixed bed adsorption of single component. The procedure employed was as follows.

1. 15 ml of resin was washed with water to get rid of the salts. The height of the resin bed was measured.
2. The resin was loaded on the glass bed and backwashed with 20 weight percent ethanol in water solution and then back-washed with water till the fluid on the top of the bed looked clear.
3. A feed solution was prepared with benzaldehyde, benzyl alcohol or benzoic acid. A GC of the feed was taken to quantify the concentration.
4. The feed was passed downward through the bed at a superficial velocity of 2.7 cm/min.
5. GC of the waste stream was taken at a regular interval to analyze the concentration of the adsorbate in the outlet.

Experiments were performed with 20ml and 25 ml of resin. The diameter of the bed was also varied. The concentration for benzoic acid was again measured by following the pH. The results of the experiments are tabulated in table C.3.1 to C.3.12

Table C-3.1 Benzaldehyde Breakthrough Behavior, Experiment-1

Adsorbate	Benzaldehyde
Height of bed	6.35 cm
Superficial velocity	2.7 cm/min
Diameter of bed	2.22 cm
Adsorbate concentration in the feed	0.83 mol/m^3
Time, minutes	C/C_o
60	0.000
180	0.015
300	0.061
360	0.050
420	0.080
480	0.280
540	0.690
600	0.886
660	0.920

Table C.3.2 Benzaldehyde Breakthrough Behavior, Experiment -2

Adsorbate	Benzaldehyde
Height of bed	8.53 cm
Superficial velocity	2.7 cm/min
Diameter of bed	2.22 cm
Adsorbate concentration in the feed	1.13 mol/m^3
Time, minutes	C/C_o
30	0.000
150	0.010
270	0.021
330	0.009
390	0.007
450	0.054
510	0.060
570	0.250
630	0.720
690	0.920

Table C-3.3 Benzaldehyde Breakthrough Behavior, Experiment -3

Adsorbate	Benzaldehyde
Height of bed	12.19 cm
Superficial velocity	2.7 cm/min
Diameter of bed	6.03 cm
Adsorbate concentration in the feed	1.05 mol/m^3
Time, minutes	C/C_o
60	0.013
180	0.010
300	0.015
360	0.020
420	0.022
480	0.024
600	0.026
660	0.030
720	0.070
780	0.090
840	0.210
900	0.540
960	0.870
1020	0.920

Table C-3.4 Benzaldehyde Breakthrough Behavior, Experiment -4

Adsorbate	Benzaldehyde
Height of bed	11.17 cm
Superficial velocity	2.7 cm/min
Diameter of bed	6.03 cm
Adsorbate concentration in the feed	1.09mol/m^3
Time, minutes	C/C_o
60	0.013
180	0.019
300	0.020
360	0.045
420	0.039
480	0.045
540	0.039
600	0.040
660	0.040
720	0.080
780	0.057
840	0.092
1020	0.920

Table C-3.5 Benzyl Alcohol Breakthrough Behavior, Experiment-5

Adsorbate	Benzyl alcohol
Height of bed	5.08 cm
Superficial velocity	2.7 cm/min
Diameter of bed	2.22 cm
Adsorbate concentration in the feed	0.63 mol/m^3
Time, minutes	C/C_o
30	0.000
60	0.001
90	0.002
120	0.160
155	0.530
190	0.860
210	0.920
240	0.924

Table C.3.6 Benzyl Alcohol Breakthrough Behavior, Experiment-6

Adsorbate	Benzyl alcohol
Height of bed	6.60 cm
Superficial velocity	2.7 cm/min
Diameter of bed	2.22 cm
Adsorbate concentration in the feed	0.48 mol/m^3
Time, minutes	C/C_o
30	0.000
60	0.000
90	0.000
150	0.050
180	0.201
210	0.450
227	0.663
256	0.812
273	0.839

Table C-3.7 Benzyl Alcohol Breakthrough Behavior, Experiment-7

Adsorbate	Benzyl alcohol
Height of bed	8.12 cm
Superficial velocity	2.7 cm/min
Diameter of bed	6.03 cm
Adsorbate concentration in the feed	0.48 mol/m^3
Time, minutes	C/C_o
40	0.000
70	0.000
100	0.001
130	0.001
160	0.002
190	0.110
220	0.221
246	0.371
268	0.538
310	0.831
340	0.839

Table C-3.8 Benzyl Alcohol Breakthrough Behavior, Experiment-8

Adsorbate	Benzyl alcohol
Height of bed	8.38 cm
Superficial velocity	2.7 cm/min
Diameter of bed	6.03 cm
Adsorbate concentration in the feed	0.48 mol/m^3
Time, minutes	C/C_o
35	0.000
105	0.002
140	0.002
175	0.003
210	0.101
268	0.458
306	0.821
335	0.882
360	0.901

Table C-3.9 Benzoic Acid Breakthrough Behavior, Experiment-9

Adsorbate	Benzoic acid
Height of bed	5.08 cm
Superficial velocity	2.7 cm/min
Diameter of bed	2.22 cm
Adsorbate concentration in the feed	0.26 mol/m^3
Time, minutes	C/C_o
10	0.000
25	0.001
55	0.007
80	0.009
210	0.180
270	0.371
280	0.470
313	0.532
365	0.691
395	0.734
440	0.890
470	0.945
510	0.961

Table C-3.10 Benzoic Acid Breakthrough Behavior, Experiment-10

Adsorbate	Benzoic acid
Height of bed	8.08 cm
Superficial velocity	2.7 cm/min
Diameter of bed	2.22 cm
Adsorbate concentration in the feed	0.26 mol/m^3
Time, minutes	C/C_o
30	0.000
150	0.000
270	0.000
330	0.111
390	0.231
450	0.320
510	0.450
570	0.709
630	0.795
690	0.921
718	0.942

Table C-3.11 Benzoic Acid Breakthrough Behavior, Experiment-11

Adsorbate	Benzoic acid
Height of bed	12.19 cm
Superficial velocity	2.7 cm/min
Diameter of bed	6.03 cm
Adsorbate concentration in the feed	0.19 mol/m^3
Time, minutes	C/C_o
30	0.000
70	0.000
210	0.001
420	0.021
600	0.080
660	0.140
720	0.241
828	0.550
853	0.601
929	0.821
1035	0.939

Table C-3.12 Benzoic Acid Breakthrough Behavior, Experiment-12

Adsorbate	Benzoic acid
Height of bed	7.50 cm
Superficial velocity	2.7 cm/min
Diameter of bed	6.03 cm
Adsorbate concentration in the feed	0.19 mol/m^3
Time, minutes	C/C_o
40	0.000
170	0.002
300	0.020
360	0.150
420	0.271
480	0.451
521	0.561
600	0.830
660	0.898

C-4. Breakthrough behavior of mixtures of benzaldehyde, benzyl-alcohol and benzoic acid in a fixed bed adsorption.

Experiments were performed to study the breakthrough pattern of benzaldehyde, benzyl alcohol and benzoic acid in a liquid phase fixed bed adsorption. The procedure employed was as follows.

1. 15 ml of resin was washed with water to get rid of the salts. The height of the resin bed was measured.
2. The resin was loaded on the glass bed and backwashed with 20 percent ethanol solution and then washed with water till the fluid on the top of the bed looked clear.
3. A feed solution was prepared with benzaldehyde, benzyl alcohol or benzoic acid. A GC of the feed was taken to quantify the concentration.
4. The feed was passed through the bed at a superficial velocity of 2.52 cm/min.
5. GC of the waste stream was taken at a regular interval to analyze the concentration of the adsorbate in the outlet.

Experiments were performed with 20ml and 25 ml of resin. The superficial velocity of the bed was also varied to 3.78 and 5.04 cm/min. The concentration of benzoic acid could be followed for only one run. The experimental results were fitted with the predicted results from Moon's program for multicomponent liquid adsorption. The Freundlich constants obtained from equilibrium adsorption data were used for fitting. Parameters like temperature, ρ_b , ρ_s Freundlich constants, diameter of adsorption bed and particle diameter were constant for all the experiments. Table C.4.1 enlists values of all the parameters that were constant for all the experiments. Their values are given in units

compatible with the program. The Freundlich constant n corresponding to equation 2.9, was taken from Table 2.3. The value of n didn't undergo any change since it was dimensionless. Since Moon's program required q in kmol adsorbate/m^3 of bed, K from Table 2.3 was converted.

Table C-4.1 Constant Parameters in Multicomponent Adsorption Experiments.

Temperature	25^0C		
Diameter of bed	0.0222 m		
ρ_b	340 kg/m^3		
ρ_s	1051 kg/m^3		
Particle diameter	0.000425 m		
Adsorbate	Benzaldehyde	Benzyl alcohol	Benzoic acid
Freundlich constant K	0.509	0.194	0.254
Freundlich constant n	2.43	2.2	1.558
Mass transfer coefficient	.2E-4 m/sec	.2E-4 m/sec	.2E-4 m/sec
Surface diffusion coefficient	.26E-11 m^2/sec	.26E-11 m^2/sec	.26E-11 m^2/sec

The raw data from the experiments is given in table C.4.2 to C.4.10.

Table C-4.2 Multicomponent Breakthrough Behavior, Experiment-1

Height of bed	0.075 m		
Superficial velocity	0.00042 m/sec		
Adsorbate	Benzaldehyde	Benzyl alcohol	Benzoic acid
Adsorbate concentration in feed	0.90 mol/m^3	0.48 mol/m^3	0.20 mol/m^3
Time, minutes	C/C_o	C/C_o	C/C_o
120	0.020	0.004	-
157	0.020	0.120	-
171	0.010	0.240	-
185	0.020	0.430	-
248	0.010	1.183	-
324	0.028	1.560	-
374	0.077	1.526	-
424	0.172	1.380	-

Table C-4.3 Multicomponent Breakthrough Behavior, Experiment-2

Height of bed	0.075 m		
Superficial velocity	0.00063 m/sec		
Adsorbate	Benzaldehyde	Benzyl alcohol	Benzoic acid
Adsorbate concentration in feed	0.88 mol/m^3	0.46 mol/m^3	0.20 mol/m^3
Time, minutes	C/C_o	C/C_o	C/C_o
75	0.010	0.067	-
110	0.010	0.403	-
136	0.010	0.640	-
187	0.020	1.276	-
230	0.050	1.453	-
274	0.194	1.372	-
315	0.395	1.240	-
375	0.68	1.055	-

Table C-4.4 Multicomponent Breakthrough Behavior, Experiment-3

Height of bed	0.075 m		
Superficial velocity	0.00084 m/sec		
Adsorbate	Benzaldehyde	Benzyl alcohol	Benzoic acid
Adsorbate concentration in feed	0.88 mol/m^3	0.46 mol/m^3	0.20 mol/m^3
Time, minutes	C/C_o	C/C_o	C/C_o
38	0.004	0.047	-
75	0.011	0.309	-
110	0.025	0.793	-
136	0.043	1.195	-
187	0.194	1.360	-
210	0.289	1.295	-
230	0.355	1.240	-
274	0.61	1.184	-

Table C-4.5 Multicomponent Breakthrough Behavior, Experiment-4

Height of bed	0.106 m		
Superficial velocity	0.00042 m/sec		
Adsorbate	Benzaldehyde	Benzyl alcohol	Benzoic acid
Adsorbate concentration in feed	0.90 mol/m^3	0.50 mol/m^3	0.20 mol/m^3
Time, minutes	C/C_o	C/C_o	C/C_o
38	0.000	0.000	
75	0.000	0.000	
110	0.000	0.000	
136	0.000	0.000	
187	0.000	0.000	-
210	0.000	0.000	-
230	0.000	0.010	-
252	0.000	0.011	-
266	0.000	0.323	-
312	0.010	0.850	-
460	0.020	1.610	-
540	0.030	1.574	-
688	0.476	1.240	-
735	0.593	1.187	-
775	0.819	1.098	-

Table C-4.6 Multicomponent Breakthrough Behavior, Experiment-5

Height of bed	0.106 m		
Superficial velocity	0.00063 m/sec		
Adsorbate	Benzaldehyde	Benzyl alcohol	Benzoic acid
Adsorbate concentration in feed	0.90 mol/m^3	0.50 mol/m^3	0.20 mol/m^3
Time, minutes	C/C_o	C/C_o	C/C_o
150	0.010	0.130	-
175	0.010	0.388	-
223	0.010	1.006	-
303	0.030	1.547	-
396	0.118	1.410	-
446	0.341	1.310	-
498	0.640	1.156	-

Table C-4.7 Multicomponent Breakthrough Behavior, Experiment-6

Height of bed	0.106 m		
Superficial velocity	0.00084 m/sec		
Adsorbate	Benzaldehyde	Benzyl alcohol	Benzoic acid
Adsorbate concentration in feed	0.90 mol/m^3	0.50 mol/m^3	0.20 mol/m^3
Time, minutes	C/C_o	C/C_o	C/C_o
35	0.000	0.010	-
90	0.000	0.100	-
113	0.004	0.271	-
131	0.007	0.480	-
175	0.037	1.127	-
212	0.059	1.446	-
250	0.117	1.480	-
310	0.275	1.347	-
340	0.411	1.200	-
380	0.631	1.134	-
400	0.716	1.090	-
420	0.763	1.086	-

Table C-4.8 Multicomponent Breakthrough Behavior, Experiment-7

Height of bed	0.121 m		
Superficial velocity	0.00042 m/sec		
Adsorbate	Benzaldehyde	Benzyl alcohol	Benzoic acid
Adsorbate concentration in feed	0.90 mol/m^3	0.46 mol/m^3	0.20 mol/m^3
Time, minutes	C/C_o	C/C_o	C/C_o
35	0.000	0.000	-
70	0.000	0.000	-
140	0.030	0.012	-
325	0.020	0.150	-
389	0.020	1.028	-
489	0.010	1.532	-
549	0.010	1.647	-
609	0.020	1.594	-
670	0.030	1.507	-
760	0.010	1.380	-
812	0.028	1.280	-
870	0.077	1.190	-

Table C-.9 Multicomponent Breakthrough Behavior, Experiment-8

Height of bed	0.121 m		
Superficial velocity	0.00063 m/sec		
Adsorbate	Benzaldehyde	Benzyl alcohol	Benzoic acid
Adsorbate concentration in feed	0.90 mol/m^3	0.46 mol/m^3	0.20 mol/m^3
Time, minutes	C/C_o	C/C_o	C/C_o
97	0.015	0.037	-
189	0.010	0.360	-
247	0.030	0.980	-
299	0.010	1.401	-
411	0.103	1.521	-
520	0.371	1.326	-

Table C-4.10 Multicomponent Breakthrough Behavior, Experiment-9

Height of bed	0.121 m		
Superficial velocity	0.00084 m/sec		
Adsorbate	Benzaldehyde	Benzyl alcohol	Benzoic acid
Adsorbate concentration in feed	0.90 mol/m^3	0.46 mol/m^3	0.20 mol/m^3
Time, minutes	C/C_o	C/C_o	C/C_o
30	0.000	0.020	-
75	0.000	0.045	-
105	0.010	0.070	-
140	0.010	0.250	-
187	0.026	0.928	-
220	0.022	1.314	-
265	0.051	1.527	-
315	0.150	1.466	-
360	0.257	1.313	-
390	0.382	1.211	-
415	0.554	1.170	-

C-5. Sampling loop procedure and calculations.

The procedure for sampling the liquid phase by the sampling loop is as follows:

1. Flush the line and loop
    A. The sampling loop is set to sample position.
    B. Valve V1 and V2 are closed.
    C. Valve V3 and V4 are opened.
    D. A syringe filled with ethanol is connected to Knurl-Lok finger tightened HPLC union (a).
    E. The sample loop is cleaned. Approximately 10 cc's of ethanol is flushed through the line and sample loop and into a beaker.
    F. The syringe is removed and then air is flushed through the loop in the same manner.

2. Load the sample in the loop
    A. Valve V3 and V4 are closed.
    B. The sampling loop is set to load position.
    C. Valve V1 and V2 are opened to allow the carbon dioxide to flow through the loop.
    D. After 15-20 minutes, the loop is brought back to sample position. This transition is done very fast, so that almost all the sample is retained in the loop.
    E. Valve V1 and V2 are closed.

3. Obtain sample and measure included gas

   A. The initial burette reading is noted.

   B. Valve V4 is opened slowly to allow the sample to flow out of the loop to the 10 ml volumetric flask.

   C. A syringe with 10 ml ethanol is connected to Valve V3.

   D. Valve V3 is opened.

   E. Ethanol is pushed through the sampling loop to the volumetric flask.

   F. The overflow bottle is lowered until the water level in the bottle matches that of the burette.

   G. The liquid level of the burette is recorded.

   H. Ethanol is added to the volumetric flask till the liquid level in the flask reaches 10 ml line.

   I. Valve V4 is closed and the sample collected in the volumetric flask is analysed.

   J. The sample is then diluted to 20 % by adding 40 ml of water. The diluted sample is then injected into the gas chromatograph.

Experiments were done to accurately measure the volume of the sampling loop. The equipment configuration used to determine the volume of the sample loop was identical to that used in the composition measurements except that the sample loop was connected directly to the high pressure tank of carbon dioxide. Sample loop volumes were calculated using the equations:

$$n = \frac{P_{ambient} V_{final}}{RT_{ambient}}$$

$$V = n\nu(P_{loop}, T)$$

Where,

n= number of moles.

ν =molar volume, mol/cm^3 .

Experiments were done at room temperature.The molar volume of carbon dioxide at elevated pressure were found by interpolating values from International thermodynamic tables of the fluid state ; v. 3.

Table C-5.1 Data for Volume Determination of Sample Loop

Temp. K	Loop pressure, bar	Final volume, cc	Moles carbon dioxide x 10^4	ν carbon dioxide, cc/gmol	Loop volume, (cc)
298.15	63.44	17.0	6.95	190.47	0.132
		17.1	6.99		0.133
		17.0	6.95		0.132
298.15	58.62	13.8	5.64	235.84	0.133
		13.7	5.60		0.132
		13.7	5.60		0.132
298.15	55.86	12.1	4.95	266.67	0.132
		12.3	4.99		0.133
		12.2	5.03		0.134

It can be realized from the table that the volume of the sampling loop is 0.132 ml. So for all the composition measurements, 0.132 ml was used as the volume of the sampling loop.

Experiments were done to check the precision of the sampling loop. Walther and Maurer reported that the solubility of benzaldehyde in carbon dioxide at 313.2 K and 8.11 MPa is 0.0023 mol benzaldehyde/mol carbon dioxide. Except the regeneration chamber, The experimental setup was same as Figure 3.4 . A smaller regeneration chamber was used and it was placed in a temperature bath to elevate the temperature to 40°C. The procedure followed in operating the sampling loop was the same. However, the sample wasn't diluted to 20%.

Table C-5.2 Results for Checking precision of Sampling loop

Temp, K	Pressure MPa	GC. Reading of sample, area count	Moles of benzalde-hydex10^7	Molar density of CO_2 mol/cc	Moles of CO_2 x10^4	Mole fraction, mol/mol
313.2	7.61	0.14	9.76	0.00525	6.93	0.00141
		0.14	9.76			0.00141
313.2	8.11	0.31	21.62	0.00675	8.91	0.00242
		0.30	20.93			0.00234

The solubility obtained from experimental results is quite close to the reported value. Hence, the sampling loop can be used to quantify the concentration of benzaldehyde in the carbon dioxide stream.

APPENDIX D

COMPUTER PROGRAM

```
/*************************************************************
  PROGRAM  :   ADSORPTION MODEL
  *************************************************************
  The program  fits the experimental data to Adsorption
models and find the constants.

*************************************************************/

#include <ctype.h>
#include <stdio.h>
#include <fstream.h>
#include <iostream.h>
#include <strings.h>
#include <iomanip.h>
#include <stdlib.h>
#include <math.h>
void linear(double *x1, double *x2);
void freundlich(double *x1, double *x2);
void langmuir(double *x1, double *x2);
void lang_freu(double *x1, double *x2);

double error(double *a1, double *a2);
int datapoints,response1;

struct functionresults
{
  double a,b;
} linearresults, langresults, freuresults, lfresults,
functionresults1;

functionresults function(double *x1, double *x2);
int main()
{

  char           *filep1;
  FILE           *filep;
  int             numbers, i, j,k,z;
  ifstream        fin;
  ofstream        fout;
  char            filename[11], line[28];
```

```
  double            values[199], totnumber,y[50],q[50];
  int               r, t, b, response, response2;
  char             data[100];
  char             number[120][10];
  int              m, n, state;

  cout << "the program has been prepared for one component
"<<endl;
  cout << "please prepare indata.dat with your adsorption
data," << endl;
  cout << " or you can specify your own input file names"
<< endl;

 continue1:
  cout << " press 0 to quit or 1 to continue" << endl;
  cin >>response;

  if (response == 0)
    {
      exit(1);
    }

  cout << " enter 1 for linear adsorption model. " << endl;
  cout << " enter 2 for langmuir adsorption model. " <<
endl;
  cout << " enter 3 for freundlich adsorption model. " <<
endl;
  cout << " enter 4 for langmuir-freundlich adsorption
model. " << endl;

  cin>> response1;


/*************************************************************
    Section 2 : Data Reading

*************************************************************/

  cout << "The data is in indata.dat(1) or some other
file(0)" << endl;
  cin >> response2;
  switch (response2) {
  case 1:
    {
      filename = "Indata.dat";
      break;
    }
```

```
case 0:
  {
    cout << " what is the filename " << endl;
    cin >> filename;
    break;
  }
}


for (j = 0; j <= 120; j++)
  {
    for (n = 0; n <= 10; n++)
   {
     number[j][n]='\0';
   }
  }
state = 1;
m = -1;
n = 1;
cout<<endl;
filep = fopen(filename, "r");
if (filep != NULL)
  {
    for (j = 0; j <= 200; j++)
   {
     fgets(data, 29, filep);

     n = 1;

     for (i = 0; i <= 29; i++)
       {
         if (isdigit(data[i]) || (data[i] == '.')) {
        if (state == 1)
          {
            m = m + 1;
            n = 0;
          }
        number[m][n] = data[i];
        n = n + 1;
        state = 999;
         }
         else
        {
          state = 1;
        }
       }
```

```
        for(i=0;i<=29;i++)
          data[i]='\0';

      }

       m = 1;
       for (j = 0; j <= 120; j++)
      {
        if (isdigit(number[j][0]) || number[j][0] == '.')
          {
            values[m] = atof(number[j]);

            m = m + 1;
          }
      }
       totnumber = m - 1; /* one already added to m */
    }
  else
    {
      cout << "it doesnt open" << endl;
      exit(1);
    }



/*****************************************************************
Section 3 : Call to corresponding Function

*****************************************************************/

  datapoints= int(values[1]);
  m=2;
  for(j=1;j<=datapoints;j++)
    {
      y[j]=values[m];
      q[j]=values[m+1];
      m=m+2;
    }
  switch (response1)
    {
    case 1:
      {
     linear(y,q);
     break;
      }
    case 2:
```

```
      {
     langmuir(y,q);
     break;
      }
    case 3:
      {
     freundlich(y,q);
     break;
      }
    case 4:
      {
     lang_freu(y,q);
     break;
      }

    }
  goto continue1;

}



/*************************************************************
    Linear Adsorption Model  Q= k*Y

*************************************************************/


void linear(double *x1, double *x2)
{
  int i;
  double a,lincalc[50],linerror;
  cout<<endl;
  linearresults= function(x1,x2);
  a=(linearresults.a);
  cout<< " the equation for linear adsorption model is q =
"<<a<<" * y"<<endl;

  for(i=1;i<=datapoints;i++)
    {
      lincalc[i]=(a*x1[i]);
      cout<<x1[i]<<" "<<x2[i]<<" "<<lincalc[i]<<endl;
    }
  linerror=error(x2,lincalc);
  cout<<" the total error is "<<linerror<<endl;
}
```

```
/*************************************************************
  Freundlich Adsorption Model  Q= k*Y^n

*************************************************************/


void freundlich(double *x1, double *x2)
{
  static int m;
  int i;
  double a,n;
  double y1[50],y2[50],freerror,frecalc[50];
  m=0;
  for(i=1;i<=datapoints;i++)
    {
      y1[i]=log(x1[i]);
      y2[i]=log(x2[i]);
      if(m==0)
     {
       cout<<endl;
       m=m+1;
     }
    }
  freuresults= function(y1,y2);
  n=freuresults.a;
  a=exp(freuresults.b);
  cout<< " the equation for Freundlich adsorption model is
q = "<<a<<" * y^"<<n<<endl;
  for(i=1;i<=datapoints;i++)
    {
      frecalc[i]=(a*pow(x1[i],n));
      cout<<x1[i]<<" "<<x2[i]<<" "<<frecalc[i]<<endl;
    }
  freerror=error(x2,frecalc);
  cout<<"the total error is "<< freerror<<endl;
}


/*************************************************************
  Langmuir Adsorption Model   Q= a*Y/(1+b*Y)

*************************************************************/


void langmuir(double *x1, double *x2)
{
  int i,m;
```

```
  double a,b;
  double y1[50],y2[50],lanerror, lancalc[50];
  m=0;
  for(i=1;i<=datapoints;i++)
    {
     y1[i]=(x1[i]);
     y2[i]=(x1[i])/(x2[i]);
     if(m==0)
    {
      cout<<endl;
      m=m+1;
    }
    }

  langresults= function(y1,y2);
  a=1/langresults.b;
  b=langresults.a*a;
  cout<<endl<<" "<<b<<" "<<a<<endl;

  cout<< "the equation for Langmuir adsorption model is q
=( ";
  cout<<a<<"*y)/(1+("<<b<<"*y))"<<endl;
  for(i=1;i<=datapoints;i++)
    {
      lancalc[i]=((a*x1[i])/(1+b*x1[i]));
      cout<<x1[i]<<" "<<x2[i]<<" "<<lancalc[i]<<endl;
    }
  lanerror=error(x2,lancalc);
  cout<<" the total error is "<<lanerror<<endl;
}


/*************************************************************
  Langmuir-Freundlich Adsorption Model
Q=(a*Y^n)/(1+(b*Y^n))

*************************************************************/

void lang_freu(double *x1, double *x2)
{
  int i,j,m,k,l;
  double a,b,step;
  double y1[50],y2[50],lferror, lfcalc[50],errorlast;
  double minn,maxn,n,ntrial,finala,finalb,finaln;

  cout<<" Please specify the range of n "<<endl;
  cout<<" possible minimum of n"<<endl;
```

```
  cin >>minn;

  cout<<" possible maximum of n"<<endl;
  cin >>maxn;
  m=0;
  errorlast= 10000000;
  for(l=1;l<=3;l++)
    {

     for(j=0;j<=100;j++)
    {
      step=(maxn-minn)/100;
      ntrial=(minn+((maxn-minn)*j/100));
      for(i=1;i<=datapoints;i++)
        {
         y1[i]=pow((x1[i]),ntrial);
         y2[i]=pow((x1[i]),ntrial)/(x2[i]);
         if(m==0)
        {
          cout<<endl;
          m=m+1;
        }
        }

      lfresults= function(y1,y2);
      a=1/lfresults.b;
      b=lfresults.a*a;

      for(i=1;i<=datapoints;i++)
        lfcalc[i]=((a*(y1[i]))/(1+b*(y1[i])));
      lferror=error(lfcalc,x2);
      cout<<endl;
      if(lferror<errorlast)
        {
          finala=a;
          finalb=b;
          finaln=ntrial;
          errorlast=lferror;
        }

    }
     minn=finaln-step;
     maxn=finaln+step;

    }
  cout<< "the equation for Langmuir-Freundlich adsorption
model is";
```

```
  cout<<" q =( "<<finala<<" *
y^"<<finaln<<")/(1+("<<finalb<<"*y^"<<finaln<<"))"<<endl;

  for(i=1;i<=datapoints;i++)
    cout<<x1[i]<<" "<<x2[i]<<"
"<<((finala*pow(x1[i],finaln)/(1+finalb*(pow(x1[i],finaln))
)))<<endl;
  cout<<" the total error is "<<errorlast<<endl;
}



/*************************************************************
  Function to calculate the best fit

*************************************************************/


functionresults function(double *x1, double *x2)
{
  functionresults functionresults1;
  int i;
  double sigmax, sigmay, sigmaxy,sigmax2;
  sigmax=sigmay=sigmaxy=0;
  for(i=1;i<=datapoints;i++)
    {
      sigmax=sigmax+x1[i];
      sigmay=sigmay+x2[i];
      sigmaxy=sigmaxy+(x1[i]*x2[i]);
      sigmax2=sigmax2+(x1[i]*x1[i]);
    }
  if(response1==1)
    functionresults1.a=sigmay/sigmax;
  else
    functionresults1.a=(((double)datapoints*sigmaxy)-
(sigmax*sigmay))/(((double)datapoints*sigmax2)-
(sigmax*sigmax));
  functionresults1.b=((sigmay-
(functionresults1.a*sigmax))/(double)datapoints);
  return(functionresults1);
}

/*************************************************************
  Function to calculate the error

*************************************************************/
```

```
double error(double *a1,double *a2)
{
  int i;
  double totalerror;
  totalerror=0;

  for(i=1;i<=datapoints;i++)
    totalerror=totalerror+ pow((a2[i]-a1[i]),2);

  return( totalerror);
}
```